PREPARATION AND CHARACTERIZATION OF MICROBUBBLES FOR ULTRASOUND IMAGING

A Thesis Submitted to
the Graduate School of Engineering and Sciences of
İzmir Institute of Technology
in Partial Fulfillment of the Requirements for the Degree of

MASTER OF SCIENCE

in Biotechnology

by
Emine Aysu SAĞDİÇ

December 2012
İZMİR

We approve the thesis of **Emine Aysu SAĞDİÇ**

Examining Committee Members:

_____
Assist. Prof. Dr. Sevgi KILIÇ ÖZDEMİR
Department of Chemical Engineering
İzmir Institute of Technology

_____
Assoc. Prof. Dr. Ekrem ÖZDEMİR
Department of Chemical Engineering
İzmir Institute of Technology

_____
Prof. Dr. Hürriyet POLAT
Department of Chemistry
İzmir Institute of Technology

_____
Assist. Prof. Dr. Devrim PESEN OKVUR
Department of Molecular Biology and Genetics
İzmir Institute of Technology

_____
Prof. Dr. Mehmet E. Şengün ÖZSÖZ
Department of Biomedical Engineering
İzmir Katip Çelebi University

11 December 2012

_____   _____
Assist. Prof. Dr. Sevgi KILIÇ ÖZDEMİR   **Assoc. Prof. Dr. Ekrem ÖZDEMİR**
Supervisor, Department of Chemical   Co-Advisor, Department of
Engineering   Chemical Engineering
İzmir Institute of Technology   İzmir Institute of Technology

_____
Prof. Dr. Salih OKUR
Co-Advisor, Department of Materials
Science and Engineering
İzmir Katip Çelebi University

_____   _____
Assoc. Prof. Dr. Volga BULMUŞ   **Prof. Dr. R. Tuğrul SENGER**
Head of the Biotechnology and   Dean of the Graduate School
Bioengineering Graduate Program   of Engineering and Sciences

ACKNOWLEDGEMENTS

ABSTRACT

PREPARATION AND CHARACTERIZATION OF MICROBUBBLES FOR ULTRASOUND IMAGING

Ultrasound is widely used in clinical settings for diagnosis of diseases. However, the image quality in some cases is not at desirable level because most of the tissues have similar acoustic properties to many tumors. Microbubbles administired to the systemic circulation during imaging are known to increase the quality, creating contrast with respect to the surrounding tissues. Unfortunately, current formulations of microbubbles composed of phospholipid (mainly PC) and emulsifier have been found to be unstable for ultrasound imaging. In this study, it was aimed to engineer the shell structure of microbubbles to develop more stable, targetable microbubbles and investigate their adhesion characteristics to breast cancer cells as a model system. Our results indicated that increasing content of PEG40 St in the formulation resulted in microbubbles with higher yield and stability, being optimum at 50 mole %. Incorporation of lipopolymers as emulsifier instead of PEG40St in the formulation influenced stability adversely. Addition of a phospholipid capable of secondary interactions to the formulation had improved stability and size of the microbbubles, depending on the content and type of head group of the phospholipid. Usage of less water-soluble gas in the core of new microbubbles did not have further effect on the stability, as observed with the microbubbles of the current formulation. This result may suggest that the new microbubbles' shell is densely packed such that gas diffusion is enormously minimized/inhibited. Moreover, selected formulations developed in this study provided much more adhesion than the current formulation to the cell of interest.

ÖZET

ULTRASON GÖRÜNTÜLEMEDE KULLANILAN MİKROKÖPÜKÇÜKLERİN HAZIRLANMASI VE KARAKTERİZASYONU

Hastalık teşhisi için yapılan klinik çalışmalarda ultrason oldukça yaygın kullanım alanına sahiptir fakat birçok dokunun tumor ile benzer akustik özelliklere sahip olması nedeni ile ultrason, hastalık teşhisinde yeterli görülmemektedir. Ultrason görüntüleme sırasında sistematik dolaşıma katılan microköpükçükler çevrelediği dokularda yarattığı kontrasttan dolayı ultrason görüntü kalitesini arttıran ajanlar olarak bilinmektedir. Ne yazıkki, fosfolipid ve emülsifiyerden üretilen günümüz mikroköpükçükleri ultrason görüntülemede yeterli stabiliteye sahip değillerdir. Bu çalışmada, stabil, hedeflenebilir mikroköpükçüklerin üretilmesi amaçlanmış ve bunların meme kanseri hücre hattına yapışmaları incelenmiştir. Bu çalışmadan çıkan sonuçlar mikroköpükçük zar yapısındaki PEG40St bileşeninin %50mol olduğu durumun en yüksek mikroköpükçük verimini ve stabilitesini sağladığını ifade etmektedir. Buna ek olarak, lipo-polimer yapıdaki emülsifiyerin PEG emülsifiyerin aksine mikroköpükçük stabilitesini düşürdüğü görülmüştür. İkincil kuvvetlerle bağ yapma yeteneğinde olan bir fosfolipidin mikroköpükçük zar yapısına eklenmesi, fosfolipidin baş grubuna bağlı olarak, stabiliteyi ve mikroköpükçük boyutunu olumlu yönde etkilemiştir. Mikroköpükçük içerisinde suda oldukça az çözünürlüğe sahip olan gaz kullanımı günümüzde üretilen mikroköpüklerin aksine yeni tasarlanan mikroköpükçüklerin stabilitesine etki sağlamamıştır. Bu sonuç sayesinde yeni tasarlanan mikroköpükçüklerin zar yapısının sıkı paketlenerek gaz difüzyonunu en alt seviyeye indirdiği veya engellediği öngörüsüne ulaşılabilir. Buna ek olarak bu çalışmada geliştirilen mikroköpük çeşitlerinin hücrelere bağlanma kabiliyeti daha yüksek bulunmuştur.

TABLE OF CONTENTS

LIST OF FIGURES

LIST OF TABLES

CHAPTER 1

INTRODUCTION

Today, routine clinical applications without ultrasound (US) cannot be imagined in medicine since ultrasound provides cost-efficient, non-invasive and well-developed modalities for imaging and diagnostics. Ultrasonography is a non-invasive diagnostic technique offering pictures of organs and structures inside the body. In principle, ultrasound pressure wave pulses reflected or scattered by the interfaces between different structures in the body. Some of these reflected sound waves return to the transducer placed on the skin. These signals are converted into electrical pulses digitized by the imaging system. Thanks to this way, an image based on scattered sound signals is generated (Riess, Schutt et al. 2003). The interpretation of an ultrasound is dependent on body structure and the skill of the operator. When imaging solid organs such as the liver, abnormal areas are not visible in nearly 40 to 50% of cases since normal liver, kidney or spleen has similar acoustic properties to many tumors (Table 1.1) indicating that ultrasound has until recently been limited by the lack of effective contrast agents compared to X-ray radiology and magnetic resonance imaging.

Table 1.1. Comparison of speed of sounds of some materials.

Material	Speed of sound (meters/second)	Acoustic Impedance
Air	330	0.0004
Water	1480	1.48
Blood	1570	1.61
Kidney	1560	1.62
Soft Tissue and Tumors	1540 (Average)	1.63
Liver	1550	1.65
Muscle	1580	1.70

A contrast agent alters image contrast by highlighting tissue borders that helps the diagnostician to distinguish between normal and abnormal conditions in a body (Figure 1.1). Regardless of the capability of an imaging technique to display structural

detail, contrast agents are curial to increase the amount of information obtained by the technique. Besides improving the contrast between pathologic and background tissues, a contrast agent will provide meaningful physiologic information when its rate of entry and elimination are monitored over time in a region of interest. An effective ultrasound contrast agent should provide differential backscatter which requires that the acoustic impedance between these tissues must be made different (Klibanov, Rasche et al. 2002). Microbubble is a type of contrast agent involving a gas core. Microbubbles are injected intravenously to the patient and remain in the vasculature. Since sound travels in gas more slowly than it does in liquid, microbubbles creates acoustic impedance mismatch between tissues and they are very effective ultrasound scatterers due to their high compressibility (Table 1.1). In the lead of insonification, microbubbles start to vibrate as the gas acts in response to the pressure change of the ultrasound by volume pulsations.
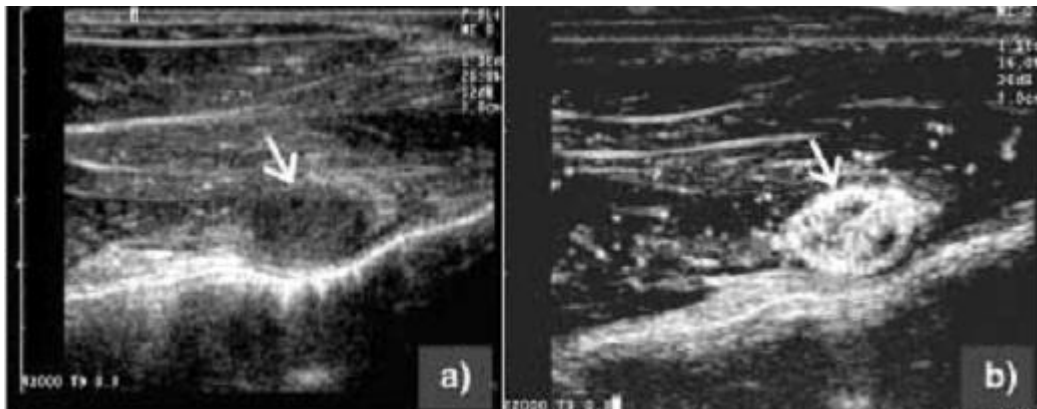
Figure 1.1. Images of a tumor (arrow) implanted in the thigh of a rabbit before (a) and after (b) the intravenous administration of microbubbles

Microbubbles are stabilized against dissolution by using main shell components such as lipids, albumin, biocompatible synthetic polymers and surfactants (Sharon and Lis 1982; Kim, Kim et al. 2000; Kim, Kim et al. 2004; Talu, Lozano et al. 2006). Because membranes of endothelial cells are mainly composed of neutral phosphocholine-based phospholipids, they are the most preferred main materials for encapsulation; however, these phospholipid monolayers show low stability due to their weak interaction between each other. Moreover, it is known that surfactant alone (such as phospholipid) cannot produce microbubbles (Kwan and Borden 2012). Therefore, forming stable microbubbles is achieved by adding PEG-emulsifier which mimics

carbohydrate layer on cell membrane which is important in improving blood compatibility of cell membrane, keeping other cells at a distance and avoiding protein-protein interaction (Sharon and Lis 1982; Klibanov 1999; Kim, Kim et al. 2000; Kim, Kim et al. 2004). It has been reported that PEG was effective in prevention of platelet adhesion (Kim, Kim et al. 2000). Thus, by using PEG-emulsifier can also prevent embolism problems in vascular system. Microbubble size is also a critical parameter that must be controlled between set limits (Riess, Schutt et al. 2003). The intensity of scattering with bubbles is proportional to the sixth power of the radius of the bubble, thus, larger bubbles provides better scattering intensity. However, since microbubbles larger than 8μm are trapped in the lung capillaries, acceptable sizes of microbubbles are in the range of 1–8μm.

It is known that exposure to ultrasound can improve cellular uptake of small-molecule drugs (Zderic, Vaezy et al. 2002). Although, high ultrasound energy is needed to induce gas cavitation which is responsible for cellular uptake, it may cause acoustic damage. Since microbubbles lower the high ultrasound energy level to safe intensity levels by acting as cavitation nuclei, they offer a different approach to facilitate the US triggered drug uptake (Figure 1.2) (van Wamel, Kooiman et al. 2006). Drug delivery using a microbubble can be performed in two ways, namely: 1) binding a therapeutic agent to or integrating it into bubble and 2) co-administration of the microbubble and a therapeutic agent (Deckers and Moonen 2010). The co-administration method is also called as sonoporation, in this route, microbubbles activated with ultrasound improve drug uptake by tissues or cells. In previous studies, a transient increase in porosity and permeability of the cell membrane was observed; however sonoporation mechanism is unclear (Hernot and Klibanov 2008; Schneider 2008). Drug uptake experiments were conducted with different ultrasound settings using different cell types such as aortic smooth muscle cells, endothelial cells (van Wamel, Kooiman et al. 2006; Meijering, Juffermans et al. 2009), *Xenopus laevis* (Zhou, Cui et al. 2008) and tumor cells (Schlicher, Radhakrishna et al. 2006; Karshafian, Bevan et al. 2009). To study sonoporation induced by microbubbles, electron microscopy, optical imaging and electrophysiological measurements have been used (Schlicher, Radhakrishna et al. 2006; van Wamel, Kooiman et al. 2006).
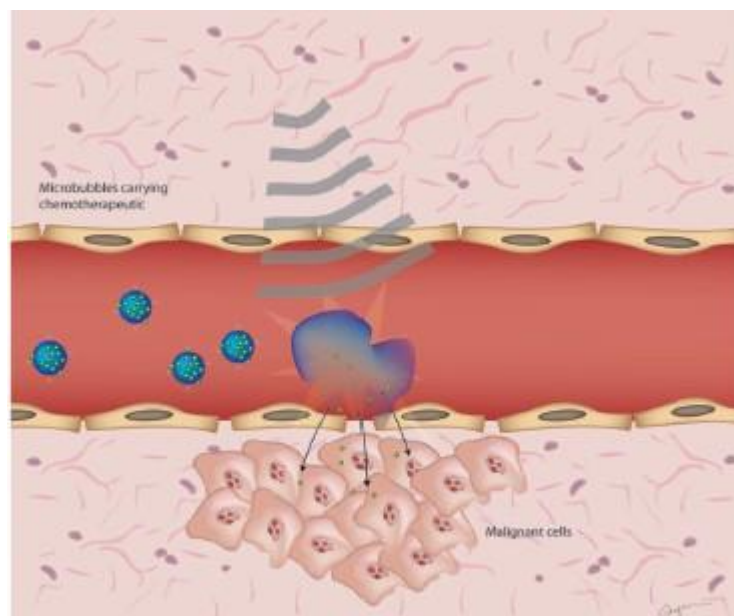
Figure 1.2. Schematic representation of the sonoporation.
(Source: Kaneko and Willmann 2012)

In current literature, microbubbles have been prepared with 1,2-Distearoyl-*sn*-glycero-3-phosphocholine (DSPC) and PEG40St at a molar ratio of 9:1 (Borden and Longo 2002; Talu, Lozano et al. 2006; Sirsi, Feshitan et al. 2010; Swanson, Mohan et al. 2010). However, our results showed that microbubbles prepared with the current formulation have been found to be unstable at body temperature. Therefore, different formulation of microbubble shell should be investigate to produce more stable microbubbles. Thus far, there are few studies about microbubble stability. These investigations involves the effect of saturated phospholipids with the same head-group and various acyl chains and effect of emulsifier type on microbubble stability (Borden and Longo 2002; Lozano and Longo 2009; Cox and Thomas 2010; Kwan and Borden 2010) but any enhancement in microbubble stability has been observed. For this purpose, following in this thesis, several phospholipids with different head-groups and same acyl chains have been focused to produce microbubbles with an appropriate stability, size, and high adhesion capacity to cell of interest. The selected range of phospholipid candidates, having capability of hydrogen bonding, includes DSPC, DSPG, DSPA, Stearoyl-rac-glycerol and DSPE. Other phospholipid candidates, having capability of ionic interaction, involves DSPS, DSTAP and Stearyl amine. Moreover, the effect of cholesterol, emulsifier and gas type on microbubble stability was also examined at close to body temperature. In addition, the effect of temperature and sub-

phase on microbubble stability was studied. In final section, adhesion of microbubbles species (selected for their stability) to cultured human breast cancer cell line were investigated at various shear rates.

This thesis has been divided into five chapters. In chapter one, a general introduction for contrast agents used in ultrasound imaging and the objective of this thesis are introduced. In chapter two, a literature survey about the properties of microbubble shell compounds, techniques used in production and characterization of microbubbles, stability studies and targeted microbubbles are presented. In chapter three, the preparation procedures of the microbubbles, stability experiments and also characterization of targeted microbubbles is explained in details. In addition, the physical characterization method of microbubbles is given. In chapter four, development of stable microbubbles by using different components and gases and adhesion rates of stable bubbles to a breast cancer cell line are presented and discussed in this thesis. Finally, the conclusions and some recommendations are listed in chapter five.

CHAPTER 2

LITERATURE SURVEY

2.1. Microbubble Shell Components

For long circulation time, microbubbles need to be stable in vascular system of an organism. Since air microbubble without a shell with initial diameter of 2μm in water at 37°C is theoretically predicted to fully dissolve within 25ms (Chomas, Dayton et al. 2001), stability of microbubbles can be provided encapsulating air bubble with a thin shell. This thin shell should be composed of molecules which are amphiphiles consisting of two different parts for production of gas filled microbubbles. One of these parts is called as hydrophilic (head group) and the other part is called as hydrophobic (tail group). Amphiphilic molecules are ordered such that head group face towards the gas phase and tail group of these molecules face towards the aqueous phase (Langmuir and Langmuir 1927; Fahy, Subramaniam et al. 2009). These amphiphilic molecules used in microbubble shell might be composed of lipids, protein (albumin), surfactants or biocompatible polymers (Hernot and Klibanov 2008). Although all of these molecules are used for encapsulation, phospholipids are the most preferred component for production of microbubbles due to their flexibility and biocompatibility. To understand the advantages of lipid coated microbubbles, initially the difference between lipids and the other components should be understood.

2.1.1. Protein Coated Microbubbles

Albumin is the most used protein for encapsulation of microbubbles as a protein. Commercially, Albunex® is the first protein-coated microbubbles approved by the US Food and Drug Administration (FDA). This microbubble suspension consists of $7x10^8$ #/mL microbubbles and filled with F-propane gas. Their sizes are between 1 and 15 μm in diameter (Christiansen, Kryvi et al. 1994). Albunex® is produced by sonication method and stable for at least two years at 4°C. Another protein coated commercial

microbubble was developed by Optison™ consisting of a ready-to-use suspension of microcapsules of albumin. These microbubbles are filled with perfluorocarbon gas (PFC) which has much longer circulation persistence in vivo (Podell, Burrascano et al. 1999). However, after injection, these microbubbles are expected to nucleate and convert into gas bubbles of approximately 2–5μm in diameter (Forsberg, Roy et al. 1998; Riess, Schutt et al. 2003). Besides commercial ones there are also some studies about this type of microbubbles in the current literature. More recently, protein-shelled microbubbles have designed for carrying targeting ligands (Korpanty, Grayburn et al. 2005) and genes. Although, albumin shells tend to be rigid, introduce the typical immunogenicity issues can be occurred which is associated with animal-derived materials (Ferrara, Pollard et al. 2007). Indeed, allergy to the albumin products found in some agents is a disadvantage in patient safety (Raisinghani and DeMaria 2002). Moreover, compared to phospholipid-MBs, protein-shelled microbubbles possess larger shell volumes and can potentially embed higher drug loads; however, a greater shell thickness can impair the acoustic properties of microbubbles.

2.1.2. Polymer Coated Microbubbles

Biocompatible polymer shell make the microbubbles more stable compared to lipid and albumin shell due to its bulk nature. However, it reduces the echogenicity and drug delivery activity (Sirsi and Borden 2009). At low ultrasound intensity, the stiff polymeric shell will not oscillate actively. As ultrasound pressure is increased up to a critical value, shell cracks form causing gas escape (Hernot and Klibanov 2008). On the contrary, at low acoustic power, a lipid based microbubble oscillates in linear manner. The pressure variations caused by ultrasound change the microbubble volume and therefore its diameter. This behavior of lipid-coated microbubbles increases transmitted frequency which offers good quality of ultrasound images and also it provides resistance to acoustic power. Although polymer-coated microbubbles have disadvantages, thus far, they have been studied in gene and drug delivery systems (Lu, Liang et al. 2003; Lentacker, De Geest et al. 2006). Beside drug delivery systems, polymer-coated microbubbles have been studied in terms of their stability by *Wheatley et al*. They used ionotropic gelation of alginate in production of microbubbles and reported that microbubble diameters ranged between 30μm and 40μm and were hence

too large for medical applications (Wheatley, Schrope et al. 1990). After that same researchers developed a new polymer-coated microbubble formulation (biodegradable copolymer poly(D,L-lactide-co-glycolide) (PLGA)) having size distribution ranged from 2 to 20µm in diameter (Narayan and Wheatley 1999). In 1997, *Bjerknes et al.* produced microbubbles using double-ester polymer with ethylidene units. Size distribution of these microbubbles ranged from 1 to 20 µm. However, they had crumpled shapes.

2.1.3. Surfactant Coated Microbubbles

Microbubbles were also stabilized by mixtures of the synthetic surfactants such as Span, Tween and sucrose stearate. *Wheatley et al.* developed a series of surfactant-stabilized microbubbles used in ultrasound imaging by using Span-type and Tween-type surfactants (Singhal, Moser et al. 1993). The stability of shell was investigated using Langmuir Blodget method. They also developed a new contrast agent ST68 prepared with surfactant 41 and investigated acoustic properties of this agent (Wheatley and Singhal 1995). In 2010, *Xing et al.* fabricated novel perfluorocarbon-filled microbubbles using ultrasonication of a surfactant mixture of sorbitan monostearate (Span 60) and polyoxyethylene 40 stearate (PEG40S) in aqueous media (Xing, Ke et al. 2010). Microbubbles developed by *Dressaire et al.* were stable in suspension for over a year and showed remarkable polygonal domains on their surface however they were not stable upon dilution (Dressaire, Bee et al. 2008).

2.1.4. Lipid Coated Microbubbles

In microbubble shell phospholipids are highly oriented due to hydrophobic forces and held together through physical associations such as secondary forces rather than covalent bonding (Borden, Kruse et al. 2005). Therefore, lipid shell reseals after expansion or fracture to stabilize the gas core. Furthermore, lipid microbubbles are more acoustically responsive and preferred as more desirable vehicles for ultrasound-triggered drug release (Sirsi and Borden 2009). However, lipid-coated microbubbles having relatively thin shell does not allow a high payload of drugs to be incorporated.

The lipid shell of a microbubble also mimics the cell membrane thus it is bio-inspired and provides remarkable stability.

There are several commercially available lipid-coated microbubble formulations approved to use in diagnostic ultrasound, such as Definity® and SonoVue®. Definity is the commercial microbubble which is initially developed by ImaRx (USA). These microbubbles have been prepared with the mixture of dipalmitoylphosphatidylcholine (DPPC), a methyl-poly(ethylene glycol) dipalmitoylphosphatidylethanolamine (MPEG5000 DPPE) and a small amount of negatively charged dipalmitoylphosphatidic acid (DPPA). SonoVue has been developed by Bracco International and prepared by using sulfur hexafluoride in the gas core. The product consists of a lyophilized phospholipid/poly(ethylene glycol)/palmitic acid powder and has a shelf life of two years at room temperature (Riess, Schutt et al. 2003). Besides commercial lipid-coated microbubbles, thus far there are also several investigations about formulation of lipid-microbubbles. These observations will be discussed in stability of microbubbles.

2.2. Current Methods Used in Lipid-Coated Microbubble Production

Production of microbubbles used in medical applications requires a sophisticated manufacturing process, characterization and safety control. In designing microbubble manufacturing process and characterization is the one of the significant prerequisites since they should be smaller enough to cross the capillary system for in vivo usage. Besides of crossing capillaries, they should provide sufficient scattering intensity. The intensity of scattering is proportional to the sixth power of the radius of the bubble; hence microbubble size must be controlled between set limits which are in the range of 1–7 μm, preferably around 3 μm. For these purpose, variety of methods have been developed to produce ideal microbubbles. The most commonly used methods were given as follows.

2.2.1. Mechanical Agitation Method

On the industrial scale mechanical agitation method is a common approach for production of lipid-coated microbubbles (Bekeredjian, Chen et al. 2003). This method is utilized to prepare the commercial product Definity®. The mechanical agitation method

consists of two steps. Initially, lipid/emulsifier film is formed using traditional method. After lipid/emulsifier dispersion is filled into vials, their head spaces are filled with gas. These vials are placed in a mechanical agitator (Vialmix® for Definity®) and then shaken at several thousand oscillations per minute. Gas-liquid interface in lipid/emulsifier suspension is quickly improved by the dispersing of gas into the aqueous phase during mechanical agitation. This enhanced contact interface between liquid phase and gas phase is stabilized by phospholipid monolayers. In this technique, some parameter should be controlled. Some of these parameters are agitation time, viscosity of the microbubble suspension, temperature, concentration of lipids and proportion of vial head-space to fill volume. This method is versatile and gentle for targeting ligands.

2.2.2. Probe-Type Sonication Method

Probe-type sonication method is the common production method for lipid-coated microbubbles. The origins of this method were described by *Li and Fogler* (Li and Fogler 1978; Li and Fogler 1978). This method consists of two stages. Lipids and emulsifiers which are found on water surface exists instable form. This instable situation results in entrainment of bubbles into the aqueous medium and following cavitation in the medium results in droplet breakup to a critical size. In the first step, unstable growth of droplets (bubbles) occurs. In the second step, until a stable size is reached, continual cavitation provides breakdown of larger droplets. The breakdown mechanism associated with the type of deformation and flow pattern around the droplets. The droplets reaches their as surface tension forces balance the inertial forces on the droplet. Thanks to this method microbubble core gas is dispersed into the aqueous solution by using ultrasound probe-type sonication. For the production of lipid coated microbubbles the temperature must be kept below the phase-transition temperature of the phospholipids. In current literature, lipid coated microbubbles are currently produced using this method (Borden and Longo 2002; Gerber, Krafft et al. 2006; Borden, Feshitan et al. 2009; Kaya, Gregory V et al. 2009; Lozano and Longo 2009; Wrenn, Mleczko et al. 2009; Kwan and Borden 2010; Swanson, Mohan et al. 2010; Xing, Ke et al. 2010).

2.2.3. Flow Focusing Device

Flow focusing device is mainly used to produce monodisperse microbubbles in laboratory-scale. This method involves passing the core gas and shell components through a nozzle into a water bath. The diameter primarily scales with the liquid and gas flow rates, with the continuous-phase surface tension having a negligible effect (Hettiarachchi, Talu et al. 2007). This method requires small volumes of fluids, and the based on variable flows. The gaseous thread is surrounded by continuous liquid film in the orifice. Because of the high surface energy of this formation, this thread is not stable and it breaks to release a bubble into the outlet channel. In each period of the process, a single bubble is formed. In 2001, *Alfonso M. Gañán-Calvo and José M. Gordillo* reported a simple microfluidics phenomenon allowing the effective mass production of monodisperse microbubbles having diameters of 100-210μm (Gañán-Calvo and Gordillo 2001). They obtained closed expressions for the bubble diameter as a function of the liquid and gas properties, flow parameters and geometry. In 2006, *Talu et al.* demonstrated long-term stabilization of monodisperse microbubbles produced by flow focusing by using lipid encapsulation (Talu, Lozano et al. 2006). By using this method, they produced microbubbles having a diameter of 51 μm which is too large for intravascular administration. After that same investigators produced nitrogen-filled microbubbles having a diameter of 1.5 μm and maintaining their size at least for 9hr (Talu, Hettiarachchi et al. 2008).

2.2.4. Electrohydrodynamic Atomization

Electrohydrodynamic atomization (EHDA) is a well-known method where a suspension is passed through a capillary needle at a constant flow rate under the effect of an electric field (Jaworek and Krupa 1999; Farook, Zhang et al. 2007). The most important difference between flow focusing device and EHDA is that in flow focusing the orifice size is independent from flow rates whereas in EHDA the microbubble size is dependent on the change in flow rates. Therefore the EHDA technique offers more process control opportunities (Farook, Stride et al. 2007). With decreasing the bubble size depending on applied voltage is also required to select the suitable values to achieve the minimum bubble size. Moreover microbubble diameter decreases with

increasing the flow rate (Farook, Stride et al. 2007). Characteristics of EHDA have been investigated by *Farook et al.* using a model glycerol-air system (Farook, Stride et al. 2007). They elucidated modes of microbubbling by changing applied voltage and liquid and air flow rates; therefore the parametric plot, providing a basis for the selection of flow rates, is invented in order to identify gas and liquid rate administration. In 2007, same investigators improved this system as co-axial electrohydrodynamic jetting to produce smaller microbubbles (2–8μm) by using outer needle and co-axial twin needle arrangement with electrohydrodynamic atomization in the stable cone-jet mode as air flowed through the inner needle at the same time (Farook, Zhang et al. 2007). *Pancholi et al.* also produced small bubbles having a diameter range between 3-7 μm by using same technique (Pancholi, Farook et al. 2008).

2.3. Current Methods Used in Microbubble Characterization

To characterize a microbubble is one of the most challenging tasks. Due to their flotation in the upright direction because of the buoyancy and sensitivity towards shear stress, the analysis of microbubble population is often complicated.

To measure the microbubble size distribution, electrical zone sensing is the most commonly used method (Christiansen, French et al. 2003; Borden, Pu et al. 2004; Bekeredjian, Kuecherer et al. 2007; Leong-Poi, Kuliszewski et al. 2007; Borden, Feshitan et al. 2009; Wrenn, Mleczko et al. 2009; Swanson, Mohan et al. 2010). This technique analyses the vesicles in terms of size and number based on the impedance change in an electromagnetic field when a particle existing in an electrolyte solution, passes through a small aperture, which is located between two electrodes. The size range of this method is between 0.4 μm and 1,200 μm and called as Coulter Counter.

Another particle counting method used to characterize microbubbles is the Light blockage technique (Lum, Borden et al. 2006; Talu, Hettiarachchi et al. 2006; Bekeredjian, Kuecherer et al. 2007). In this system, particles flow through a region of uniform light one at a time and their light shades are detected. The size capacity of this method ranges from 0.5μm to 400μm. With this method, due to rapid buoyancy microbubbles, the analysis of the large microbubbles cannot be performed.

Static light is another suitable and reliable method to detect the particle size distribution of microbubbles (Lentacker, De Geest et al. 2006; Lentacker, De Smedt et

al. 2006). With this method, particles are measured in a short time and measurement is independent from buoyancy effects. The size range of this method is between 40–2 mm. to obtain feasible results by using this technique an elaborate optical is needed.

Dynamic light scattering (DLS), is a less commonly used method for analyzing microbubble suspensions (Hernot and Klibanov 2008). Due to the bouncy of the microbubbles fluctuations in the intensity of scattered light are occurred. Measurements of the microbubbles are typically on the upper end of the DLS size range.

Finally, the simplest method is light microscopy to analyze microbubbles. By using counting chambers, this method may provide reliable results of microbubble size distribution and microbubble concentration. For physical characterization of microbubbles we used this method and will be discussed in Chapter 4.

2.4. Stability of Microbubbles

2.4.1. Effect of Shell Components on Microbubble Stability

Lipid coated microbubble shell generally includes a primary stabilizing lipid and an emulsifier, often polyethylene glycol 40 stearate. These two types of components affect the stability of microbubbles. Head group of lipids in microbubble shell are often zwitterionic; however, they can be adjusted to modulate for microbubble properties. For instance, lipids having charge on their head group can be used for DNA delivery (Borden, Caskey et al. 2007). Tail group of phospholipids provide an anchor to the gas/liquid interphase. Generally, saturated di-acyl chain is utilized due to their low solubility and high packing order providing high stability (Kim, Costello et al. 2003). Emulsifiers are the crucial components to aid in microbubble generation and to prevent coalescence during foam formation by reducing the energy barrier. When lipid/emulsifier monolayer forms, the PEG molecules form a brush, which inhibits microbubble coalescence through a steric repulsive force (Kwan and Borden 2012).

The first use of microbubbles as contrast agents was introduced in 1968 by *Gramiak and Shah* (Gramiak and Shah 1968). They used agitated saline by injecting intracardiacly and observed that this injection improved aortic root delineation because of the scattering of ultrasound by air-bubbles present in the solution. After that, other agitated contrast agents such as hydrogen peroxide, indocyanine green dye, iodinated

contrast and dextrose have been utilized but it was found that they were unstable to pass through the pulmonary capillaries. Use of sonication to produce small and stable microbubbles was introduced by *Feinstein et al.* in 1984 (Feinstein, Ten Cate et al. 1984). The first commercial products developed in the early 1990s were Echovist (Schering AG, Germany) and Albunex (Molecular Biosystems Inc., USA), respectively. Echovist produced with microcrystalline galactose particles (von Bibra, Hartmann et al. 1989) whereas Albunex consists of air microbubbles prepared with heat-denatured human albumin shells (Feinstein, Cheirif et al. 1990).

In current literature, since membranes of endothelial cells are mainly composed of neutral phosphatidylcholine-based phospholipids, they are the most preferred main materials for encapsulation of gas bubbles. In 2002, Borden & Longo investigated shell resistances for a homologous series of phospholipids by comparing this model to experimental data of lipid-coated, air-filled microbubbles. It was found that microbubble stability increased monotonically with lipid hydrophobic chain length (Borden and Longo 2002). Another study about stability of microbubbles based on hydrocarbon group of phospholipids has been published by *Cox and Thomas*. They investigated effect of hydrocarbon saturation on stability microbubbles and found that unsaturated lipid-coated bubbles shrink slowly and vanished entirely by time, while saturated lipid-coated persist for longer times (Cox and Thomas 2010). In 2010, *Swanson and Mohan* also examined the effect of lipid acyl chain length on stability of microbubble population. They observed that DSPC lipids with 18 carbons provided more stable microbubbles compared with DPPC lipids with 16 carbons (Swanson, Mohan et al. 2010). Beside lipids, stability of microbubbles by changing emulsifier type was also investigated by some researchers. One of them is the study of *Longo et al.* (Lozano and Longo 2009). They investigated the impact of the DSPE-PEG2000 species and PC chain-length on microbubble dissolution rate and surface contour. They observed that film microstructure and collapse behavior for all chain lengths (n= 14-20) by using fluorescence microscopy of dissolving microbubbles was indicative of primarily condensed phase monolayers, unlike similar coatings involving polyethyleneglycol (40) stearate (PEG40St) that are either expanded phase monolayers and found that the microbubbles having a diameter of 15μm and involving DSPE-PEG2000 persisted approximately 4× longer in comparison to microbubbles containing PEG40St.

2.4.2. Effect of Temperature on Microbubble Stability

Hyperthermia (HT) is a strategy in cancer therapy based on heating selective tumour cells in the range of 41-45°C (Guiot, Pastore et al. 2006). Adding HT to radiotherapy showed an important treatment on clinical bases (15 of 22 studies were succeeded) (Overgaard 1989). Effective temperature control is an essential prognostic factor for the treatment using HT with radiotherapy because total time and rate of heating, and a fluctuation in temperature might avoid or at least reduce monitoring (Kapp and Cox 1995). For temperature monitoring of heated tissues, ultrasound which is a cost effective and non-invasive imaging technique studied by some authors (Straube and Arthur 1994; Seip and Ebbini 1995; Zuna, Novak et al. 2000; Varghese, Zagzebski et al. 2002) based on attenuation, speed of sound waves and reflectivity in tissues can be used. However, there are limitations about monitoring local temperature in heated tissues. To reduce these limitations, improvement in the ultrasound signal in a selected tissue which requires a contrast agent, such as microbubble, is needed. Therefore, microbubbles should be resistance to high temperature and there are a few studies performed with commercial microbubbles (SonoVue®, Bracco) of SF_6 coated with phospholipid investigating the thermal response of microbubbles (Guiot, Cavalli et al. 2004; Guiot, Pastore et al. 2006; Mulvana, Stride et al. 2010). However, these investigations did not examine the change in concentration of microbubbles with the temperature; they are based on the effect of temperature on bubble diameter and acoustic attenuation. Moreover, since the formula of the commercial bubbles is not known, the effects of temperature on lipid coated microbubbles currently studied still have not been investigated (Currently studied microbubbles are encapsulated with phospholipids and PEG40S at a molar ratio of 9:1). In addition to these studies, heat-sensitive microbubbles for cancer ablation prepared with biodegradable poly lactic-co-glycolic acid shell instead of phospholipid have been produced by *J. Huang* and found that these microbubbles were just detected by ultrasound after being heated to 55°C for 10 minutes (Huang 2009).

2.5. Targeted Microbubbles

Several studies have been performed to design microbubbles for detection of the diseased tissues by ultrasound imaging (Weller, Villanueva et al. 2005; Bachmann, Klibanov et al. 2006). Targeted microbubbles are the contrast agents which are expected to allow earlier and safe detection of pathology since they bind to tumors without eliminating by leukocytes during circulation. There are two methods used for targeting of microbubbles to cell of interest; passive and active targeting. Passive targeting strategy is based on size and shell structure by specially accumulating in regions of interest. Accumulation in the reticuloendothelial system (Kono, Steinbach et al. 2002; Hohmann, Albrecht et al. 2003) within phagocytotic cells at inflammation sites (Lindner, Song et al. 2001), and within tumors can be given as examples for passive targeting. In current literature, there are several investigations related to passive targeting of microbubbles. One of these is the study of *Goldberg et al*. In their investigations, they examined whether lymphatic channels and sentinel lymph nodes with and without metastases can be detected with microbubbles or not with passive targeting and observed that using contrast agents is curial materials to visualize the lymph channels and sentinel nodes (Goldberg, Merton et al. 2004). Passive targeting has also been illustrated by *Wisner et al.*(Wisner, Ferrara et al. 2003). They observed that subcutaneous injection of contrast media caused enhancement of 85% of sentinel lymph nodes in dogs by using passive targeting strategy.

Active targeting refers to the attachment of antibodies or ligands providing microbubble to bind to cell of interest. Ligands/antibodies are recognized by disease antigens. In order to bind the biotinylated microbubbles with biotinylated antibodies, avidin/biotin chemistry is often preferred since they have extremely high equilibrium association constant. Biotin has one binding site for avidin whereas avidin has four binding site to biotin (Livnah, Bayer et al. 1993). Avidin serves as a bridge between biotinylated components. These molecules bind each other strongly but non-covalently. The binding speed of these two molecules is so fast and highly resistant to physiochemical factors such as high temperature, pH and organic solvents. Since natural avidin shows non-specific binding to cells, streptavidin is generally used for targeted microbubbles. Streptavidin is a bacterial analog of avidin isolated from *Streptomyces avidinii* and has lower non- specific binding because of its non-glycosylated nature

(Bayer, Ben-Hur et al. 1989). Currently, there are several research focused on active targeting of inflammation (Lindner, Song et al. 2001), thrombus (Takeuchi, Ogunyankin et al. 1999) and angiogenesis (Ellegala, Leong-Poi et al. 2003; Leong-Poi, Christiansen et al. 2003). Villanueva et al. demonstrated that microbubbles targeted to ICAM-1 via surface conjugation with anti-ICAM-1 monoclonal antibodies adhered to inflammatory cultured endothelial cells in 1998 (Villanueva, Jankowski et al. 1998). In 2002, Weller et al. observed that the adhesion of this targeted bubbles is dependent on the antibody density and the shear conditions (Weller, Villanueva et al. 2002). After that, In 2005, *Weller et al.* described that targeting contrast agents to multiple molecular epitopes increased binding to inflammatory endothelium (Weller, Villanueva et al. 2005). Another investigation about targeted microbubbles has been performed by *Takalkar et al.* In that study, they found that adhesion and retention of targeted lipid-coated microbubbles is possible under physiologic flow conditions and is influenced by surface density of the target receptor and shear stress (Takalkar, Klibanov et al. 2004).
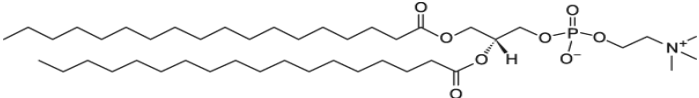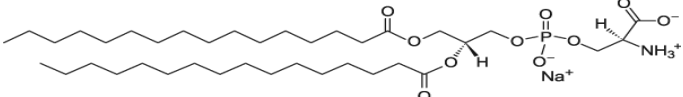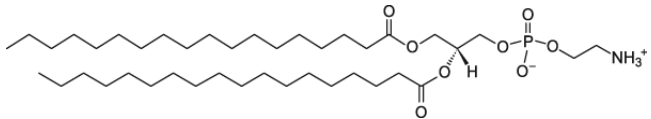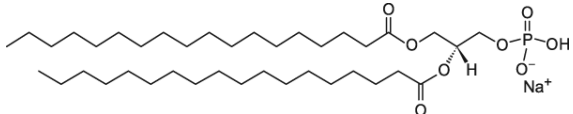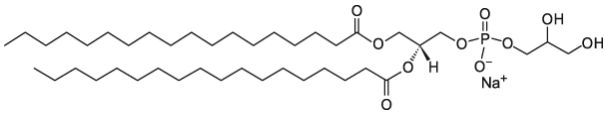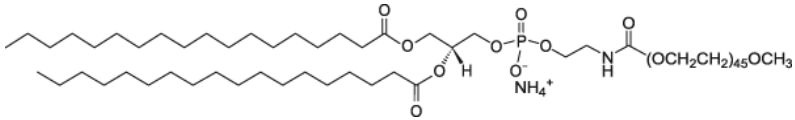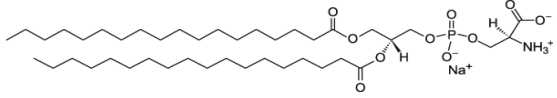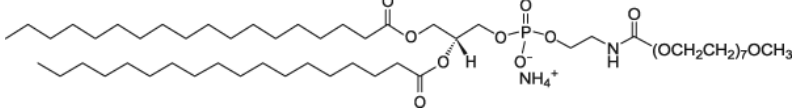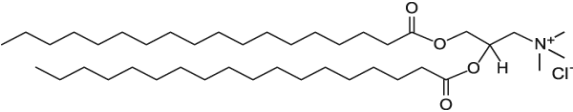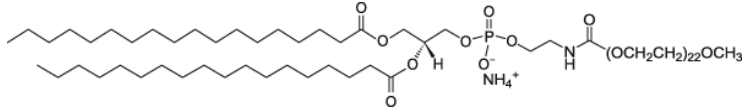
CHAPTER 3

MATERIALS AND METHODS

3.1. Materials

The microbubble shell components (Table 3.1), 1,2-Distearoyl-sn-glycero-3-phosphocholine (DSPC), 1,2-dioctadecanoyl-sn-glycero-3-phosphoethanolamine (DSPE), 1,2-distearoyl-sn-glycero-3-phosphate (sodium salt) (DSPA), cholesterol, Stearyl amine (octadecylamine), 1-stearoyl-rac-glycerol and polyoxyethylene glycol (40) steareat (PEG40St) and PEG8St were purchased from Sigma-Aldrich (St. Louis, MO) and 1,2-dioctadecanoyl-sn-glycero-3-phospho-(1'-rac-glycerol) (sodium salt) (DSPG), DSPE-PEG$_n$ (n=350, 1000, 2000), 1,2-distearoyl-sn-glycero-3-phospho-L-serine (sodium salt) (DSPS) and distearoyl (C 18:0)-trimethyl ammonium propane (DSTAP) were purchased from Avanti Lipids. All glassware was cleaned with 5% volume of chromic acid and rinsed with deionized water. Air and decafluorobutane (perfluorocarbon gas, TSCA Inventory) was used as gas to form microbubbles. Lipid and emulsifier were dissolved in chloroform (Sigma-Aldrich). Phosphate buffer saline (PBS was prepared by mixing 0.12 mM of NaCl, 5.08 mM of NaH$_2$PO$_4$, and 11.6 mM of Na$_2$HPO$_4$), propylene glycol (Sigma-Aldrich) combinations were used as hydration and storage solution. All buffer materials were purchased from MERCK. The pH of the buffer solution was adjusted to 7.2 by using NaOH (MERCK). Centrifugation was performed with centrifuge (Nuve, NF200).

Table 3.1. Microbubble shell components and their chemical structures.

Components	Chemical Sturctures
DSPC	
DPPS sodium salt	
DSPE,approx	
DSPA-NA,approx	
DSPG	
1-stearoyl-rac-glycerol	$CH_3(CH_2)_{15}CH_2$ ... OH, OH
Octadecylamine	$CH_3(CH_2)_{16}CH_2NH_2$
DSPE-PEG2000	$(OCH_2CH_2)_{45}OCH_3$
DSPS	
DSPE-PEG350	$(OCH_2CH_2)_7OCH_3$
DSTAP	
DSPE-PEG1000	$(OCH_2CH_2)_{22}OCH_3$

3.2. Production of Microbubbles

Air-filled microbubbles coated with lipids were produced through high power tip sonication of a lipid/emulsifier aqueous solution. Briefly, mixture of lipid/emulsifier at various molar ratios was dissolved in chloroform, evaporated with nitrogen and incubated overnight at 25°C under vacuum. The dried lipid/emulsifier film then hydrated with 4 ml PBS and propylene glycol at molar ratio of 4:1 at the main phase transition temperature of the phospholipid (55°C). The homogenous mixture dispersed with sonication was then sonicated with a probe type sonicator (MISONICS) at the air-solution interface continuously at 50 AMP to form microbubbles. After that, the produced suspension was diluted with 5 ml PBS and the milky part of the suspension which is found at the bottom of the vial was transferred into 2-mL tubes. Washing and collecting all microbubbles from the suspension into a cake by centrifugation was operated at 2000 rpm for 4 minutes. All cakes were re-suspended in PBS until the infranatant was no longer turbid (after each re-suspension, centrifugation was repeated). The infranatant part of the suspension which is the result of the centrifugation consisting of residual lipids and vesicles were discarded. Finally, the final cake was concentrated to 1 ml PBS and propylene glycol at molar ratio of 4:1 and stored in 2 ml tubes. Before the analysis each sample was stored at 4°C over night. For the study about the effect of gas type on microbubble stability, at sonication step we used closed system in order to avoid the air entrance to the lipid/emulsifier suspension. This closed system, first, vacuumed to remove the air from the system. After that perfluorocarbon gas was released to the system containing vial filled with lipid/emulsifier suspension.

3.3. Physical Characterization

Concentration and size distribution of microbubbles was determined using counting chamber (Thoma glass) with a binocular microscope attached to a digital camera (TUCSEN). Special software (NIH, ImageJ) for image data processing and determining the size of the microbubbles was used. Counts and determination of size distribution were performed through a 10X objective. The stability of microbubbles was tested at 38°C using a circulating bath to conduct the experiments rapidly and to

observe the behavior of the microbubble population at body temperature. The image analysis of each microbubble was performed every hour.

3.4. Confocal Microscopy Analysis

Confocal microscope was performed on Olympus IX71 with 40X objectives for all microbubble species. For all microbubble species, fluorescein DHPE (N - (Fluorescein - 5 - Thiocarbamoyl) - 1,2 – Dihexadecanoyl -sn- Glycero-3-phosphoethanolamine, Triethylammonium Salt) was added to DSPC:PEG40St mixture at mol fraction of 0.1 in order to demonstrate the shell morphology of microbubbles. Images were captured with Andor Revolution digital camera and processed with ImageJ. Microbubbles were imaged after being sandwiched between two glass cover slides. Then, slide was turned over in order to image microbubbles that were stuck to the bottom slide. Hence, artifacts in domain morphology created by contact with slide were avoided.

3.5. Temperature Studies

The temperature experiments were conducted at 4°C, 10°C, 20°C, 30°C, 38°C and 48°C using a circulating bath. For this study, microbubbles prepared with DSPC and PEG40St at molar ratios of 9:1 was used. Image analysis of the microbubbles for temperature experiments at 48°C and 38°C was performed every 10 minutes, for temperature experiments at 4°C, 10°C and 20°C was performed every hour. Series of photos were taken at different times, until almost all of the microbubbles were disappeared.

3.6. Sub-phase Studies

Microbubble solutions were prepared with DSPC and PEG40S at molar ratio of 8:2. Every solution was hydrated with PBS and PG mixture at volume ratio of 4:1 at 55˚C (phase transition temperature of DSPC). Storage solutions used were PBS, sucrose solution at different concentrations (0.3M, 0.6M, 1M, 1.2M and 1.5M) and PBS:PG

mixture at different volume ratios (4:1, 4:2, 4:3, 4:4). Each experiments were conducted at 38°C using a circulation bath. To determine the behavior and the life time of bubbles by time, several photos were taken with a special camera attached a optic microscope and analyzed with a special software (ImageJ). Each photo was taken every 1 hour.

3.7. Targeted Microbubbles

3.7.1. Streptavidin Quantification

Biotinylated lipid-coated, air filled microbubbles were prepared with DSPC:PEG40St:DSPE-PEG2000 at molar ratios of 5:4.2:0.8 and 9:0.2:0.8 and DSPC:PEG40St:DSPE-PEG2000:DSPG at a molar ratio of 2:4.2:0.8:3. These biotin carrying microbubbles then diluted to 10^6 per mL with PBS. After that these diluted biotin carrying microbubbles were incubated with various percentage of phycoerythrin (PE) labeled streptavidin (0%, 10%, 25%, 50%, 75%, 100% and 200% corresponding to 0μg/mL, 1 μg/mL, 2.5 μg/mL, 5 μg/mL, 7.5 μg/mL, 10 μg/mL and 20 μg/mL, respectively) (streptavidin-PE) for 30 min. To avoid unbound streptavidin-PE microbubble suspensions were washed twice with PBS. Samples of these microbubbles were analyzed for fluorescence with 10,000 events per sample by using flow cytometry (Facscanto, BD).

3.7.2. Preparation and Characterization of Targeted Microbubbles

Biotin carrying microbubbles described above were conjugated with Epidermal Growth Factor (Invitrogen, EGF, ligand) using a streptavidin-biotin bridge. Briefly, after production of biotinylated microbubbles, they were diluted to 10^6/mL and incubated with streptavidin for 30min. After washing with PBS twice, they were incubated with biotinylated EGF and washed again with PBS twice. Targeted microbubbles were thus prepared with biotinylated EGF coupled to the phospholipids located in the microbubble shell through a biotin–streptavidin bridge (Figure 3.1).
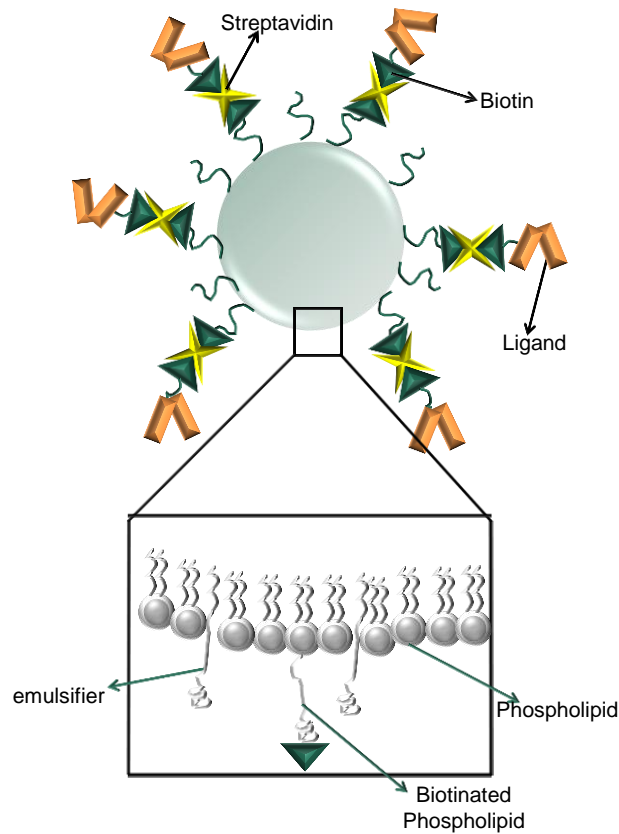
Figure 3.1. Schematic illustration of targeted microbubbles via streptavidin-biotin bridge.

A rectangular parallel plate flow chamber comprising a transparent polydimethylsiloxane (PDMS) block and a standard microscope slide was used to examine adhesion of microbubbles to cultured MDA-MB-231 (breast cancer cell line). The inlet port was connected to a syringe pump (Figure 3.2). A syringe was filled with imaging buffer (HEPES buffer) and put into the syringe pump. MDA-MB-231 first cultured in microscope slide and adapted to the PDMS block. Microbubbles 2×10^6 ml^{-1} were infused through the flow chamber at various shear rates (76 s^{-1}, 152 s^{-1} and 229 s^{-1}) for 3 min. Then adhered microbubbles to cells were incubated for 3 min. After that imaging buffer was drawn through the flow chamber at same shear rates for additional 3 min and their adhesion to the target surface was evaluated. Control experiments were performed with microbubbles with no EGF and with BSA instead of EGF. Analysis of adhered microbubbles to cells was performed under a light microscope through a 10X objective. Several photos were taken after washing step and bubble number per cell was quantified using Image*J* program.
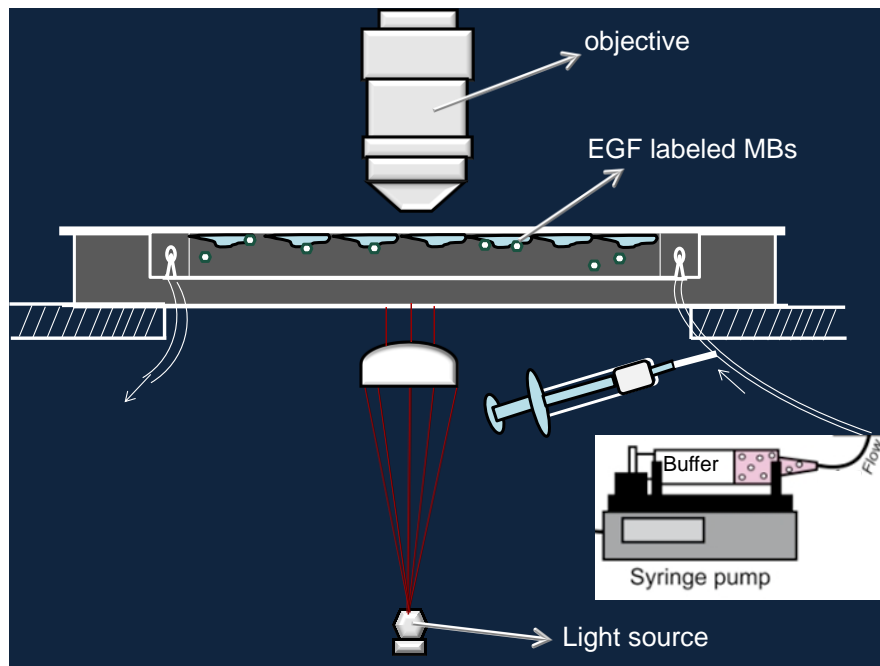
Figure 3.2. Experimental setup up used to examine adhesion of microbubbles to cultured MDA-MB-231 (breast cancer cell line).

CHAPTER 4

RESULTS AND DISCUSSION

4.1. Effect of Temperature on Microbubble Stability

In this section, the effect of temperature on microbubble stability was investigated. For this experiment, microbubbles were produced with the mixture of DSPC and PEG40St at molar ratio of 9:1 and their temperature responds were tested at the temperatures of 4°C, 10°C, 20°C, 30°C, 38°C and 48°C. To understand the behavior of microbubble population, change in concentration and size distribution by time was examined at these temperatures. To mimic the conditions encountered during administration, microbubbles storage temperature was changed abruptly from 4°C to higher temperatures systematically and the changes in their behavior were observed. Change in concentration by time for microbubble prepared with DSPC and PEG40St at molar ratios of 9:1 is given in Figure 4.1. Each measured microbubble number was divided by the initial number of same bubble species to obtain the normalized number. At 4°C (storage condition) the number of microbubbles remained constant over days. This also indicates that reproducible results can be obtained with the optical microscopy. As the temperature of the microbubbles was increased, onset time (the time period at which the number of microbubbles stays constant) becomes shorter. Accordingly, d_{50} of microbubbles started to increase in the same order at the end of this time period (Figure 4.2). Both the decrease in number of microbubbles and increase in microbubble size were the most dramatic at 48°C. This dramatic change may be caused by the abrupt temperature change since microbubbles stored at 4°C was immediately put in a circulating bath at 48°C.
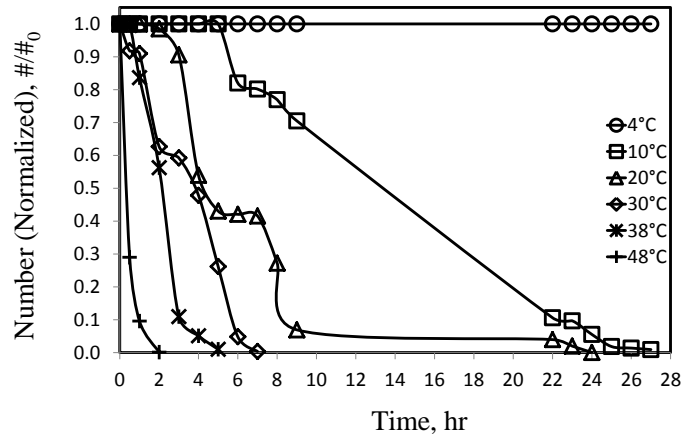
Figure 4.1. Change in number (normalized) of microbubbles prepared with the mixture of DSPC and $PEG_{40}St$ at a molar ratio of 9:1 by time at various temperatures.
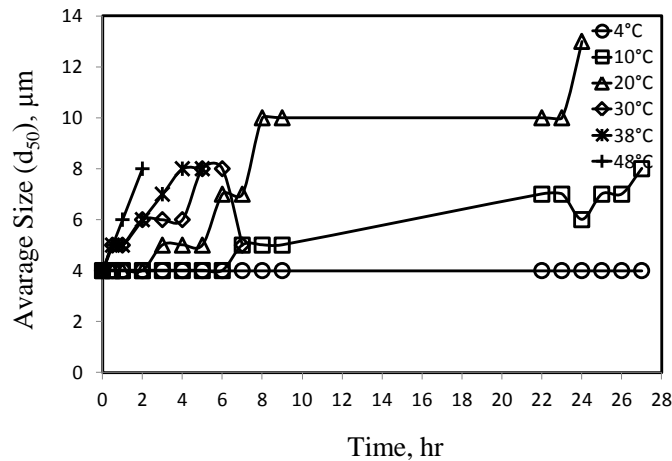
Figure 4.2. Change in diameter of microbubbles by time at various temperatures for mixtures of DSPC/PEG40St at molar ratios of 9:1.

Current believe is that for a microbubble to be stable, lipid monolayer should form a fully condensed coating around the gas bubble with negligible surface tension and gas permeability (Borden and Longo 2002; Pu, Longo et al. 2005). As seen in Figure 4.1 and Figure 4.2, microbubbles can maintain both their number and size under 20°C for 2 hours. But, at higher temperatures, especially at 38°C (close to body temperature), number of microbubbles maintained constant for less than 30 minutes. It is known that monolayer around the gas core, provides the resistance to gas exchange from and/or to the aqueous environment, stabilizing the microbubbles. Borden et al. showed that resistance of microbubble shell to gas dissolution increased with the increase of chain length of the phospholipids (Borden and Longo 2002). Previous

studies also showed that hydrocarbon thickness for lipids decreases and the area per lipid increases with increasing temperature (Figure 4.3) (Petrache, Dodd et al. 2000).
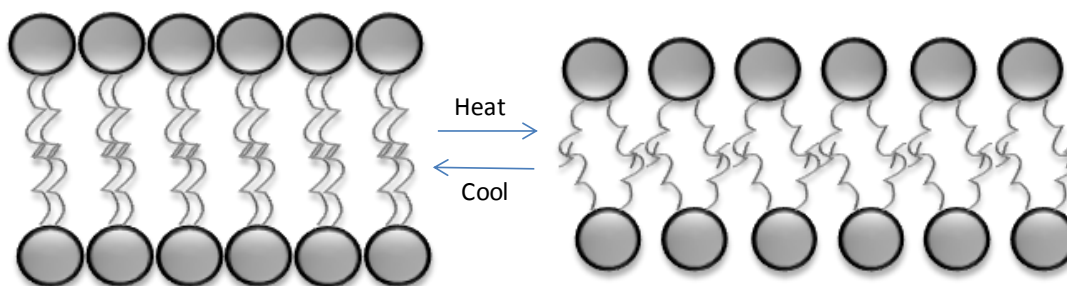
Figure 4.3. Schematic illustration of the change in thickness and distance between phospholipids.

We surmise that the observed changes in the size and counts of microbubble over time with increasing temperature are resulting from the disorder in the monolayer structure of the microbubbles, suggesting that hydrocarbon layer has reduced length and lipid per area increases due to the thermal effect thus causing increase in the surface tension and change in size of the microbubbles. It is noteworthy to mention that, growth in microbubble size was initially not very substantial especially below $20^{o}C$ for the first 2 hours. Therefore, it can be said that average microbubble size and counts were not substantially affected during onset time. It may be possible that during this equilibration period, reduced hydrocarbon thickness in the monolayer with increasing temperature may be compensated with the conformational changes in the form of ethylene oxide chain of PEG40 stearate. Upon this time period which depends on the temperature, we observed that the counts of microbubbles decreased, size of the microbubbles increased. However, the increase in size of the microbubbles was much larger than expansion of the gas core, assuming constant mass of gas bubble in ideal state and spherical in shape. When we consider the decrease in number of bubbles with increased average size together, we arrived the conclusion that microbubbles were fused together because lipid monolayer can no longer hold low surface tension and lipid molecules may reorder themselves to achieve a new thermodynamically stable shell structure. The current study shows that as a proof-of-concept, elevated temperatures can be used to investigate the behavior of microbubbles in a logical time interval and microbubble response changes accordingly with increasing temperature.

4.2. Development of a Method for Analysis of Microbubbles

The size and count evaluation of microbubbles require use of a very reliable and precise measurement techniques and should be modified since methods which are currently used to analyze have some limitations (methods used to analyze microbubble suspensions has been given in Chapter 2). Laser diffraction and electrical zone sensing is the most preferred techniques to measure the size and number of microbubbles because it has broad measuring range, it is independent of buoyancy effects and it has stirring option. However, these techniques measure all of the particles besides microbubbles such as micelles, liposomes and the other dust particles. Another technique used for analysis is the Light blockage is another technique for analysis of microbubbles. However, measurements of Light blockage are limited in the nanometer range. Dynamic light scattering (DLS), also called photon correlation spectroscopy (PCS), is a less frequently used method to analyze microbubbles since measurements are typically on the upper end of the DLS size range.

In this study, we employed optical microscopy to measure the size and concentrations of microbubbles. To verify the reproducibility and reliability of size and count measurements, we conducted a series of experiments in which different volumes of microbubble suspension was placed on a counting chamber. Images obtained using a 4X objective for each volume of microbubble suspension are shown in Figure 4.4. When 2μL and 5μL of microbubble suspension was put on the counting chamber, microbubbles accumulated in the middle region. For 20μL, 50μL and 100μL of microbubble suspension, microbubbles accumulated in the corners and distribution was not homogenous. When we put 10 μL of sample, we obtained the most homogenous image.
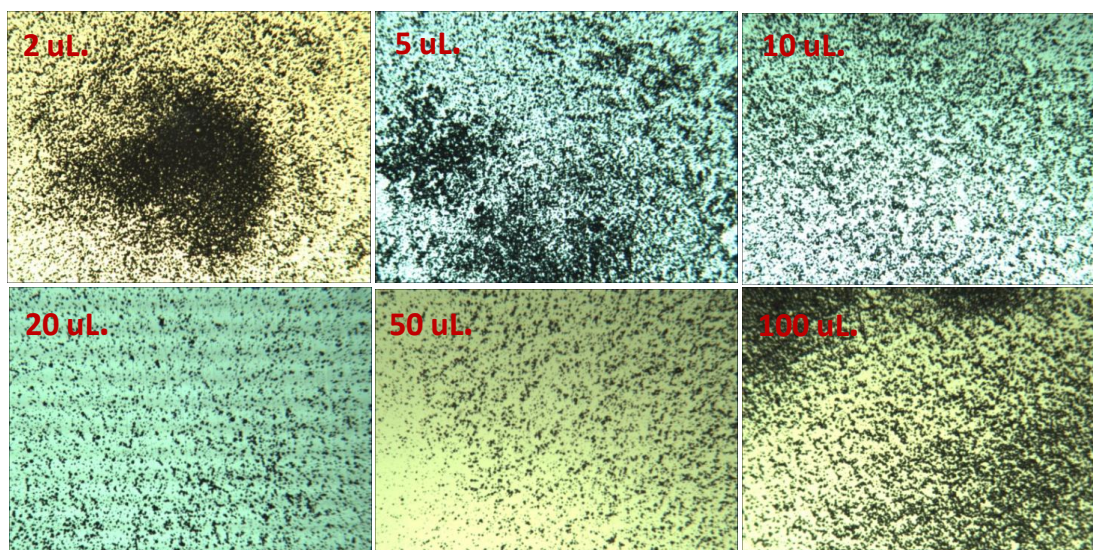
Figure 4.4. Microscope images of various volume of microbubble suspensions taken through 4X objective.

Size distributions of microbubbles for different volumes of the suspension are given in Figure 4.5. In Figure 4.5, size distributions taken from 5 different regions of microbubbles (Images are not shown) were compared. As seen, very accurate and reproducible counts were obtained again with 10μL of sample spreaded on the counting chamber.
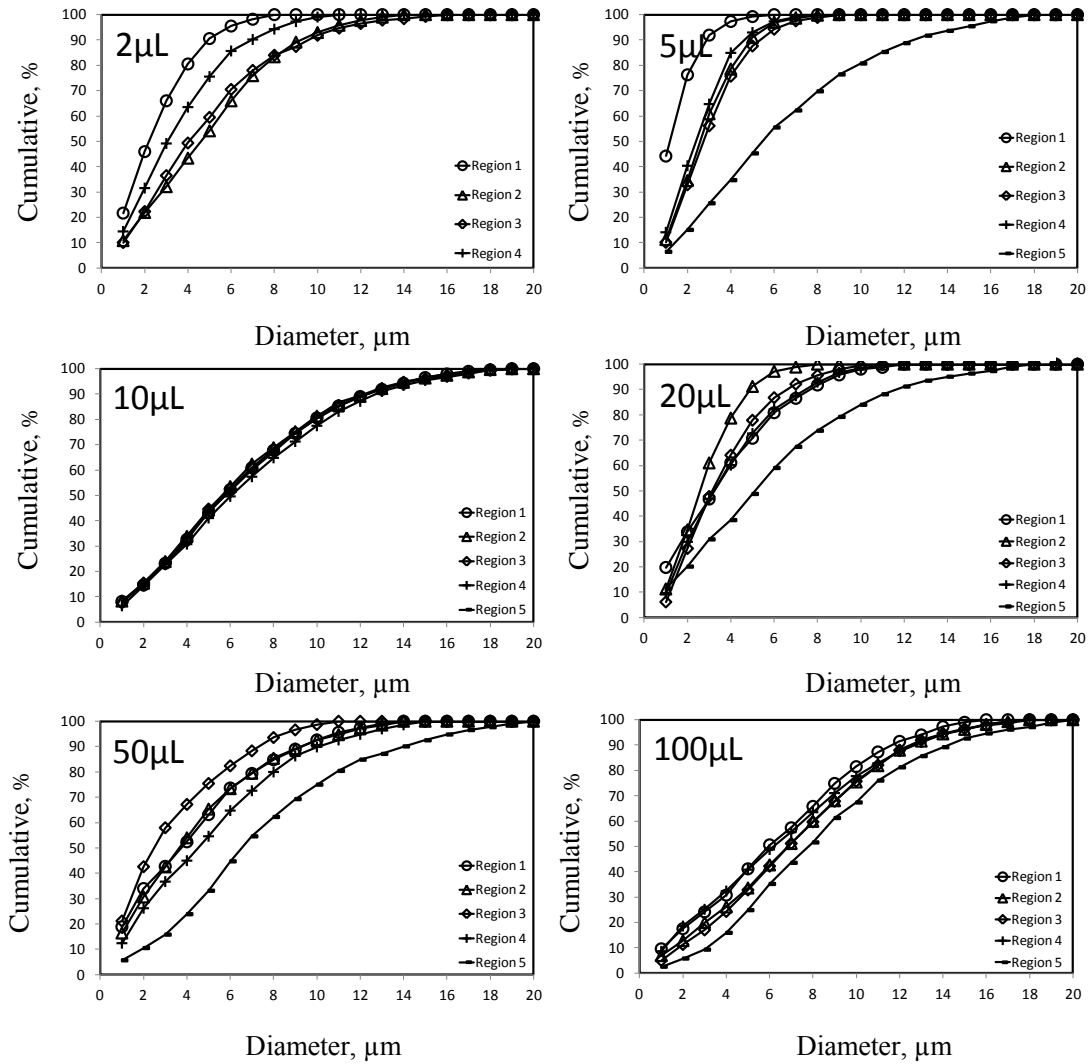
Figure 4.5. Size distributions of microbubbles from different regions for each volume.

Furthermore, number of microbubbles for each volume was also investigated using imageJ. Number of the microbubbles was measured at 5 different regions of the counting chamber. From the comparison of microbubble number in different regions obtained for different volumes of spreaded solution, it can be said that reproducible and reliable size and counts measurements can be obtained when 10µL of sample spread on the counting chamber (Figure 4.6).
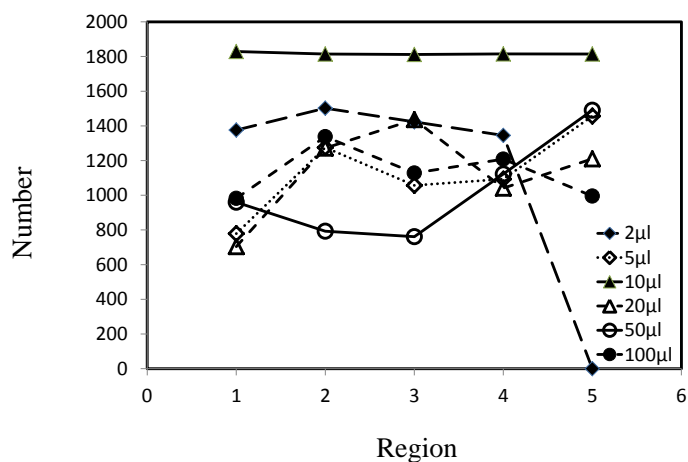
Figure 4.6. Number of microbubbles from different regions for each volume.

For 2µL and 5µL of microbubble suspension, suspension did not fill the gap between the cover slip and Thoma glass, as a result of this, aggregation occurred. For 20µL, 50µL and 100µL of microbubble suspension, suspension overflowed from the counting chamber. Therefore, accumulation of the microbubbles occurred at the corners of the counting chamber. In the rest of our study, we selected to work 10µL volume of suspension.

In the current literature, Electrical zone sensing (Coulter Counter) is often used to obtain size and number of microbubbles. Moreover, it has been reported that image analysis is not a trustable method (Coester, Tinkov et al. 2009). However, electrical zone sensing does not show the particles which are analyzed. Hence, liposomes of some dust particles in the suspension might be analyzed with this system. Furthermore, only limited volume of the sample can analyzed with Coulter Counter as in image analysis. Though, we showed repeatable result by using image analysis with this study.

4.3. Effect of Emulsifier on Microbubble Stability

4.3.1. Effect of Mol Fraction of PEG40St on Microbubble Stability

Current formulation of lipid based microbubbles consist of mostly with 1,2-Distearoyl-*sn*-glycero-3-phosphocholine (DSPC) and PEG40St at a molar ratio of 9:1 (Borden and Longo 2002; Talu, Lozano et al. 2006; Sirsi, Feshitan et al. 2010; Swanson, Mohan et al. 2010). Best to our knowledge, there is only one study about microbubble production by using different percentages of $PEG_{40}St$, but in that study Span60 as a surfactant was used instead of phospholipids (Xing, Ke et al. 2010); Herein, we investigate effect of PEG40St amount on air-filled, lipid-coated microbubble stability. For this purpose, we prepared microbubbles with DSPC and PEG40St at various (9:1, 8:2, 7:3, 6:4, 5:5, 4:6, 3:7, 1:9 and 0:10) molar ratios. It is noteworthy to mention here that without DSPC, PEG40St alone (molar ratio of 0:10) did not produce microbubbles. In reporting of microbubble concentration only the microbubbles with diameter less than 10μm were counted. Figure 4.7 shows the change in yield obtained with different concentration of the emulsifier. As seen from the figure, yield increases with increasing emulsifier content up to 40%. But further increase in emulsifier content resulted in a decrease in the yield. Maximum yield was obtained with the formulation containing 40 % of PEG stearate, which is almost 4 times higher than the one obtained with the current microbubble formulation containing 10 % of PEG stearate. In medical practice, this means reduced cost of microbubbles since both the yield increases and the lipid content (most expensive component in the formulation) decreases. The comparison of microbubble sizes is given in Figure 4.8 indicating that the size of microbubbles reduced with increasing amount of PEG40St. Since PEG40St is a cone-shaped molecule due to the larger cross sectional areas of head group, they are more likely to form micelles in aqueous media (Jebrail, Schmidt et al. 2008) indicating that they can produce monolayer structures as microbubbles (Dickey and Faller 2008). Moreover, as reported in the literature, curvature on bubble increases (Hristova and Needham 1994; Kenworthy, Hristova et al. 1995; Jebrail, Schmidt et al. 2008). The high curvature on the microbubble means small bubbles. This result had importance since the size of the microbubbles is crucial for clinical applications. To cross pulmonary capillaries, size of

microbubbles should be smaller than 8 μm in diameter (Riess, Schutt et al. 2003). Hence, it is important to observe high yield of small bubbles.

The change in the concentration of microbubbles at 38°C with time is shown in Figure 4.9. Results were reported as normalized numbers. In other words, microbubbles number counted at each time was normalized with the number counted at the initial time for that particular formulation. As seen from the figure, microbubbles retained their concentration constant for some time depending on their formulation (different molar ratio of DSPC-PEG40St). We named that time duration as onset time. At the end of the onset time, microbubble concentration decreased continuously with time. Moreover, change in size distribution of microbubbles species were also examined with time. As seen in Figure 4.12, while microbubble population prepared with the mixture of DSPC and PEG40St at a molar ratio of 9:1 was converted to large bubbles within minutes indicating that this microbubble species might cause embolism problems, microbubbles involving 50mol% of PEG40St preserved their sizes for hours. Further increase in the PEG content (PEG40St amount more that 50%) was decreased the size stability of microbubbles (Figure 4.13, Figure 4.14, Figure 4.15) Onset times for different microbubble formulations are compared in Figure 4.10-A. As seen, onset time increases with increasing emulsifier concentration up to 50% and remain the same in 60 %. However, the further increase in the PEG content yielded microbubbles with less onset time. This situation is described in Figure 4.11. As known, PEG40St is an amphiphilic molecule consisting of both hydrophobic and hydrophilic parts. Apart from phospholipids, hydrophilic parts of these molecules are longer than phospholipids'. Hence, when high amounts of PEG40St are used in microbubble shell, they go towards to the liquid phase and squeeze out from the shell structure and shell becomes unordered. This unordered shell structure causes gas escape from the microbubble and cause instability. As opposed to the previous literature stating PEG40St squeeze out at high packing densities(Borden, Pu et al. 2004); we observed that microbubble formulation with 50% of PEG yielded more stable microbubbles.

Figure 4.10-B shows half-life of microbubbles for mixture of DSPC:PEG40St at different molar ratios indicating that the half-life of the bubbles increased with increasing the PEG40St amount up to 50%. Though, further increase of PEG40St caused a sharp decrease in stability.

It is important to note at this point that during the time course of measurements, sampling of microbubbles was done from a single tube. In other words, the same tube

was removed for the bath and the microbubble solution was homogenized by up and down motion before each measurement. This means that the microbubbles were subjected to some shear, affecting microbubble stability. This effect can be clearly understood from the measurement taken after overnight waiting. As seen in Figure 4.9, during overnight (between 8th-23th hours) the change in microbubble concentration was much less than the other times.
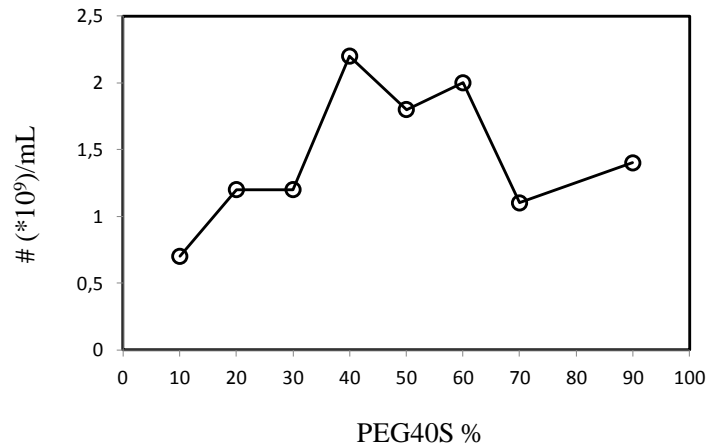
Figure 4.7. Microbubble concentration per mL for mixtures of DSPC/PEG40St at various molar ratios of PEG40S.
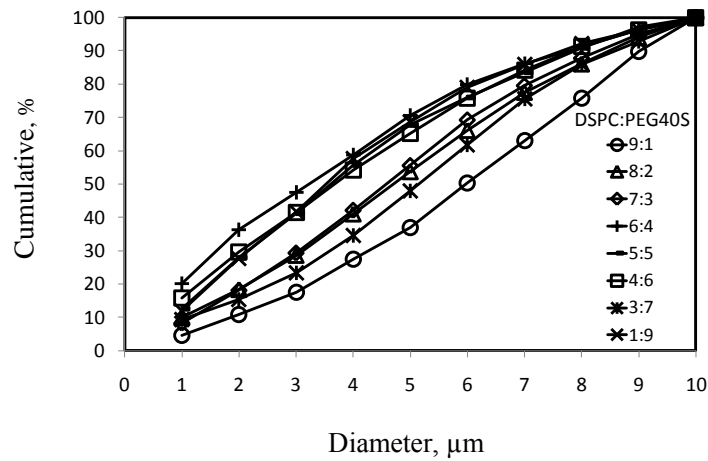
Figure 4.8. Size distributions of microbubbles for mixtures of DSPC/PEG40S at various molar ratios.
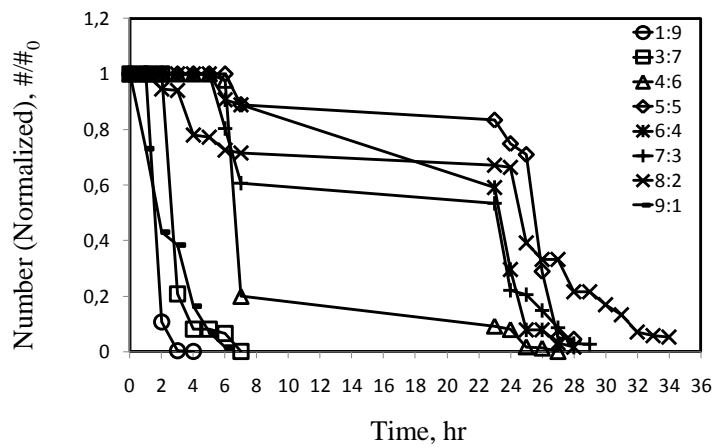
Figure 4.9. Change in concentration of microbubbles by time for mixtures of DSPC/PEG40St at various molar ratios of PEG40St at 38°C.
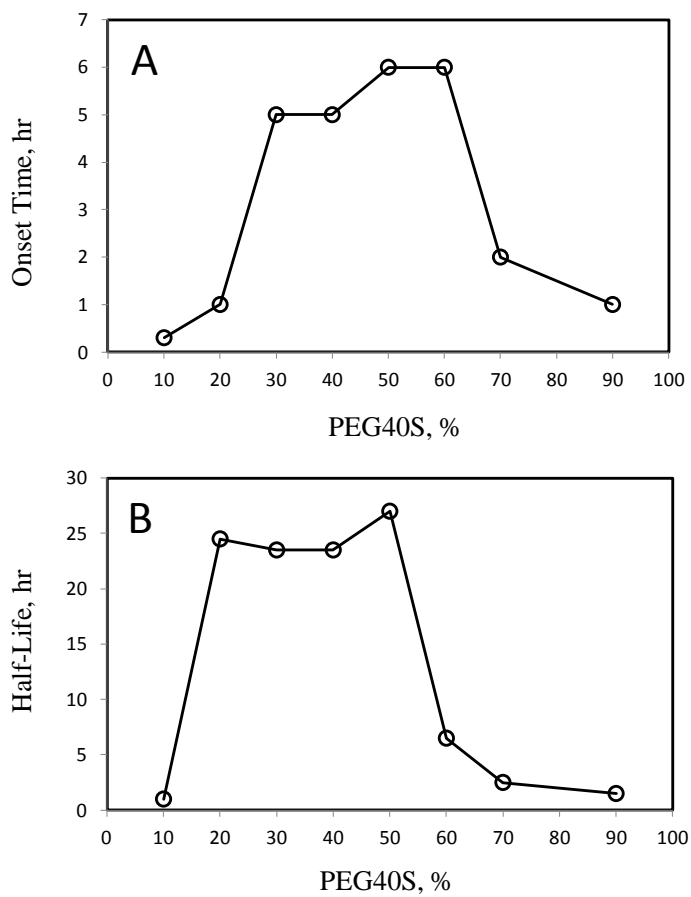
Figure 4.10. (A) Onset time and (B) half-life of microbubbles for mixtures of DSPC/PEG40St at various molar ratios of PEG40St at 38°C
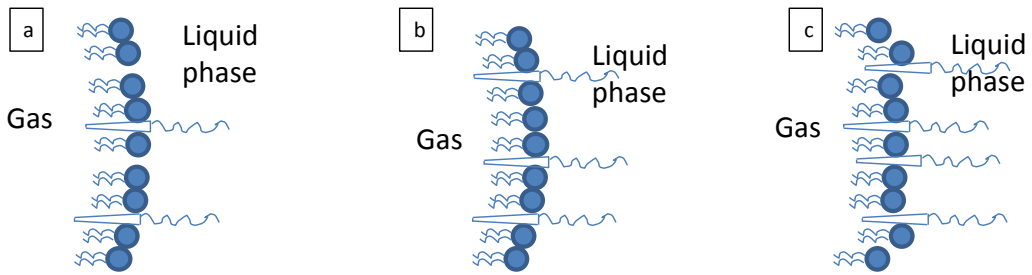
Figure 4.11. Schematic illustration of microbubble shell consisting of (a) low, (b) sufficient and (c) high amount of PEG40St
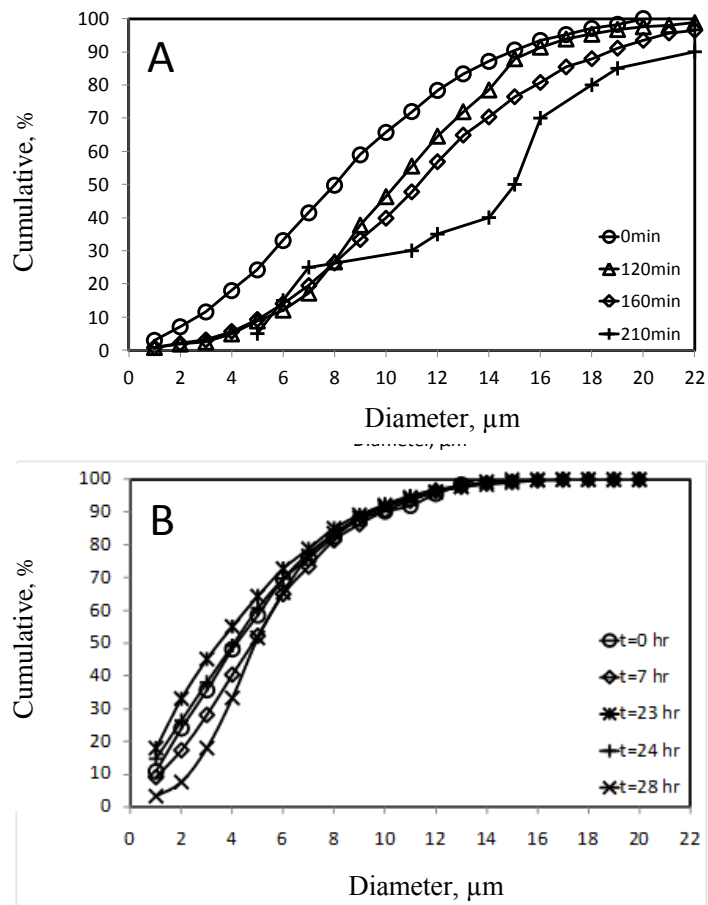
Figure 4.12. Microbubble size distribution for mixtures of DSPC/PEG40St at a molar ratios of (A) 9:1 and (B) 5:5.
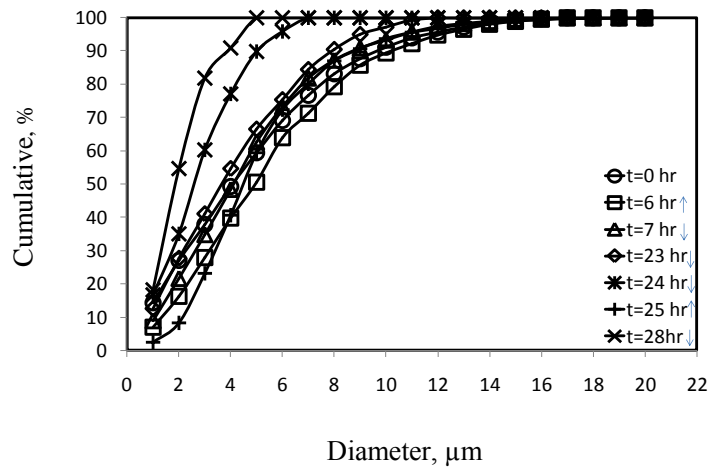
Figure 4.13. Size distribution for mixtures of DSPC/PEG40St at a molar ratio of 4:6.
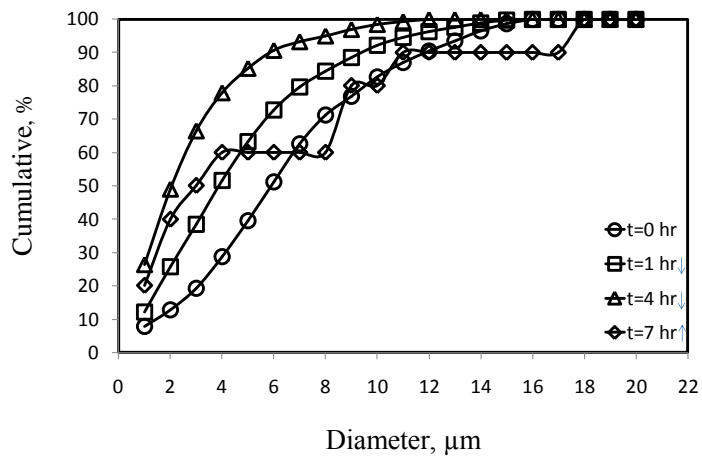
Figure 4.14. Size distribution for mixtures of DSPC/PEG40St at a molar ratio of 3:7.
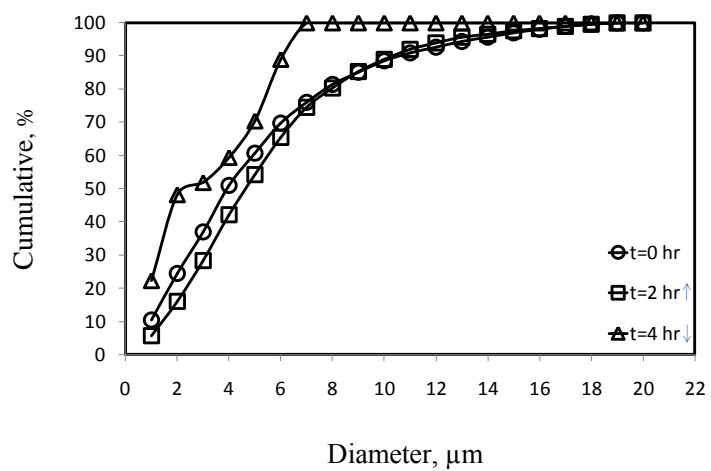
Figure 4.15. Size distribution for mixtures of DSPC/PEG40St at a molar ratio of 1:9.

As expected from sonication-based synthesis process, size of the microbubbles yielded by all formulation of microbubbles was polydisperse. Figure 4.10 and Figure 4.12-A indicated that 50mol% $PEG_{40}St$ results in formation of more stable microbubbles because, as *Xing et al.* reported, while this PEG molecule forming as an energy barrier around the shell prevents the coalescence among microbubbles, and thus it inhibits the repulsive forces between the phospholipid molecules (Xing, Ke et al. 2010). But as the percentage of $PEG_{40}S$ was increased from 50% to 70%, decrease in concentration of microbubbles became faster. As we examine the image of microbubbles prepared with DSPC:$PEG_{40}St$ at a molar ratio of 9:1 used commonly in current literature, we observed that the agglomeration ratio of microbubbles was very high (Figure 4.16). compared to 5:5 microbubbles, this result may be attributed to low amount of $PEG_{40}St$ (in the microbubbles composed of 9 to 1 molar ratio of DSPC and PEG40St).
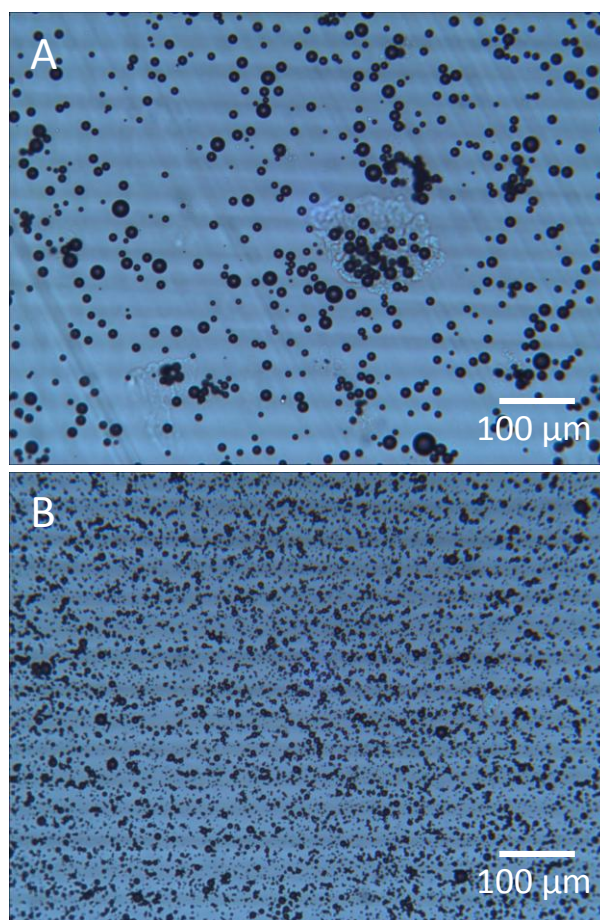
Figure 4.16. Image of microbubbles prepared with DSPC:$PEG_{40}St$ at a molar ratio of (A) 9:1 and (B) 5:5.

Effect of $PEG_{40}St$ concentration on phase behavior of monolayer was investigated by *Borden et al*. using Langmuir-Blodgett technique and at 5mol% $PEG_{40}St$ squeeze-out plateau was observed and the length of the plateau increased with rising PEG concentration. All squeeze-out plateaus were observed at around surface pressures of 35mN/m (Borden, Pu et al. 2004). According to *Borden et al.* (Borden, Pu et al. 2004) surface pressure higher than 35mN/m cannot be attained with lipid-PEG40St mix. When we used mixture of $DSPC/PEG_{40}S$ at 50% molar fraction of $PEG_{40}St$ in the bubble shell we observed that change in diameter and concentration of these microbubbles was lower than the other mixtures (Figure 4.9 and Figure 4.12-B).

It is important to note here that, the mixture of $DSPC/PEG_{40}St$ at 10 % molar fraction of $PEG_{40}S$ showed almost same stability (in terms of change in number by time) with 90% of PEG40S (Figure 4.9), however change in diameter by time was not the same (Figure 4.12 and Figure 4.15). While change in diameter for the mixture of $DSPC/PEG_{40}St$ at 90% molar fraction of $PEG_{40}S$ was not observed for 4 hours, at the end of the 4th hour bubble size decreased (Figure 4.15); however, for the mixture of $DSPC/PEG_{40}S$ at 10% molar fraction of $PEG_{40}St$ there was a growth in bubble size (Figure 4.12).

According to the previous observations in the literature, described previously, microbubbles lose their spherical geometry and smooth surface and appear to crumple (Figure 4.17) since gas inside the bubbles diffuse through the shell wall and dissolve into liquid phase (Wrenn, Mleczko et al. 2009). This behavior has been reported by Borden and Longo and called as 'zippering effect'. They observed that zippering process depends on phospholipid chain length and with decreasing chain length, continual bubble shrinkage without crumpling increase (Borden and Longo 2002). Figure 4.17 indicates that microbubbles prepared with the mixture of DSPC and PEG40St at a molar ratio of 5:5 started to lose their spherical geometry and appear to crumple after 24hr.

Figure 4.17. Microbubbles coated with DSPC and PEG40S at a molar ratio of 5:5. The arrow shows the microbubble appearing to crumple after 24hr.

To investigate the miscibility characteristics of DSPC and PEG-emulsifier, microbubbles labeled with FITC were monitored using Confocal microscope. Microbubbles coated with DSPC and PEG40St were smaller than 10µm in diameter and exhibited uniformly fluorescent shell (Figure 4.18). Dark domains represent phospholipids (DSPC) and bright patches represent emulsifier (PEG40St). As expected, with increasing molar fraction of PEG40S, area of bright patches also increased. Besides, PEG40St was fully immiscible with DSPC indicating that there was a phase separation between lipids and PEG-emulsifier. However, this phase separation was seen more clearly in microbubbles prepared with DSPC and PEG40S at molar ratios of 6:4 and 5:5. Surprisingly, for the mixture of DSPC and PEG40S at a molar ratio of 7:3 phases were well distributed on bubble shell. As *Borden et al.* reported, each microbubble had a unique compression state because of this, the fluorescence intensity varied from bubble to bubble (images not given) and this variation does not depend on the size of microbubbles (Borden, Pu et al. 2004). On the other hand, most of the microbubbles had a characteristic morphology for each microbubble species can be seen after observing many microbubbles on microscopic slide.
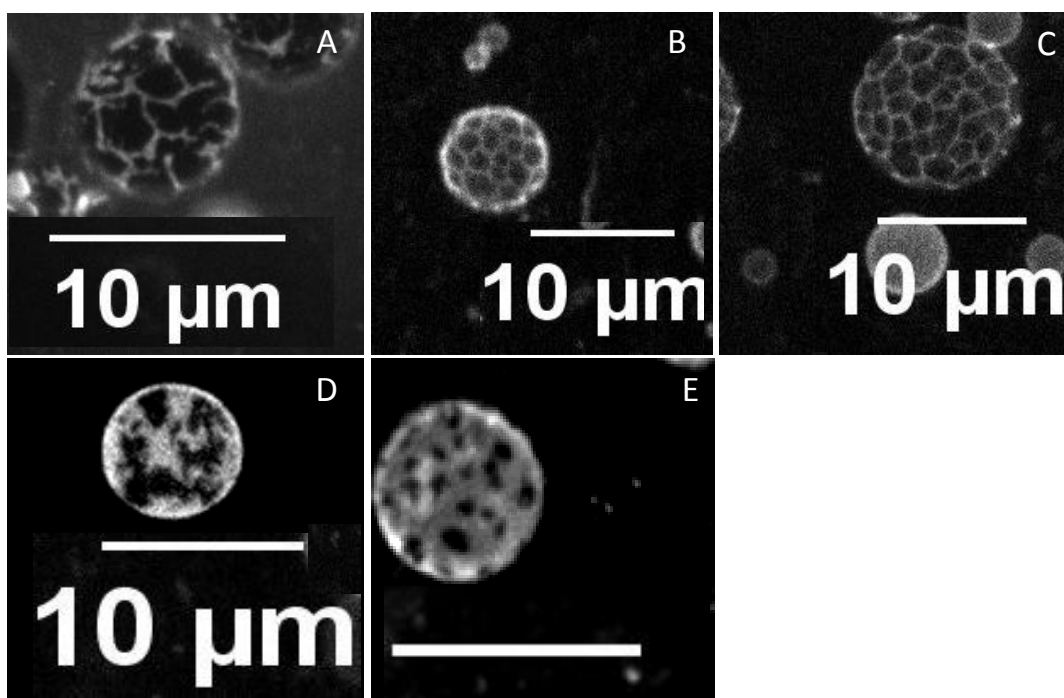
Figure 4.18. Fluorescent images of microbubbles taken with Confocal microscope. Shell contains DSPC:PEG40S:FITC at a molar ratio of (A) 8.9:1:0.1, (B) 7.9:1:0.1, (C) 6.9:1:0.1, (D) 5.9:1:0.1 and (E) 4.9:1:0.1

4.3.2. Effect of Emulsifier Chain Length on Microbubble Stability

As given in the introduction part of this thesis, it is known that phospholipids alone cannot produce microbubbles. Therefore, forming stable microbubbles is achieved by adding emulsifiers which is also an amphiphilic molecule like phospholipids. In chain packing of molecules as monolayer, molecular structure of emulsifier components is an important factor and associated with the stability at the air–water interface (Shen, Powell et al. 2008). Currently, PEG40St is used to produce stable microbubbles since PEG is known to be effective in prevention of platelet adhesion (Kim, Kim et al. 2000). In this section, we used different emulsifiers with different chain lengths (PEG8St and DSPE-PEG$_n$, n=350, 1000, 2000) and investigated their performance in production of stable microbubbles. DSPE-PEG$_n$ includes PEG molecule like PEG 40 Stearate which is currently used in production of microbubbles, however they are attached to a lipid (DSPE) and called as lipo-polymers. In this study, microbubbles were produced with DSPC and DSPE-PEG$_n$ at molar ratios of 9:1 and 5:5 and with DSPC and PEG8St. It is noteworthy to mention here that mixtures of DSPC and PEG8St, DSPC and DSPE-PEG$_{350}$ and DSPC and DSPE-PEG$_{1000}$ at a molar ratio of 9:1 did not produce

microbubbles. We obtained viscous suspension with the mixture of DSPC and PEG8St and with the mixture of DSPC and DSPE-PEG$_{350}$ (Figure 4.19). Stability of microbubbles coated with DSPC and DSPE-PEG$_n$ was compared with the microbubbles prepared with mixture of DSPC and PEG40St in   Figure 4.20. It is clearly seen that substitution of the PEGylated-emulsifier (PEG40St) by lipo-polymer decreased the microbubble stability (Figure 4.20) and produced larger bubbles (Figure 4.21). However, when we used all these emulsifiers at a mol fraction of 0.1, stability of microbubble species did not change (Figure 4.20). Furthermore, we did not observe any significant changes in stability of microbubbles with varying the mol fraction of emulsifier. Therefore, we can say that decrease in stability is related to using different type of emulsifier. As reported above since PEG molecules have larger cross sectional areas of head group and thus conical shapes, they are considered to cause formation of smaller microbubbles (Dickey and Faller 2008). In another words, due to their conical shapes, they result in microbubbles with high degree of curvature structure of microbubbles. Although DSPE-PEG$_n$ emulsifiers also include PEG molecules, due to their smaller cross sectional area of head group compared to hydrophobic tail of lipid (DSPC) they formed large bubbles compared to PEG40St. Since DSPE having two hydrocarbon chains in its tail, it interrupts conical shape of lipo-polymer emulsifier (DSPE-PEG$_n$) (Figure 4.22). Hence, DSPE-PEG$_n$ led to low curvature in microbubble shell including DSPC and this circumstance cause formation of larger bubbles.
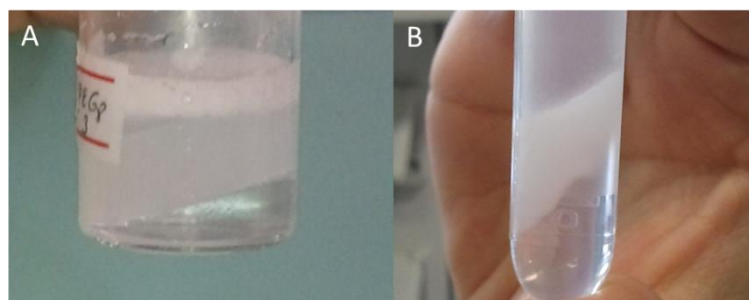
Figure 4.19. Microbubble suspensions prepared with (A) DSPC:PEG8St and (B) DSPC:DSPE-PEG$_{350}$.
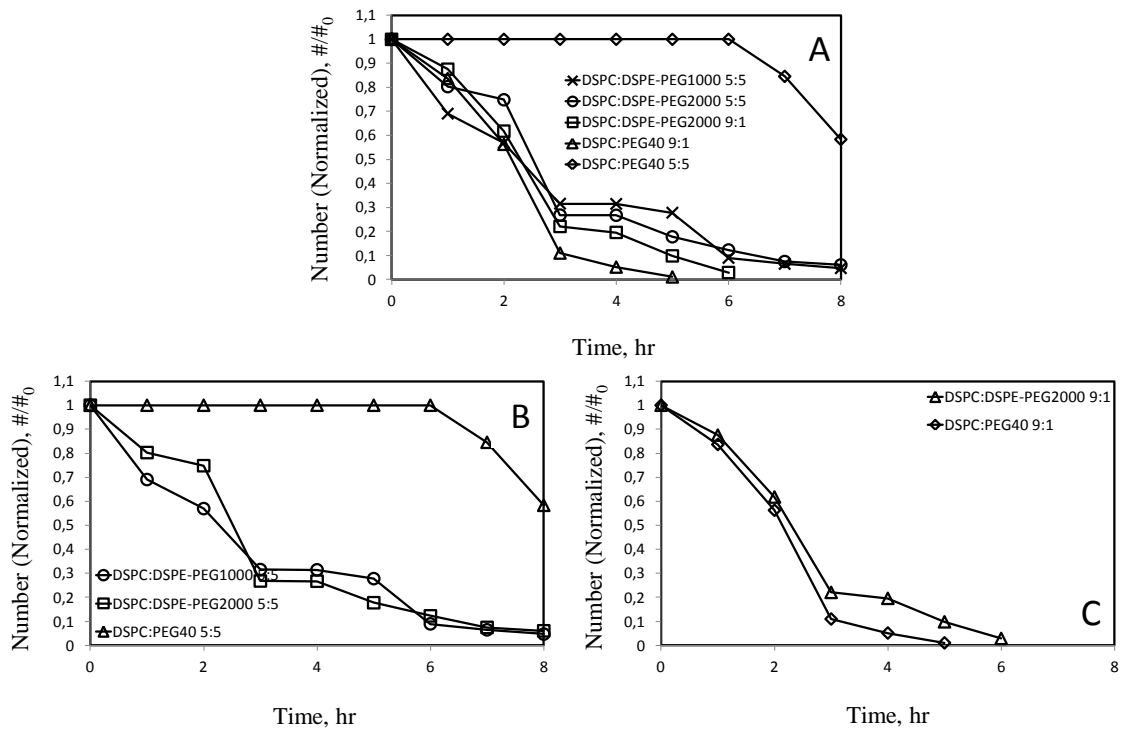
Figure 4.20. Change in concentration of microbubble species by time at 38°C
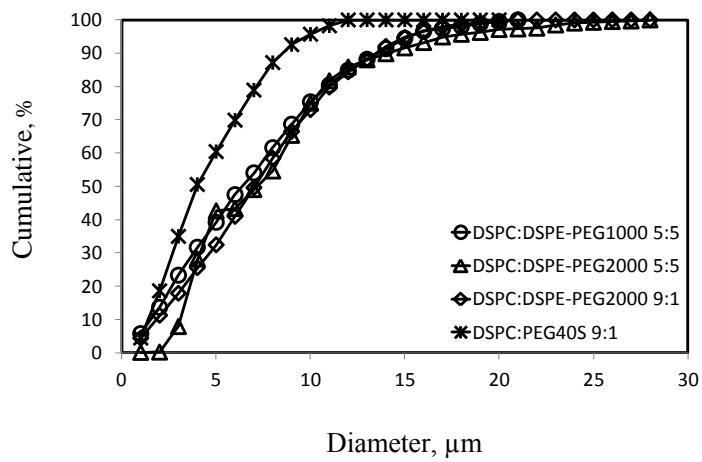
Figure 4.21. Size distribution of microbubble species
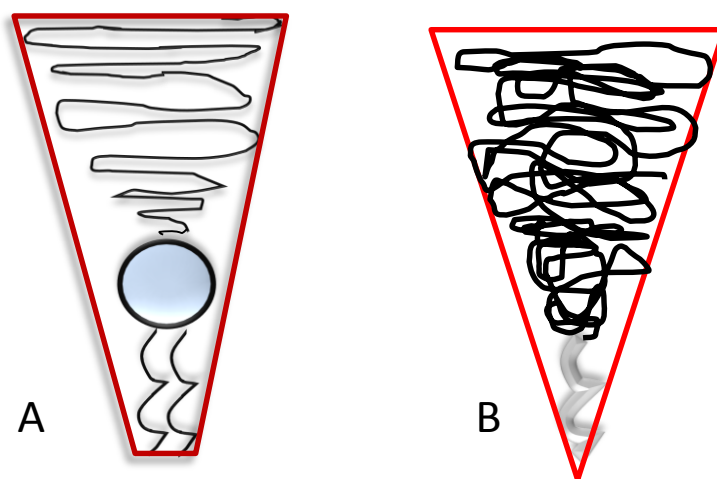
Figure 4.22. Schematic illustration of the structure of (A) DSPE-PEG2000 and (B) PEG40St.

Thus far, apart from PEG40St; monostearin/monopalmitin-rich food emulsifier (MYVATEX) and PEG-lipid (DSPE-PEG$_{2000}$) was used to produce microbubbles (Shen, Powell et al. 2008; Lozano and Longo 2009). *Lozano and Longo* produced DSPC coated microbubbles containing 10 mol% DSPE-PEG2000 and investigated dissolution behavior of a single microbubble having a diameter of 15µm. They observed that microbubbles coated with DSPC and DSPE-PEG$_{2000}$ at a molar ratio of 9:1 remained their stability approximately 4× longer in comparison to microbubbles containing PEG40St (Lozano and Longo 2009). In their report they did not investigate the stability of microbubble population, they only examined single microbubble (15 µm) dissolution behavior. In our study, we investigated stability of microbubble population over time at 38°C. Beside change in number and size, we also reported size distribution of these bubbles. As examining the stability of microbubbles coated with DSPC and DSPE-PEG2000 in terms of population, we observed that using lipo-polymer instead of PEG-emulsifier decreased microbubble concentration dramatically over time at body temperature indicating that if these microbubble species are used intravenously, ultrasound imaging will be ended in a few minutes. This unstable behavior of microbubble population is also similar to the other microbubble species that we discussed in this section. Since time required for ultrasound imaging is approximately 10min-40min (Williams, Hudson et al. 2011), this time is not sufficient for the detection of the diseases. As a result, our findings indicate that lipopolymers are not suitable emulsifiers for production of microbubbles used in medical applications.

4.4. Effect of Sub-phase on Microbubble Stability

Microbubbles are complex structures, where numerous factors play crucial role in the stability. There is gas exchange between gas core and surrounding medium, as well as favorable/unfavorable interactions between the shell components. In this section of the study, the effect of storage solution was studied on microbubble stability. To investigate effect of viscosity on microbubble stability, microbubbles prepared with DSPC and PEG40St at a molar ratio of 8:2 were stored in solution including propylene glycol at different concentration. Production of microbubbles resulted in a polydisperse suspension of approximately 10^9 particles mL^-1. Results are shown in Figure 4.23. As illustrated in the figure, the initial addition of propylene glycol enhanced microbubble stability. Further increase in propylene glycol amount in storage solution of microbubbles increased the onset time of microbubbles. But after that number of microbubbles decreased faster at higher concentration of propylene glycol. This situation caused lower half-life of microbubbles at higher concentration of propylene glycol. This dramatic decrease in the half-life of microbubbles might be due to the high viscosity causing burst of microbubbles. Sampling of microbubbles was performed from the same tube. Shear forces may be operative in burst for microbubbles at high viscosities.

Figure 4.23. Change in concentration of microbubbles by time for mixtures of DSPC/PEG40St at a molar ratio of 8:2 in mixture of PBS and PG at various volume ratios at 38°C.

Propylene glycol is more viscous than water. Due to its OH group, it has the ability of making hydrogen bonding with the molecules such as with oxygen of including free the phosphate group of phospholipids and water. In current literature, to enhance the stability of microbubbles, 10% glycerin, 10% propylene glycol and 80% water was used and it has been reported that these mixture improved the stability of microbubbles due to the viscosity of aqueous solution (Talu, Lozano et al. 2006). However, in our study, it was observed that the reason of the stability of microbubbles is not only the viscosity, but also hydrogen bonding between phospholipids located on the microbubble shell and the molecules in the mixture of storage solution. Because the microbubbles are gas-filled and therefore they float at the gas-water interphase, the hydrogen bonding between shell materials and propylene glycol might decrease the drainage rate. We surmise that the decrease in drainage rate around the microbubbles inhibited drying of microbubbles, and thus enhanced the microbubble stability.

Furthermore, we also investigated change in diameter of microbubbles stored in the mixture of PBS and PG at various volume ratios by time at 38C. Change of size of microbubbles is given in Figure 4.24. As shown in the figure, except microbubbles stored in the mixture of PBS and PG at a volume ratio of 4:4, all of the microbubble population showed a growth. At the same time, number of these microbubbles decreased. From these two figures we observed that initially, small bubbles might burst or large bubbles initially burst then other large bubbles grew by the effect of temperature over time. Microbubbles showing the least growth were the microbubbles stored in the mixture of PBS and PG at a volume ratio of 4:1. Therefore, both in terms of size and number we observed the maximum stability at a volume of 4:1.
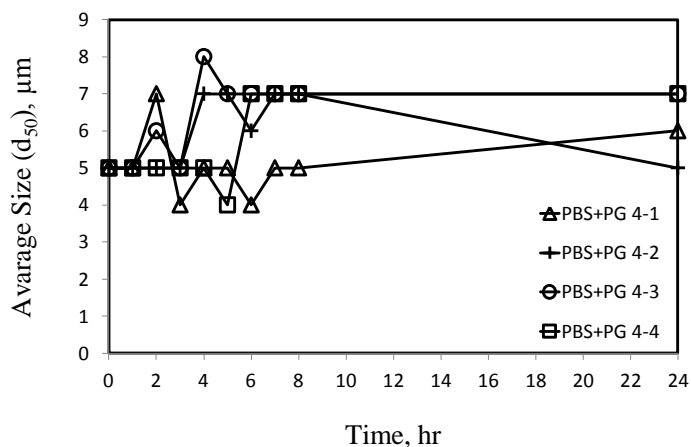
Figure 4.24. Change in diameter of microbubbles by time for mixtures of DSPC/PEG40St at a molar ratio of 8:2 in mixture of PBS and PG at various volume ratios at 38°C.

Craig et al. has reported that 0.3M of sucrose concentration inhibits the bubble (without shell) coalescence (Henry and Craig 2009). In our study, the effect of sucrose concentration in PBS on bubble stability was also investigated. Change in concentration is given in Figure 4.25. As illustrated in Figure 4.25, addition of 0.3M sucrose to PBS did not enhance the stability of microbubbles. First increase in sucrose concentration to 0.6M showed a low decrease in number of microbubbles dramatically indicating that it increased the microbubble stability. However, further increases in sucrose concentration decreased microbubble stability gradually. As for change in diameter of microbubbles over time, we can say that the most stable microbubble was the one stored in 0.6M of sucrose. To sum up, when sucrose concentration was increased from 0.6 M to higher molarities, life time of bubbles decreased. Hence, we can say that the optimum molarity of sucrose solution is 0.6M for storage of bubbles to stay stable for longer time.
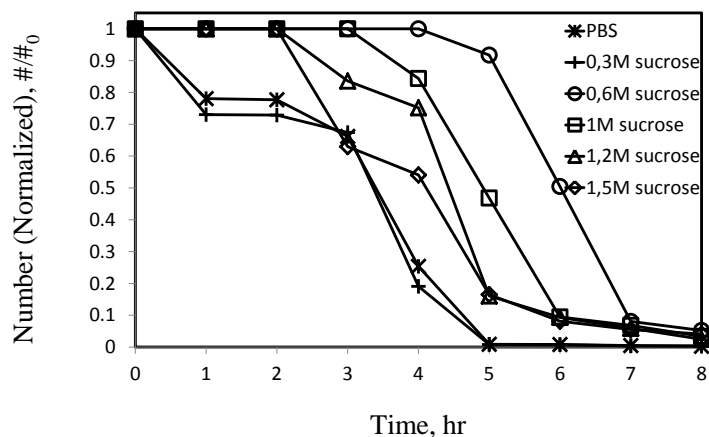
Figure 4.25. Change in concentration of microbubbles by time for mixtures of DSPC/PEG40St at a molar ratio of 8:2 in mixture of sucrose and PBS at various molar ratios at 38°C.

Finally, we compared the effect of different storage solutions on microbubble stability. The formulations of the mixtures were selected for their optimum molarities and volume ratios where we obtained the highest stability. For PBS and PG mixture and sucrose solution we selected 4:1 volume ratio and 0.6M, respectively. Comparison of these mixtures was given in Figure 4.26. As shown in the figure, we obtained the highest onset time by using 0.6M sucrose solution. But after that microbubbles stored in this solution disappeared within 1 hour. If we compare the half-life of the microbubbles, the highest stability was obtained with the mixture of PBS and PG at a volume ratio of 4:1. Without additives (only with PBS) we obtained the lowest microbubble stability.
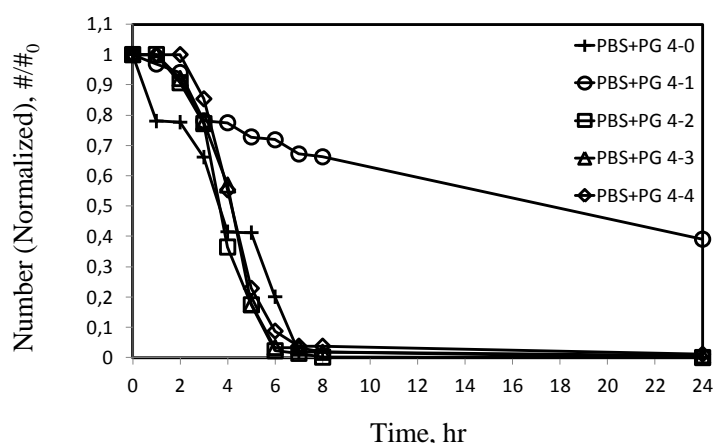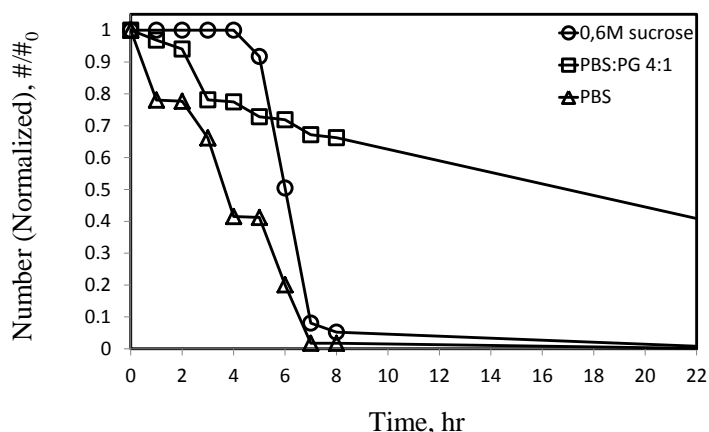

Figure 4.26. Change in concentration of microbubbles over time for mixtures of DSPC/PEG40St at a molar ratio of 8:2 in different mixtures at 38°C.

Bubble stability was performed in different storage solutions at 38°C and sampling was done from the same tube as before. We surmise that shear forces again were operative in decreasing the number of microbubbles. Our results showed that PBS and PG mixture is the most suitable solution for storage of bubbles to stay stable for longer time probably because the capability of propylene glycol to make hydrogen bonding of is high and it decrease the drainage rate between the microbubbles (Vaddi, Ho et al. 2002).

4.5. Effect of Components of Microbubble Shell on Stability

4.5.1. Effect of Hydrogen Bonding on Microbubble Stability

To investigate the effect of hydrogen bonding between the components on microbubble stability, three different phospholipids capable of hydrogen bonding (DSPG, DSPA, DSPE and Stearoyl-rac-glycerol) were added to the mixtures of DSPC and PEG40St.

Effect of DSPG on microbubble stability: Beside much studied phosphatidylcholines, phosphatidylglycerols are among the most common lipids in nature (Zhao, Róg et al. 2008). These phospholipids are mostly present in higher plants and they are one of the major components of bacterial membranes (Dowhan 1997). In eukaryotic cell membranes phosphatidylglycerol (PG) amount is low, but they are present in mitochondria and red blood cells. Studies shows that bacteria has capability to adjust their relative concentrations of PGs when exposed to toxic organic solvents (Weber and De Bont 1996; Isken and de Bont 1998). Thanks to some modifications in head-group composition, membrane permeability changes and therefore stability is provided (Zhao, Róg et al. 2008). For this purpose, PGs was used in microbubble shell to provide microbubble stability. Initially, we examined effect of emulsifier (PEG40S) amount on DSPG coated microbubble stability and use this information to optimize mol fraction of PEG40S in microbubble shell composed of DSPC, PEG40S and DSPG. For this purpose, we prepared microbubbles with DSPG and PEG40S at various (9:1, 8:2, 7:3, 6:4 and 5:5) molar ratios. Production of microbubbles using sonication of DSPG/PEG40St mixture resulted in a polydisperse suspension of approximately 10^9 particles mL^{-1}. To detect the physical stability of these microbubble species, change in

concentration and size distribution was examined at 38°C for each formulation. Effect of PEG40St on stability of DSPG coated microbubbles is given in Figure 4.27 indicating that onset time (the time that microbubbles remain stable in number) and half-life of microbubbles increase as percentage of PEG40St molecule increase. Same results have been found in our previous study for DSPC coated microbubbles. Therefore, molar fraction of PEG40St was kept constant at 50mole% for examination of effect of DSPG molecule on microbubble stability. Besides, it is noteworthy that microbubbles coated with DSPG contained smaller vesicles in contrast to current formulation of microbubbles (DSPC/PEG40St at a molar ratio of 9:1) (Figure 4.28). This is in contrast to the behavior of neutral phospholipids such as DSPC which was in good agreement with the current literature (Lentz, Alford et al. 1982). As shown in Figure 4.28, for DSPG, 97% of microbubbles were smaller than 10μm and it was 80% for DSPC. Therefore, it can be said that head group of phospholipid is an important factor determining size of microbubbles.
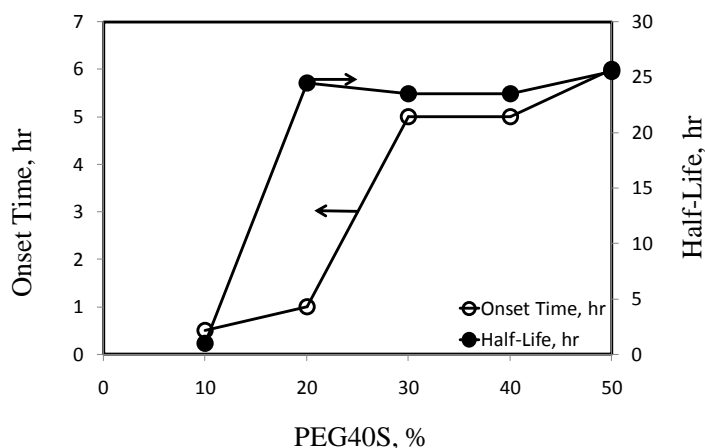
Figure 4.27. Onset time and half-life of microbubbles composed of DSPG/PEG40St at various molar ratios of PEG40St: 10%, 20%, 30%, 40% and 50%.
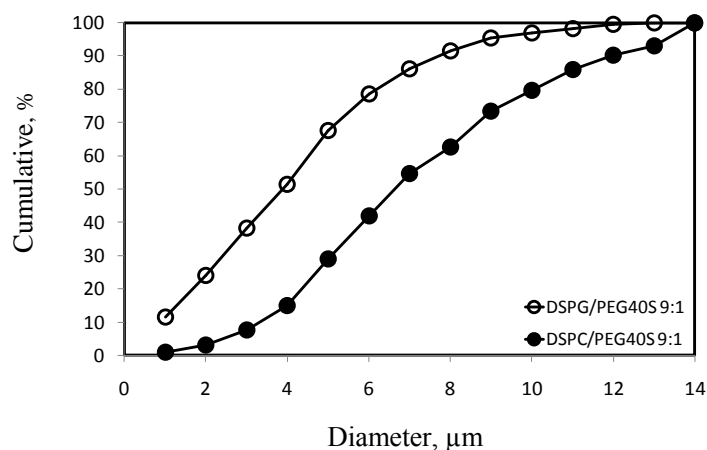
Figure 4.28. Size distribution of microbubbles containing different phospholipid (DSPC and DSPG) in the shell structure. Molar composition of the shell was kept constant at 9:1
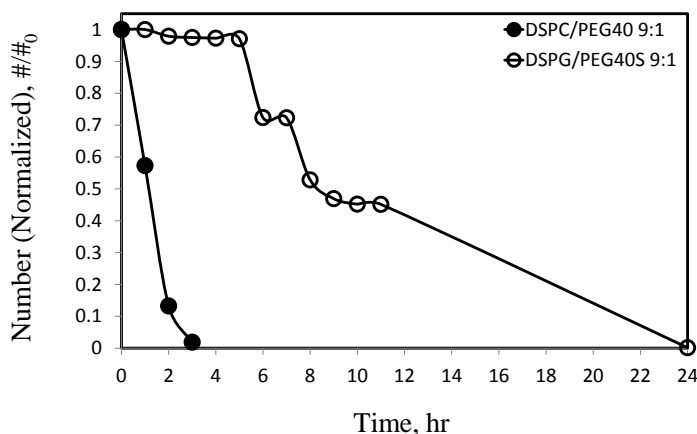
Figure 4.29. Change in number (normalized) of microbubbles by time at 38°C.

It was also observed that decrease in concentration of microbubbles coated with DSPG was less than with DSPC at 38°C. This result suggests that microbubbles with a longer lifetime can be prepared using DSPG. Figure 4.29 illustrates change in concentration of microbubbles coated with DSPC and DSPG over time at 38°C. Each measured microbubble number was divided by the initial number of same bubble species to obtain the normalized number. Both change in concentration and initial size distribution for DSPG coated microbubbles indicates that utilization of DSPG in microbubble production might be a good approach for medical applications.

Beside DSPC and PEG40S, 1,2-dioctadecanoyl-sn-glycero-3-phospho-(1'-rac-glycerol) (sodium salt) (DSPG) was used as an additional lipid in the microbubble formulation by changing the mol% of DSPG. Moreover, molar fraction of PEG40S was

kept constant at 50mole% as explained above. For this purpose, mixtures for microbubbles were prepared with DSPC, PEG40S and DSPG at molar ratios of 0:5:5, 1:5:4, 2:5:3, 3:5:4 and 4:5:1. Figure 4.30 shows onset times and half-life of microbubbles for mixtures of DSPC:PEG40St:DSPG at various molar ratios of DSPG. The highest onset time was observed at molar ratio of 2:5:3 at 38°C. Initial addition of the DSPG content in the mixture caused a decrease in stability. However, the increase of DSPG in the mixture (up to 30%) caused a sharp increase in lifetime of bubbles. Again, further increase of DSPG caused a sudden decrease in stability. As reported by Lentz et al., head group of DSPG repel each other. These fluctuations in onset times may be due to intermolecular interactions between DSPG molecules indicating that head group of DSPG repel each other and causes phase separation (Lentz, Alford et al. 1982).
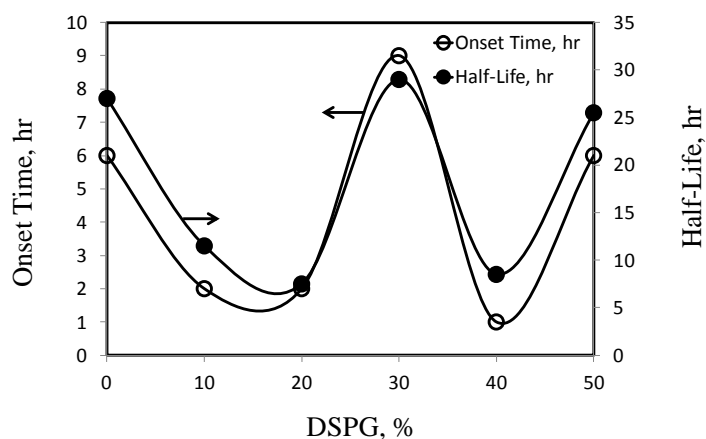
Figure 4.30. Onset time and half-life of microbubbles for mixtures of DSPC/ PEG40S/DSPG at various molar ratios of DSPG at 38°C. molar ratio of PEG40St was kept constant at 50mole%.

The comparison of microbubble sizes is given in Figure 4.31 showing that DSPG reduced diameter of DSPC-containing microbubble. For example, when for mixture of DSPC and PEG40St 80% of microbubbles were less than 8um; inclusion of 10mol% DSPG increased bubble (less than 8µm) amount to 90%. However further increase of DSPG (up to 40mol%) increased bubble size. Similar result was obtained by Lentz et al. for liposomes coated with PC and PG. They have reported that at higher PG content, liposomes were unstable and converted to large vesicles because mixture of components rich in DSPG do not mix randomly (Lentz, Alford et al. 1982).
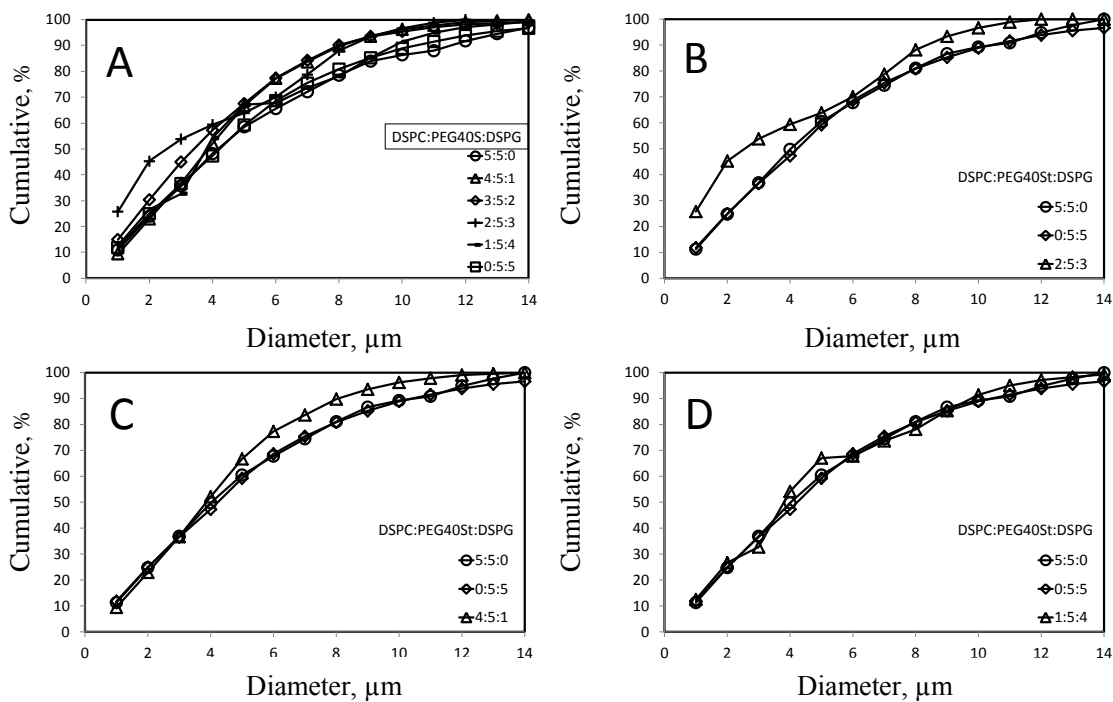
Figure 4.31. Size distributions of microbubbles for mixtures of DSPC/ PEG40S/ DSPG at various molar ratios.

Moreover, Figure 4.32 illustrates change in size distribution of microbubbles for mixtures of DSPC/PEG40St/DSPG at molar ratios of 9:1:0 and 2:5:3. Unlike the microbubbles prepared with DSPC and PEG40St at a molar ratio of 9:1, diameter of microbubbles prepared with our new formulation (DSPC/PEG40St/DSPG 2:5:3) did not increase by time at body temperature. For all clinical applications, this may be desirable to use microbubbles with this formulation to avoid embolism problems during administration of microbubbles intravenously.
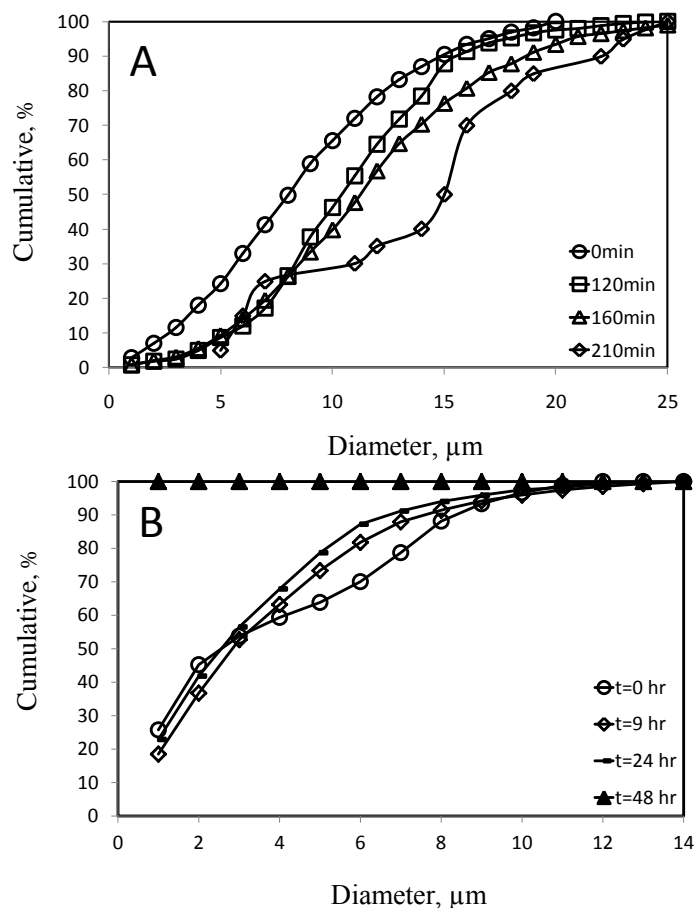
Figure 4.32. Change in microbubble size distribution for mixtures of DSPC/ PEG40S/DSPG at molar ratios of (A) 9:1:0 and (B) 2:5:3.

Medical applications for microbubbles require optimal circulation time and small diameter (1-8µm) at body temperature. In our previous study, we have reported that microbubbles prepared with DSPC and PEG40St at a molar ratio of 9:1 (current formulation in literature) were unstable at body temperature and found that with increasing PEG40St molecule up to 50mol%, we obtained stable and smaller microbubbles having 6hr onset time. In this study, keeping the PEG40St at 50mol% constant, we added DSPG molecule to the microbubble shell formulation to produce microbubbles. We found that when DSPG was increased up to 30mol%, the number of microbubbles remain constant for 9 hours at 38°C (Figure 4.29). It was also observed that DSPG molecule reduced size of microbubbles. Since DSPG forms hydrogen bonds effectively at each of oxygen acceptor groups between DSPC and themselves, this may be the factor in obtaining more stable and smaller microbubbles. Another reason of getting small sized microbubbles may be that larger head group of DSPG compared to DSPC possesses more conical shape causing microbubbles with high curvature (Jebrail,

Schmidt et al. 2008). Moreover, it is known that to provide the stability of foams (microbubble is a type of foam), the rate of drainage of the microbubbles should be decreased (Shah, Djabbarah et al. 1978; Koczo, Lobo et al. 1992; Askvik, Are Gundersen et al. 1999; Hédreul and Frens 2001). Therefore, we anticipate that OH groups in DSPG forms hydrogen bonds with sub-phase (PBS:Propylene glycol mixture) solution forming athin liquid layer around the microbubbles as a result of this, the drainage rate of aqueous solution between the microbubbles decreases resulting in more stable microbubbles.

Effect of DSPA on microbubble stability: It is known that the physical properties of PA based phospholipid influence membrane curvature. Moreover, PA may be involved in vesicle formation by promoting membrane curvature in living organisms (Kooijman, Chupin et al. 2005). For this purpose to we used DSPA as an additional component in microbubble production. In this study, microbubbles were produced by using DSPC, PEG40St and DSPA at various molar ratios (4:5:1, 3:5:2, 2:5:3, 1:5:4 and 0:5:5) to investigate the effect of DSPA amount on bubble stability at 38°C. Change in microbubble stability for each formulation by time at 38°C is illustrated in Figure 4.33. As shown in the figure, initial addition of the DSPA content in the mixture had no effect on life time of microbubbles. However, further increases of DSPA caused a sharp decrease in stability.
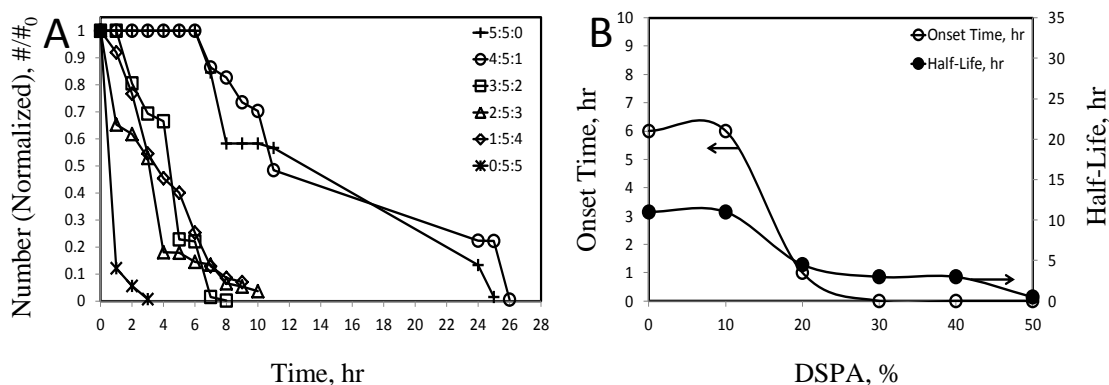
Figure 4.33. (A) Change in concentration and (B) onset time and half-life of microbubbles by time at 38°C for mixtures of DSPC/PEG40S/DSPA at various molar ratios.

Furthermore, microbubbles including DSPA contained large vesicles compared to the microbubbles prepared with DSPC and PEG40St at a molar ratio of 5:5. The comparison of the size distribution of these two microbubble population is given in

Figure 4.35. Without DSPA, most of the microbubbles had a diameter between 1 and 6μm. However, when DSPA molecule was added to the microbubble shell, size range of microbubbles shifted to the between 4 and 10μm. Since DSPA lipids have a small head group compared to the DSPC lipids, these lipids may aggregate to form Hexagonal II phase (type II lipids) (Figure 4.34) (Dickey and Faller 2008). This packing of the lipid head groups reduces their contact with the aqueous phase. Type II lipids also facilitate fusion however type I lipids inhibit this process (Polozov and Gawrisch 2004; Pu, Longo et al. 2005). On the other hand, to produce microbubble we need to create Hexagonal I phase which have polar head groups facing out, and the hydrophobic, hydrocarbon chains facing the interior. This conformation is similar to micelle structure. The only difference is that in microbubbles, the interior is filled with gas. Moreover, fusion must be avoided. The shape of a lipid is not only depends on its chemical structure but also depends on intermolecular interactions with neighboring lipids and other molecules. Therefore, addition of DSPA molecule in bubble shell reduced the possibility to get microbubbles with high curvature and formed large bubbles. Since capability of making hydrogen bonding of DSPA molecule is too low (Dickey and Faller 2008), increasing the DSPA content in microbubble shell did not result in the same effect observed with DSPG containing microbubbles.
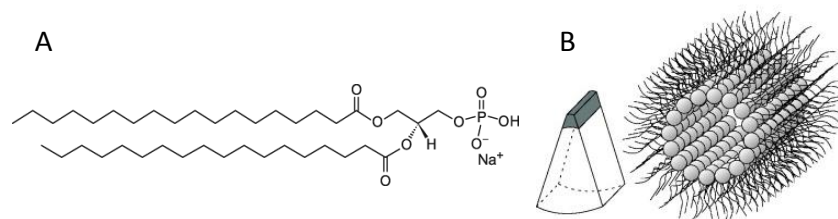
Figure 4.34. (A) Chemical structure and lipid packing of DSPA
(Source: Perutková, Daniel et al. 2009)
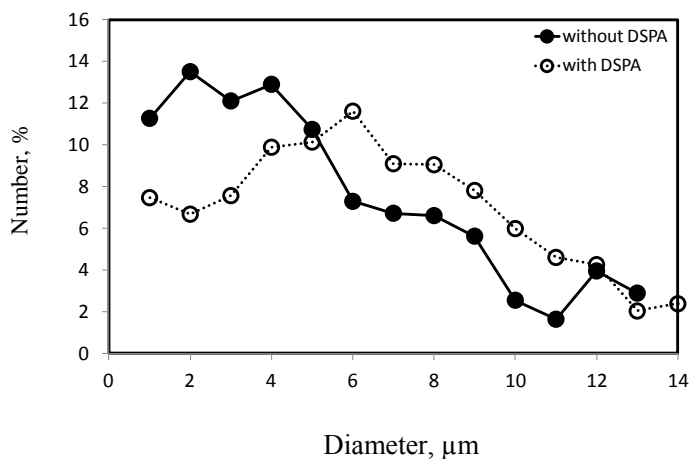
Figure 4.35. Size distribution of microbubbles with DSPA (DSPC:PEG40St:DSPA 4:5:1) and without DSPA (DSPC:PEG40St:DSPA 5:5:0)

Besides, change in diameter of microbubbles was also investigated at 38°C over time. This result is shown in Figure 4.36. As seen in the figure, for the microbubbles produced by using DSPC, PEG40St and DSPA at a molar ratio of 4:5:1, we can say that although number of microbubbles did not change within 6hr, average diameter of the bubbles decreased with time. This means that these microbubble species shrank with time. The reason of the shrinking was the diffusion of the gas in the core of microbubbles (Borden and Longo 2002). This dissolution behavior is the one of the reason of bubble destruction. Moreover, for the other formulations of the microbubbles including DSPA, the destruction of the microbubbles began from the large bubbles. Therefore, DSPA is not suitable for the microbubble production.
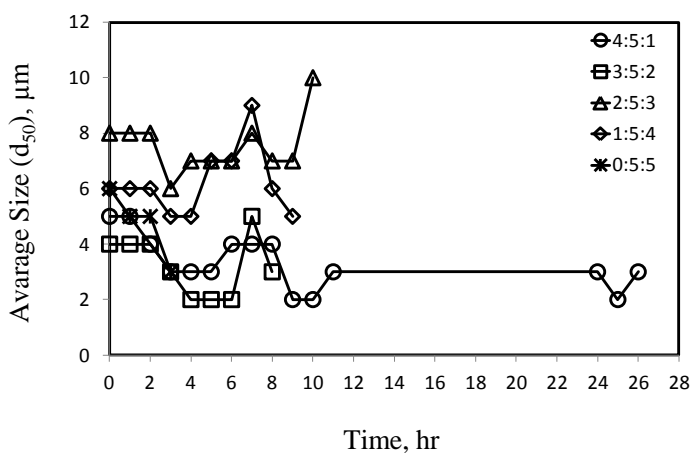
Figure 4.36. Change in diameter of microbubbles by time at 38°C for mixtures of DSPC/PEG40S/DSPA at various molar ratios.

Best to our knowledge, there is only one study about PC and PA coated phospholipids. *Hettiarachchi et al.* produced microbubbles by using DPPC, DPPA, DSPE-PEG$_{5000}$ at a molar ratio of 8.1:0.8:1 with microfluidic channels (Langner and Kubica 1999). They did not observe any change in the size of microbubbles from minutes to hours after generation. However, distance between exiting microbubbles decreased and coalesce of bubbles occurred because of the lower shell resistance in the expansion chamber. In that study, microbubbles were visualized at same frame and it was reported that they were size-stable microbubbles. In our study, we investigated stability of bubble population ($1.2*10^9$) at close to 38°C. Moreover, we used DSPC and DSPA as lipids and PEG40St as en emulsifier and found that bubbles were unstable.

Effect of DSPE on microbubble stability: Another additional component that we used was DSPE since it is known phosphatidylcholine (PC) and phosphatidylethanolamine (PE) together form the majority of the total phospholipids in most eukaryotic cell membranes (Silvius, Brown et al. 1986; Bagatolli and Gratton 2000). The inner monolayers of plasma bilayers are enriched in PE (Polozov and Gawrisch 2004). In this study, microbubbles were produced with DSPC, PEG40St and DSPE at various molar ratios of DSPE (4:5:1, 3:5:2, 2:5:3, 1:5:4 and 0:5:5) to observe the effect of DSPE amount on microbubble stability. Change in concentration of microbubbles is shown in Figure 4.37. As seen from the figure, first addition of the DSPE molecule decreased the number of microbubbles dramatically by time. Further increase in DSPE amount in microbubble shell increased the microbubble stability slightly. When the molar fraction of DSPE was increased up to 0.3, decrease in concentration of microbubbles occurred more slowly. As we continued to increase the DSPE amount, we observed that stability of microbubbles reduced much more dramatically. In terms of change in bubble concentration, 30mol% of DSPE provided the most stable microbubbles for the mixtures of DSPC, PEG40St and DSPE.
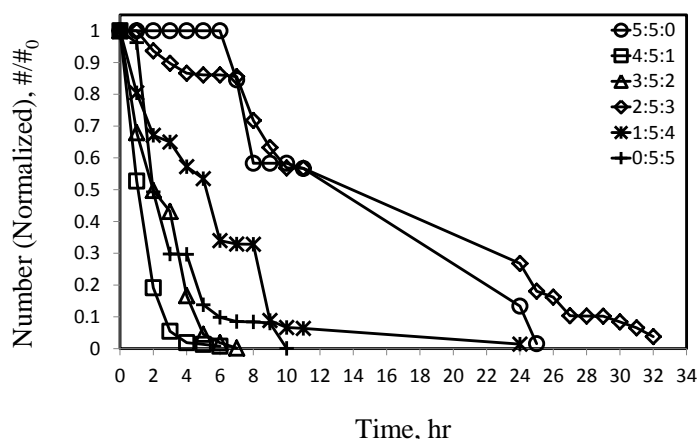
Figure 4.37. Change in number (normalized) of microbubbles prepared with the mixture of DSPC, PEG$_{40}$St and DSPE at various molar ratio of DSPE.
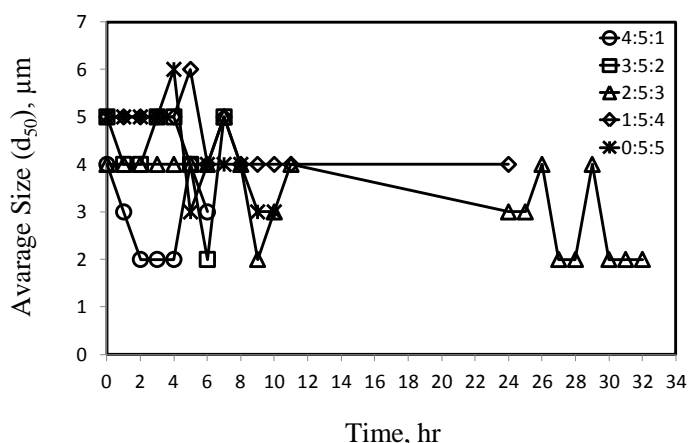
Figure 4.38. Change in diameter of microbubbles by time at 38°C for mixtures of DSPC/PEG40S/DSPE at various molar ratios.

We also investigated change in microbubbles size over time at 38°C. Results are illustrated in Figure 4.38. as explained before, average size (d$_{50}$) refers to the microbubble size at which 50% of total population is smaller. As shown in the figure, the destruction of microbubble began from the large ones as expected because large bubbles are not stable (Borden, Feshitan et al. 2009). Both number and size of microbubbles were almost constant over 6hr. Therefore, we can say that optimum molar fraction of DSPE that we should use is 0.3.

Furthermore, we compared size distribution of the microbubbles prepared with DSPE and without DSPE (Figure 4.39). As show in figure, size distribution of both microbubble species were almost the same indicating that addition of DSPE molecule at a molar fraction of 0.3 had no effect on size distribution. However, microbubble (having

a diameter less than 10μm) yield was too low with this microbubble species (DSPC:PEG40St:DSPE at a molar ratio of 2:5:3).
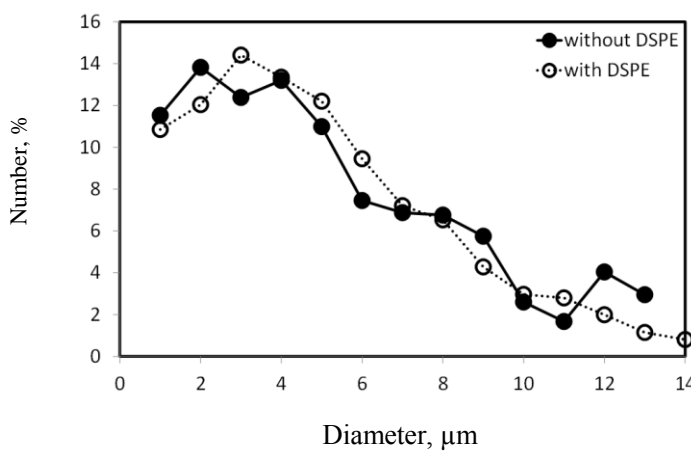
Figure 4.39. Size distribution of microbubbles with DSPE (DSPC:PEG40St:DSPE 4:5:1) and without DSPE (DSPC:PEG40St:DSPE 5:5:0)

The reason of this might be small head groups of DSPE, where only three H atoms are attached to the N atom as compared to the three methyl groups attached to the N atom in PC lipids, resulting in the formation of the non-lamellar inverted hexagonal phase (Dickey and Faller 2008). Besides, the relationship of water molecules increases the size of lipid head group. PC lipids have 25 water molecules in their hydration shell, whereas PE has only about 11. The head-group of PC is thus not only structurally larger than PE head group, but this difference is further enhanced by a difference in the relative hydration of the head-groups (Langner and Kubica 1999). Therefore, with addition of DSPE in the microbubble shell, stability of microbubbles did not enhance. Beside, cost of microbubbles produced with addition of is higher due to the decrease in the yield.

Effect of Stearoyl-rac-glycerol on microbubble stability: Stearoyl-rac-glycerol is a molecule which has the same head group (except phosphate group) with DSPG. On the other hand, Stearoyl-rac-glycerol has single hydrocarbon tail whereas DSPG has double hydrocarbon tail. We have studied the effect of stearoyl-rac-glycerol on microbubble stability. To observe the optimum amount of this component, we kept the emulsifier molar fraction at 0.5 and changed stearoyl-rac-glycerol molar fraction (4:5:1, 3:5:2, 2:5:3, 1:5:4 and 0:5:5). However, the solutions containing 50mole% of PEG40St did not produce any microbubbles due to chemical structure of stearoyl-rac-glycerol (

Figure 4.40). As seen, hydrophobic part of this component consists of single tail in contrast to phospholipids; hence, it is thought that this component interferes with the curvature structure of microbubble including high amount of PEG40St (Figure 4.41). Therefore in order to investigate the effect of emulsifier amount on stability of microbubbles containing stearoyl-rac-glycerol, microbubbles with DSPC:PEG40St:Stearoyl-rac-glycerol at molar ratios of 5:3:2 and 7:1:2 were prepared. Comparison of the microbubble stabilities (DSPC:PEG40St:Stearoyl-rac-glycerol at molar ratios of 5:5:0, 5:3:2 and 7:1:2) was given in Figure 4.42. As seen, although molar fractions of the PEG40St were different, onset times of the microbubbles prepared with stearoyl-rac-glycerol at a molar ratio of 5:3:2 were found to be the same with the microbubbles prepared with DSPC and PEG40St at a molar ratio of 5:5. Another observation is that, in contrast to DSPC coated microbubbles including 10mol% PEG40St, (current formulation in the literature with onset time of 10min.) microbubbles including stearoyl-rac-glycerol maintained their number constant for 4 hours. OH groups located in the head group of stearoyl-rac-glycerol might be responsible from this enhancement. Since these OH groups in stearoyl-rac-glycerol make hydrogen bonding with the DSPC and the liquid phase, and thus provide microbubble stability. Moreover, these microbubbles were size-stable for 1 hour. Further increase in PEG40St in microbubble shell containing stearoyl-rac-glycerol caused a decrease in stability and increased the microbubble size. Average size of microbubbles containing 30mol% of stearoyl-rac-glycerol decreased within 2 hours (Figure 4.42-B) due to gas diffusion since single-tail of this component probably caused non rigid shell structure.
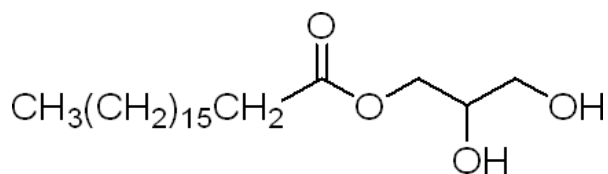
Figure 4.40. Chemical structure of Stearoyl-rac-glycerol
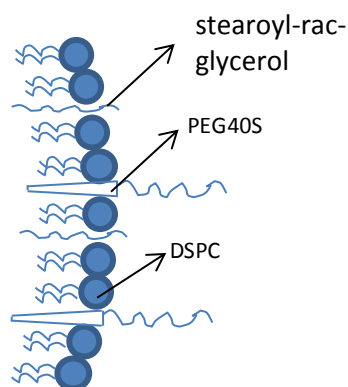
Figure 4.41. Microbubble shell structure consisting of DSPC, PEG40St and Stearoyl-rac-glycerol
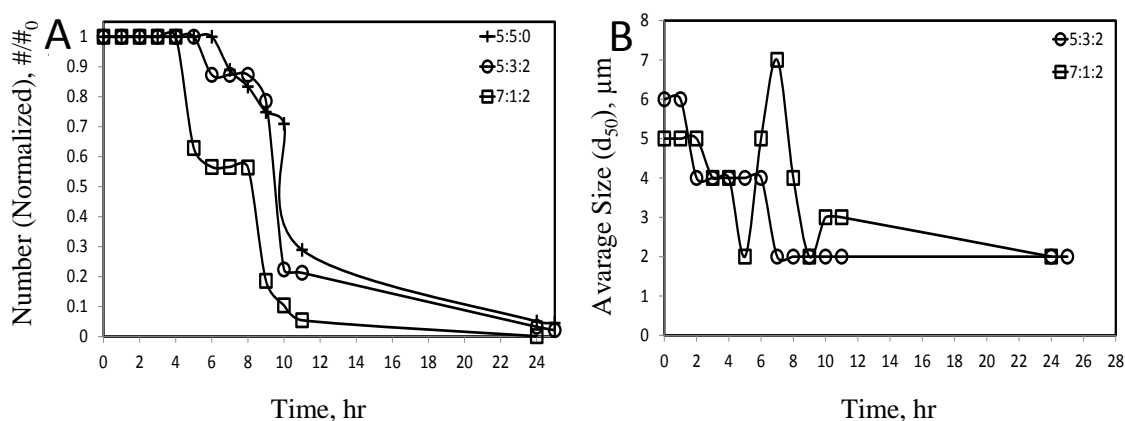
Figure 4.42. (A) Change in concentration and (B) average size of microbubbles over time at 38°C for mixtures of DSPC/PEG40S/ Stearoyl- rac-glycerol at various molar ratios.

Furthermore, comparison of the size distributions of the microbubbles prepared with stearoyl- rac-glycerol and without stearoyl- rac-glycerol is given in Figure 4.43. As illustrated, stearoyl glycerol caused production of larger microbubbles indicating that this component did not enhance production of microbubbles for medical applications. Due to short single-tail, stearoyl-rac-glycerol does not have the form of conical shape. Therefore, it is not in concert with the curvature of microbubble. That is why we obtained large microbubbles. The formulations we tried for the microbubbles containing stearoyl- rac-glycerol did not result in any better microbubble with enhanced stability than the ones without stearoyl- rac-glycerol.
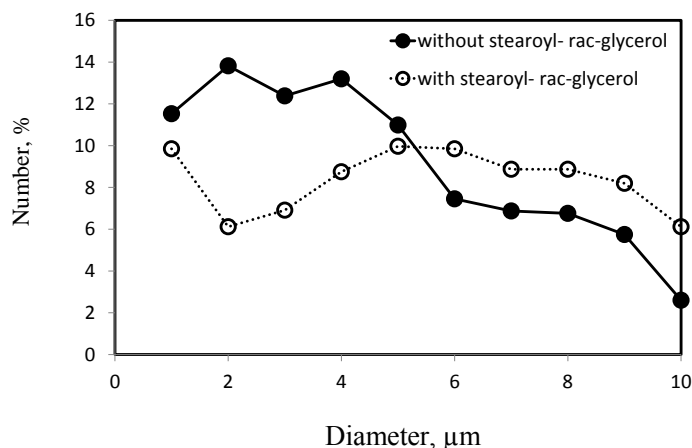
Figure 4.43. Size distribution of microbubbles with Stearoyl-rac-glycerol (DSPC: PEG40St:Stearoyl-rac-glycerol 5:3:2) and without Stearoyl-rac-glycerol (DSPC:PEG40St:Stearoyl-rac-glycerol 5:5:0)

To observe the effect of a third molecule having capability of making hydrogen bonding, stability of microbubbles including DSPG, DSPE and DSPA Stearoyl-rac-glycerol was compared. For each species we choose microbubble formulations by looking their stability. While comparing the microbubble species, we choose the microbubble formulations (for each formulation) that showed the best stability. The microbubble formulations that we compared are DSPC:PEG40St:DSPG 2:5:3, DSPC:PEG40St:DSPA 2:5:3, DSPC:PEG40St:DSPE 4:5:1 and DSPC:PEG40St: Stearoyl-rac-glycerol 5:3:2. Comparison of these microbubble species for their stability and size distribution is given in Figure 4.44. It was observed that microbubbles including DSPG at molar fraction of 0.3 showed the highest stability as compared other microbubble species. Microbubble species including DSPA molecule showed lower stability than DSPG coated microbubbles and microbubbles containing DSPE showed the lowest stability (Figure 4.44-A). Moreover, stearoyl-rac-glycerol coated microbubbles showed higher stability than DSPE coated microbubbles due to their OH groups. We think that this stability is related to molecular interactions between the components of the microbubble shell. As compared with DSPA, DSPG have 2 OH groups in its head group (Figure 4.45). It is known those OH groups have more capability of making hydrogen bonding. Moreover, PG lipids make more both inta- and intermolecular hydrogen bonds than PA lipids. Therefore, DSPA coated microbubbles are less stable than microbubbles containing DSPG. Although, stearoyl-rac-glycerol has same amount of OH groups, it showed lower stability due to its shape whereas DSPA includes single OH group in its head group for H-bonding. DSPE head group is smaller

63

than that of DSPG. DSPE resulted in less stable microbubbles than DSPA and DSPG since DSPE includes only one OH group on its head group.
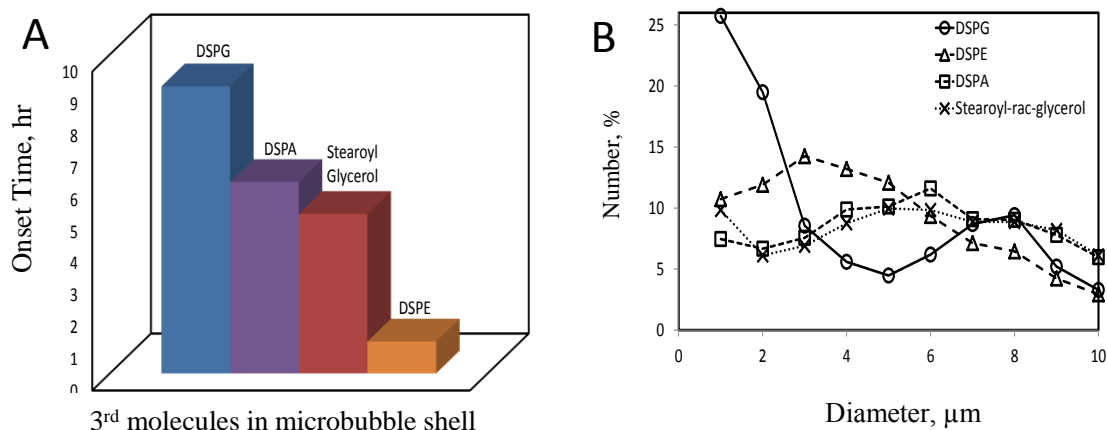
Figure 4.44. (A) Onset time and (B) size distribution of microbubbles for the mixtures including DSPG, DSPA, DSPE and Stearoyl-rac-glycerol as the third molecule.
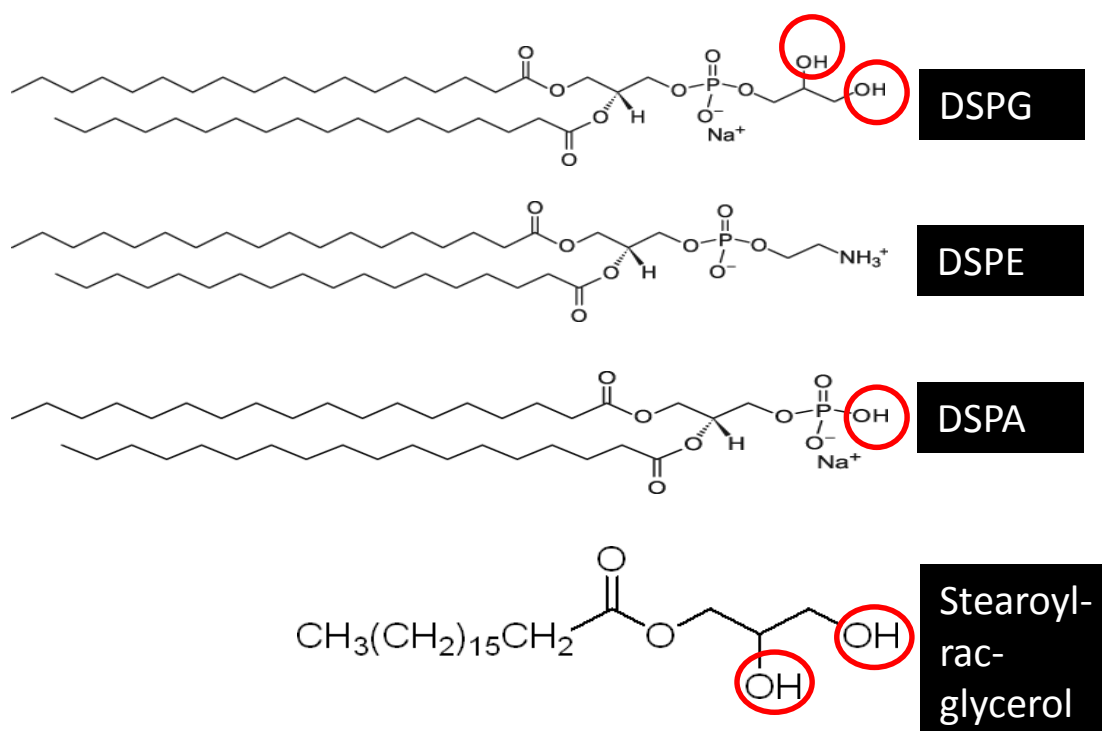
Figure 4.45. Chemical structures showing OH groups of the molecules that we used as the third component in production of microbubbles.

As mentioned above, microbubble size is very crucial for medical applications. Therefore, it is important to produce small microbubbles (in the range of 1-10um). As seen in Figure 4.44-B we produced the smallest microbubbles having diameter between

64

1 and 3μm with a high yield by using DSPG. It is known that this change in microbubble size is related to the area of the head group of lipid molecules (Dickey and Faller 2008). Large head group of lipids form conical shape and this causes microbubbles with high curvature. For example, DSPG has larger head group than DSPE and DSPA so it forms smaller microbubbles. Detailed information about the formation of microbubbles based on their head group is given above. The comparison of the head group of the third components is illustrated in Figure 4.45. As seen, DSPA have small head group when compared with DSPE and DSPG. That is why; DSPA produced larger bubbles than the other two components that we used. The reason of why we obtained large microbubbles with stearoyl-rac-glycerol is due to single hydrocarbon chain of this component. Due to its hydrocarbon group with single chain it could not form conical shape and interfere with curvature characteristics of microbubbles. As a conclusion, we think that among formulations we tried, addition of DSPG to DSPC and PEG40St produce microbubbles with enhanced stability in size.

4.5.2. Effect of Ionic Interaction on Microbubble Stability

To investigate the effect of ionic interactions between the components on microbubble stability, three different ionic molecules (DSPS, DSTAP, Stearyl amine) were added to the mixture of DSPC and PEG40St.

Effect of DSPS on microbubble stability: Phosphatidylserine (PS) is the one of the anionic phospholipids existing in eukaryotic cell membranes. Most of the PS-lipids are located in the inner monolayer of plasma membranes (at cytosolic side). When they are found in the outer leaflet of the cell membrane, they are indicative of apoptosis (Ross, Steinem et al. 2001). Since they are anionic lipids and naturally found in living organisms, PS-lipid (with C_{18}, DSPS) was used as a third component to produce microbubbles. Microbubbles were produced by using DSPC, PEG40St and DSPS at various molar ratios (4:5:1, 3:5:2, 2:5:3, 1:5:4 and 0:5:5) to investigate the effect of DSPS amount on bubble stability at 38°C. Like other investigations in this thesis, molar fraction of the PEG40St molecule in all formulations was kept constant at 0.5. Change in stability of microbubbles species is shown in Figure 4.46. As illustrated, initial addition of DSPS as a third component did not enhance the microbubble stability at 38°C. With the addition of this component to the microbubble shell, the onset time of

bubbles decreased (Figure 4.46-B). Further increase in DSPS amount in microbubble formulation remained unstable microbubble behavior. However, substation between DSPC and DSPS showed almost same stability with microbubbles prepared with only DSPC and PEG40St. Another word, DSPS coated microbubbles showed almost same stability with DSPC coated microbubbles. This may mean that phosphatidylcholine and phosphatidylserine containing microbubbles were completely immiscible. That is why we could not get stable bubble by mixing these 2 components (DSPC and DSPS). This is in a good agreement with the study of *Silvius et al.*. In their study, they have reported that at least a limited lipid phase separation, forming PS-enriched domains, attends the fusion of PC-PS vesicles containing considerably less than 70mol% PS (Silvius and Gagne 1984). Since negative charge of DSPS molecule, DSPS molecules interacted intermolecularly. Therefore, DSPC and DSPS did not mix properly.
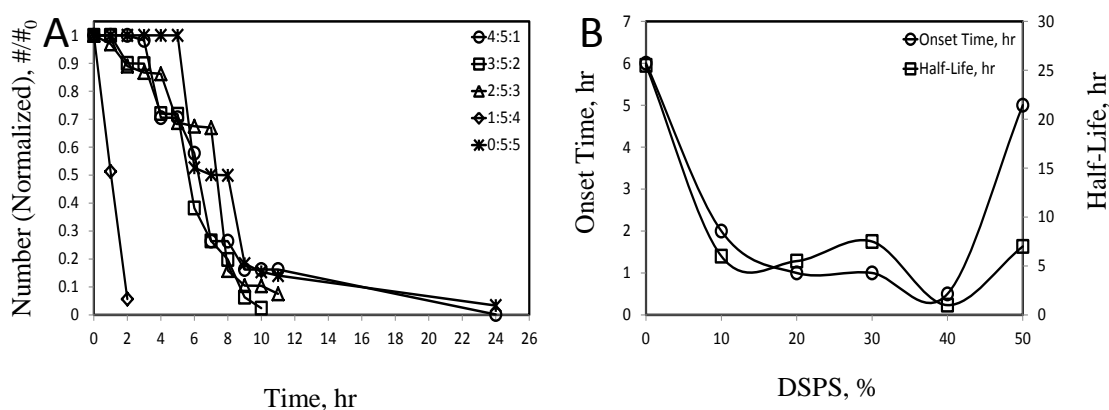
Figure 4.46. (A) Change in concentration and (B) onset time and half-life of microbubbles over time at 38°C for mixtures of DSPC/PEG40S/DSPS at various molar ratios.

Another observation is that DSPS produced smaller microbubbles due to their charges (Figure 4.47). As reported above, microbubbles including DSPS are not stable. However, in terms of microbubble size, these microbubble species are suitable for medical applications since microbubble size is a critical parameter to cross the capillary system of living organisms. Based on this, a microbubble should not be larger than 8μm (size of erythrocyte), on the other hand, they should not be very small since intensity of scattering by gas filled microbubbles is proportional to the sixth power of the radius of the bubble, so the larger the bubble, the better the scattering intensity (Riess, Schutt et al. 2003).
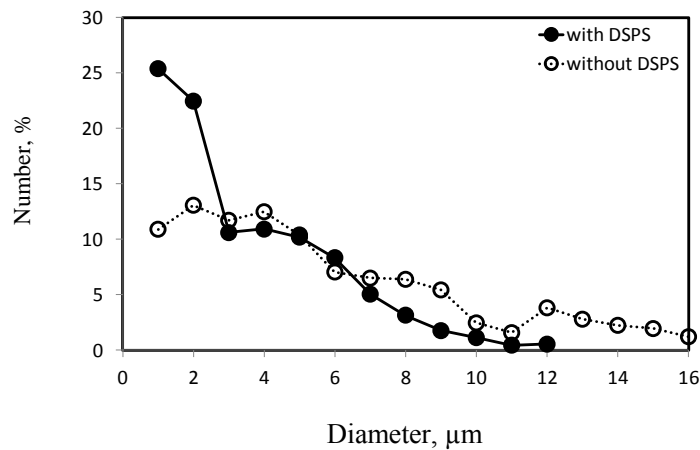
Figure 4.47. Size distribution of microbubbles with DSPS (DSPC:PEG40St:DSPS 5:4:1) and without DSPS (DSPC:PEG40St:DSPS 5:5:0)

Additionally, change in average size (d_{50}) of microbubble species was also investigated at 38°C over time (Figure 4.48). As demonstrated, there was no significant change in diameter of microbubbles over time at body temperature. Growth of microbubble was almost not seen with these formulations. This observation is also important because bubble growth with the effect of temperature (body temperature) may cause embolism problems.
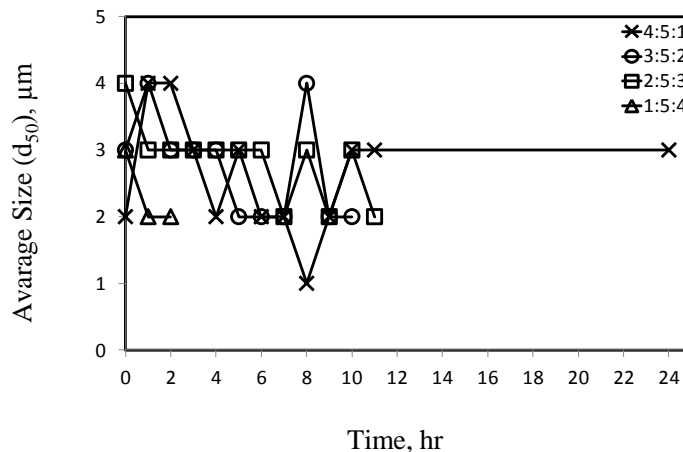
Figure 4.48. Change in diameter of microbubbles by time at 38°C for mixtures of DSPC/PEG40S/DSPS at various molar ratios.

Effect of DSTAP on microbubble stability: Another ionic component we used was DSTAP (distearoyl (C 18:0)-trimethyl ammonium propane) to produce microbubbles since it is known that addition of charged species in the microbubble shell

can have an effect on lipid packing, which is essential for microbubble stability (Borden and Longo 2002; Borden, Caskey et al. 2007). In this study, we prepared microbubbles with DSPC, PEG40St and DSTAP at various molar ratios (4:5:1, 3:5:2, 2:5:3, 1:5:4 and 0:5:5) of DSTAP by keeping PEG40St molar fraction at 0.5. Stability experiments for these species were conducted at 38°C over time. Comparison of the stability of these microbubble species including DSTAP is given in Figure 4.49. As shown, with initial addition of DSTAP to microbubble shell, onset time decreased dramatically. Further increases in the amount of the DSTAP caused little improvement in stability of microbubbles containing DSTAP.

Figure 4.49. (A) Change in concentration and (B) onset time and half-life of microbubbles over time at 38°C for mixtures of DSPC/PEG40S/DSTAP at various molar ratios.

Furthermore, change in diameter of microbubbles prepared with DSPC, PEG40St and DSTAP at various molar ratios was investigated over time at close to body temperature (Figure 4.50). Average diameter of microbubbles including DSTAP at 50mol% and 20mol% decreased over time as their numbers decreased indicating that initially large bubbles disappeared with the effect of temperature. For these molar fractions of DSTAP, microbubbles began to burst from the large ones.
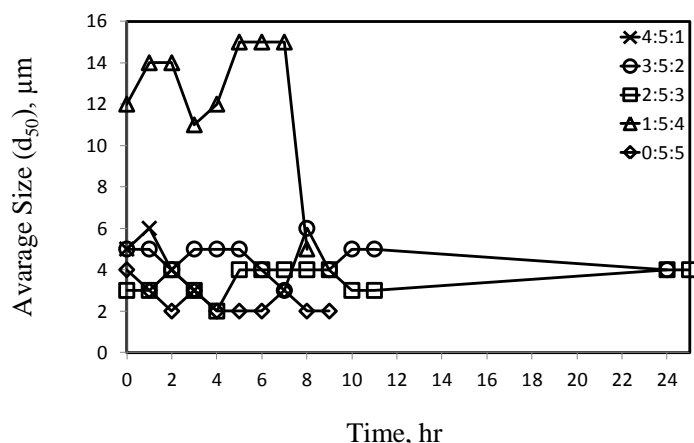
Figure 4.50. Change in diameter of microbubbles by time at 38°C for mixtures of DSPC/PEG40S/DSTAP at various molar ratios.

Another observation is that, the inclusion of DSTAP at 10 mol% increased the diameter of microbubbles in contrast to liposome behavior (Figure 4.51). Moreover, Figure 4.51-C shows that further increases in DSTAP raised microbubble diameter. *Campbell et al.* reported that addition of DOTAP (DOTAP has same head group with DSTAP, only chain lengths are different) at 10mol% both decreased the diameter of spontaneously-forming liposomes and decreased particle heterogeneity (Kwan and Borden 2012). This decrease in size occurred when DSTAP was used at 30mol% (Figure 4.51-B). Liposome and microbubble behaved different in terms of size when DSTAP was added to the microbubble shell, because, as mentioned above, liposomes consist of bilayer structure; however microbubble shell is formed of a monolayer. For microbubbles it is crucial to use conical shaped components to provide the curvature. This conical shape might be formed with the components having large head group (like PEG-emulsifiers). DSTAP is a cationic lipid having a small head group (Hexagonal II phase) compared to DSPC (Figure 4.52). Since lipid packing formed by type II lipids (Hexagonal II phase) deteriorate miceller structure, production of small and stable microbubbles with DSTAP becomes is not possible.
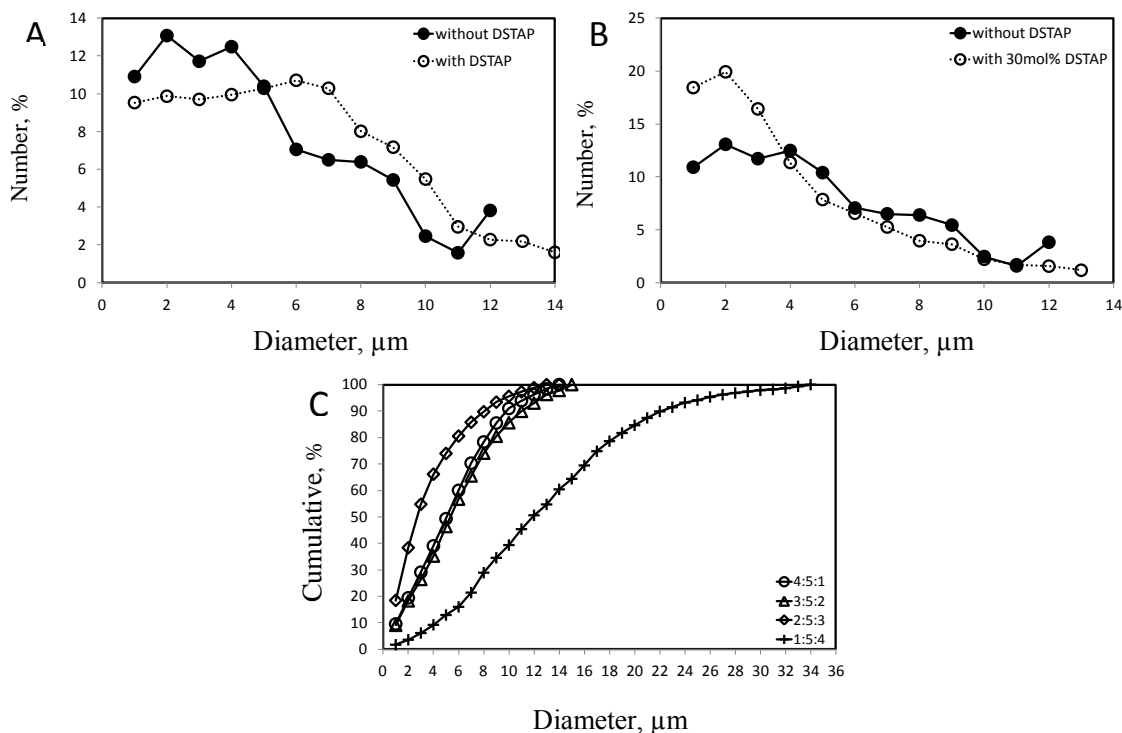
Figure 4.51. Comparison of size distributions of microbubbles prepared (A) with and without DSTAP, (B) without DSTAP and 30mol% DSTAP and (C) with DSTAP at various molar ratios.
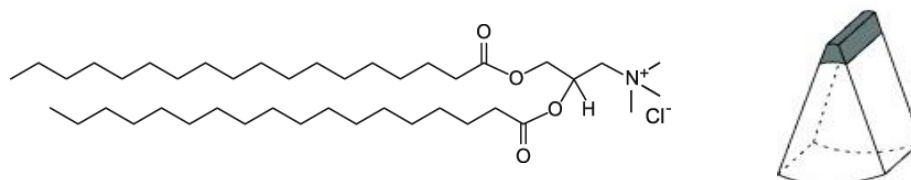
Figure 4.52. Chemical structure and lipid packing of DSTAP.

Effect of Stearyl amine (octadecylamine) on microbubble stability: It has been reported earlier that PC and stearyl amine together showed cytotoxic properties through some parasite species due to positively charge of stearyl amine (Dey, Anam et al. 2000). Besides, this component is utilized with phospholipids and cholesterol in production of stable liposomes (Riaz 1995). Although, liposomes are not foam, they participate in colloidal systems. We used stearyl amine as the third component in production of microbubbles. To optimize the stearyl amine concentration in microbubble shell, we produced microbubbles by using DSPC, PEG40St and stearyl amine at various molar ratios (4:5:1, 3:5:2, 2:5:3, 1:5:4 and 0:5:5) and investigated their stability at body

temperature. It was observed that stearyl amine at molar fractions of 0.3, 0.4 and 0.5 did not produce microbubbles while the mole fraction at PEG40St was kept constant at 0.5 similar to stearoyl-rac-glycerol, stearyl amine is also a single-tail surfactant and with high amount of PEG40St having conical shape it disrupts the curvature of the microbubble shell. Because of this, microbubbles were also produced with PEG40St at a molar fraction of 0.2. Change in number and size of these microbubbles is illustrated in Figure 4.53. With the addition of stearyl amine in microbubble shell structure, microbubble stability decreased. Decrease in emulsifier amount (PEG40St) caused little enhancement of the microbubble stability. As said before, with single-tail surfactants obtaining highly condensed monolayer seems to be less likely. This might cause gas diffusion in microbubbles. Since gas diffusion is one of destruction mechanism of microbubbles, long term stability of microbubbles cannot achieved with this component.

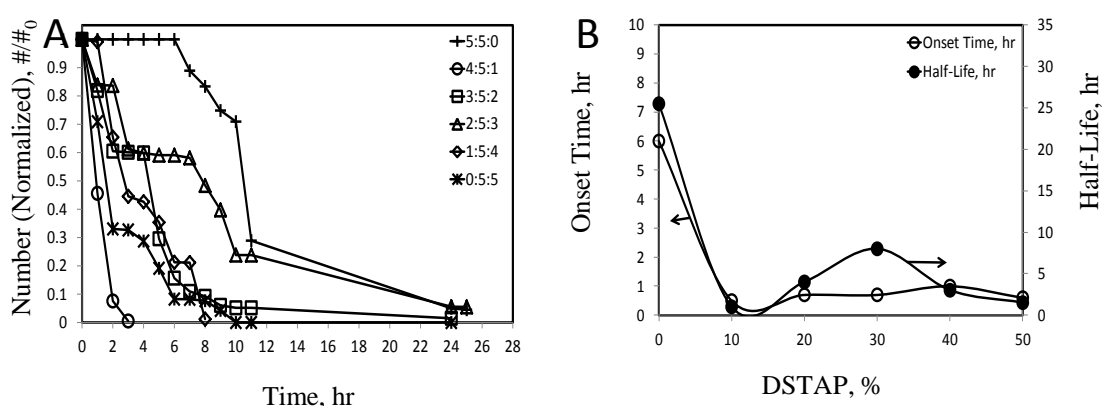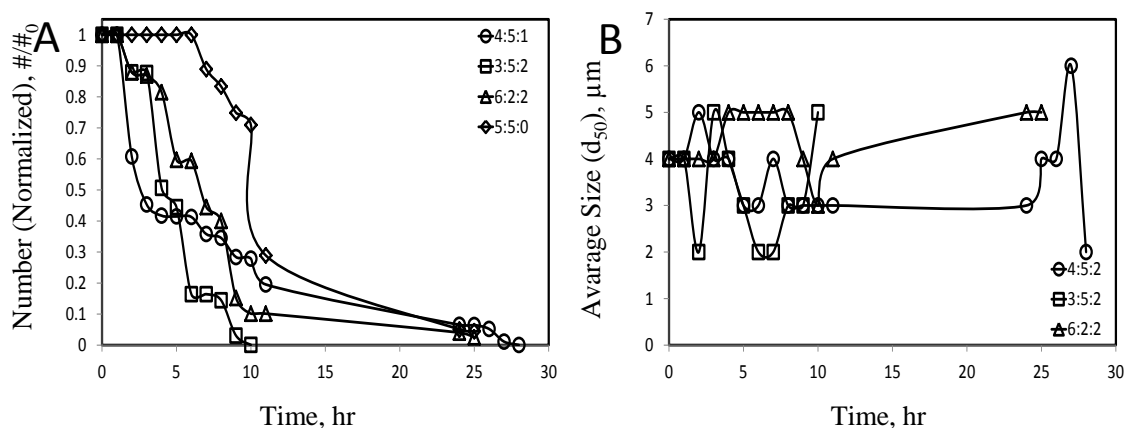Figure 4.53. (A) Change in concentration and (B) average size of microbubbles over time at 38°C for mixtures of DSPC/PEG40S/Stearyl amine at various molar ratios.

Another observation is that addition of stearyl amine in microbubble shell increased the microbubble size as expected (Figure 4.54) since curvature of the microbubble shell decreased. This indicates that production of small sized microbubbles was almost inhibited with single-tail surfactant stearyl amine. As mentioned above, for intravascular administration of microbubbles increase in diameter of microbubbles might cause embolism problems in medical applications.
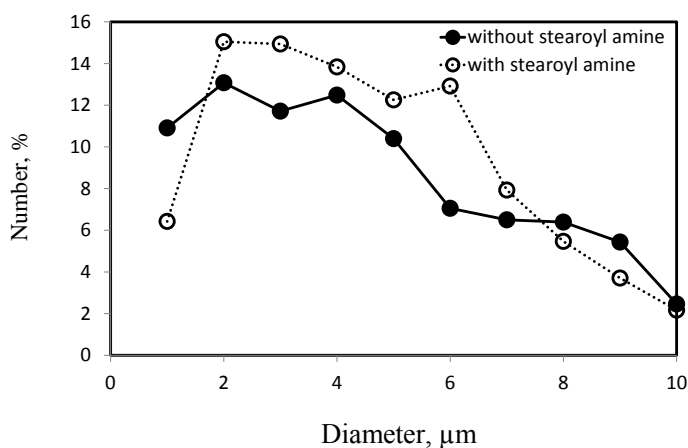
Figure 4.54. Comparison of size distributions of microbubbles prepared with and without Stearyl amine.

The effect of ionic components on microbubble stability, microbubble species consisting DSPS, DSTAP and Stearyl amine were compared for their stability. For each species microbubble formulations were chosen by considering their stability. Comparison of microbubble species was performed by choosing the microbubble formulations that exhibited the best stability. Specifically, comparison of the microbubbles was done with the formulations of DSPC:PEG40St:DSPS 4:5:1, DSPC:PEG40St:DSTAP 1:5:4 and DSPC:PEG40St:Stearyl amine 3:5:2. Comparison of these microbubble species for their stability and size distribution is given in Figure 4.55. It was observed that microbubbles consisting DSPS at a molar fraction of 0.1 exhibited the highest stability when compared with the other microbubble species at their optimum composition (Figure 4.55-A). DSTAP and stearyl amine showed lower stability than microbubbles prepared with DSPS. The higher stability of microbubbles prepared with DSPS is related to ionic interaction between the components of the microbubble shell. As seen in Figure 4.56 DSPS component having NH_3^+ group can interact with DSPC and itself. Although, stearyl amine has also NH_3^+ group, due to its single hydrocarbon chain as hydrophobic tail. It cannot form highly dense monolayer having curvature structure and therefore may cause gas diffusion. This single-tail structure also decreased the curvature of the microbubble causing formation of large sized microbubbles. DSPS produced the smallest microbubbles since it has larger head group than DSTAP (Figure 4.56). As said above, components having a large head group are much closer to the conical shape and it is known that this kind of components provide micellar formation with high curvature. And high curvature means smaller

microbubbles. Among the ionic component we tried, DSPS can be said to be the most suitable ionic component to produce stable microbubbles for intravascular administration.
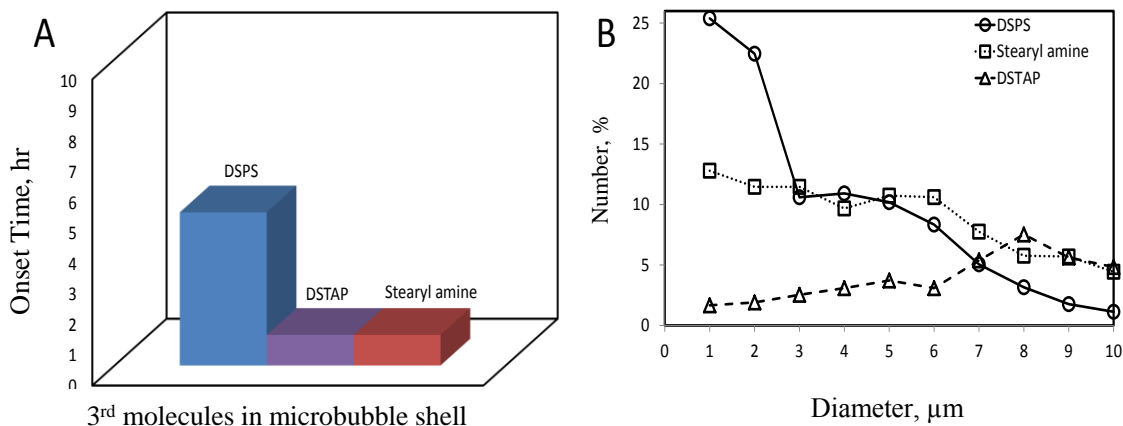
Figure 4.55. (A) Onset time and (B) size distribution of microbubbles for the mixtures including DSPS, DSTAP, DSPE and Stearyl amine as the third molecule.
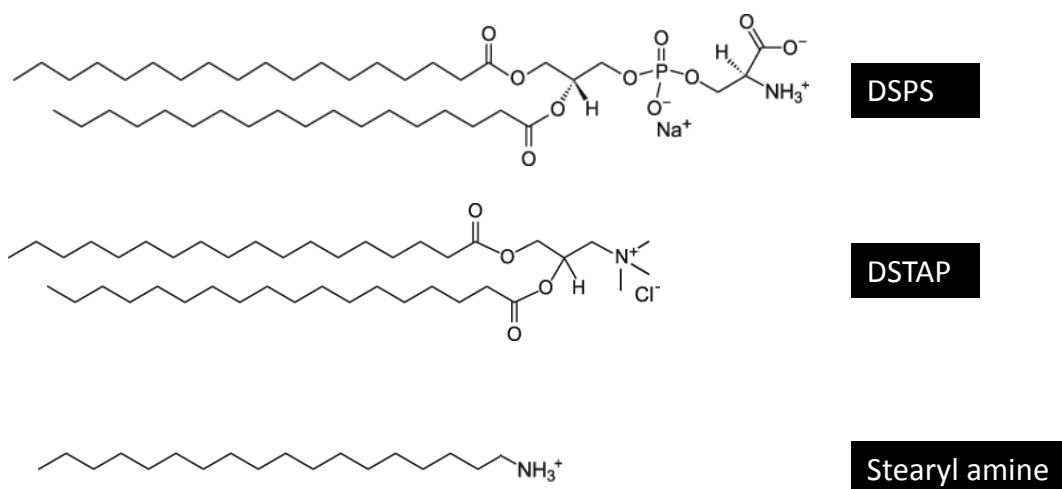
Figure 4.56. Chemical structures of the molecules that we used as the third component for production of microbubbles.

4.5.3. Effect of Cholesterol on Microbubble Stability

In living organisms cells include cholesterol molecules in their inner and outer membranes to provide lateral organization of bilayer structure and maintain the fluidity of the cell membrane (Williams, Hudson et al. 2011). Thus far, to describe the effect of

cholesterol on the organization of other lipids number of investigations were performed on model systems (Kirby, Clarke et al. 1980; Christiansen, Kryvi et al. 1994; Petrache, Dodd et al. 2000; Chomas, Dayton et al. 2001; Wydro 2011). However, there is no study about the microbubble coated with lipids and cholesterol. To investigate the effect of cholesterol molecule on microbubble stability, we added cholesterol molecule to DSPC coated microbubbles. The mixtures were prepared with DSPC, PEG40St and cholesterol at molar ratios of 5:4:1, 6:3:1 and 4:4:2 for production of microbubble species. In the first mixture we added 10mol% of cholesterol molecule and reduced the emulsifier (PEG40St) amount to 40mol%. In the second mixture again 10mol% of cholesterol molecule was used and emulsifier (PEG40St) amount was decreased, but at this time mol% of DSPC was increased to 60mol%. Then cholesterol amount was increased up to 20mol% and both DSPC and PEG40St amount was decreased. Change in number of microbubbles was shown in Figure 4.57. As shown in the figure, substitution between emulsifier and the cholesterol approximately had no effect on bubble stability at close to body temperature (38°C). Number of bubbles remained stable for 5 hours, and then concentration started to decrease dramatically. Half-life of these microbubbles was obtained as 11hr. Decreasing PEG40St amount affected bubble stability negatively. Both onset time and half-life of microbubbles reduced due to diminished effect of PEG as steric barrier (PEG chains forms a steric barrier around microbubbles) on bubble shell. Further increase in cholesterol continued to decrease microbubble stability. This behavior of microbubbles is in contrast to the liposome behavior in terms of stability. Current studies have showed that cholesterol-rich (PC/cholesterol) liposomes were stable for at least 90 min in the presence of whole blood (Kirby, Clarke et al. 1980). This difference may be due to the structures of microbubbles and liposomes because liposomes consist of bilayer membrane structure whereas microbubbles consist of monolayer membrane structure. Moreover, microbubbles include emulsifier contrary to the liposomes. Liposome instability is generally related to the finding that liposomes prepared with little or no cholesterol lose some of their phospholipid to high density lipoproteins (Kirby, Clarke et al. 1980). On the other hand, for microbubbles, it is not like this. Cholesterol, located inside the hydrophobic core of plasma membrane (plasma membrane has bilayer structure), is known to reduce the lipid bilayer's permeability. Conversely, microbubble shell has monolayer structure and head groups of the shell components should interact with aqueous phase to maintain microbubble stability. If so, localization of the cholesterol

molecule may cause irregular shape in microbubble shell. This irregular shape of the thin shell may cause dissolution of the microbubble, causing cholesterol containing microbubbles to be less stable compared to the one with no cholesterol.
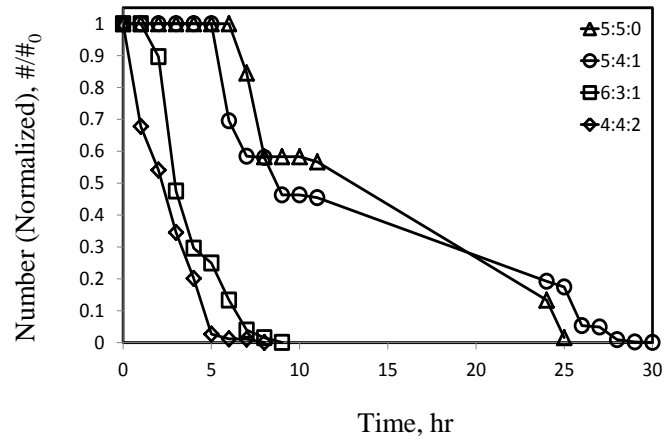
Figure 4.57. Change in number (normalized) of microbubbles prepared with the mixture of DSPC, $PEG_{40}St$ and cholesterol at various molar ratios.

Besides, population of microbubble behavior was also investigated over time at 38°C in terms of change in size of microbubbles. Change in d_{50} of microbubbles over time at 38°C is illustrated in Figure 4.58. As demonstrated, in terms of size, microbubbles prepared with DSPC, PEG40St and cholesterol at a molar ratio of 5:4:1 behaved almost the same with the microbubbles without cholesterol. For the other microbubble formulations, there were some fluctuations. However, these changes in average size were not very dramatic.
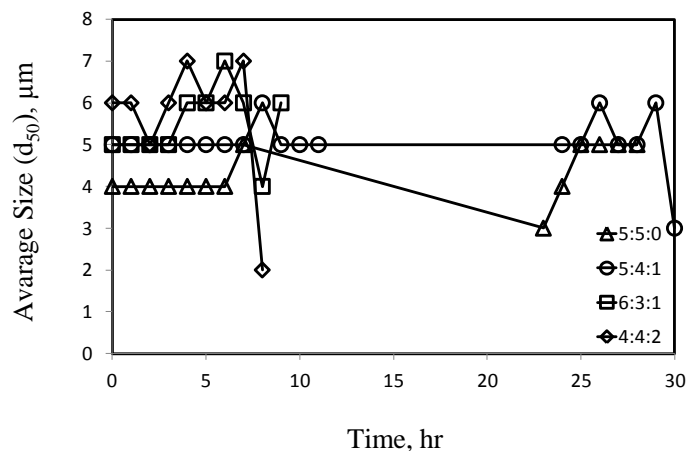
Figure 4.58. Change in diameter of microbubbles by time at 38°C for mixtures of DSPC/PEG40S/Cholesterol at various molar ratios.
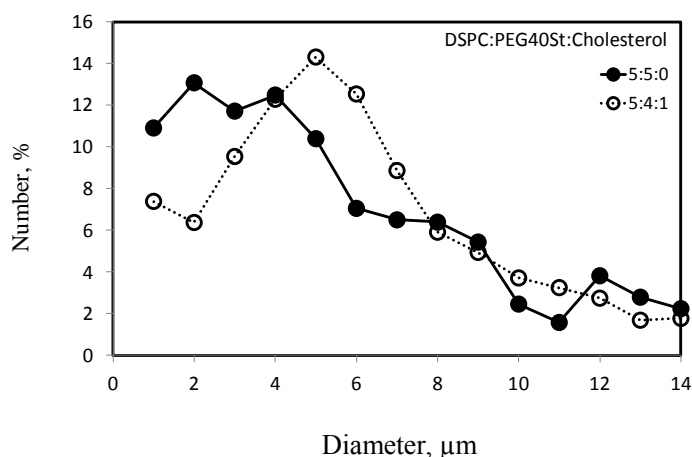
Figure 4.59. Size distribution of microbubbles with cholesterol and without cholesterol

Another observation was that cholesterol caused production of large bubbles. The comparison of the size distribution of microbubbles with and without cholesterol is given in Figure 4.59. With addition of cholesterol to the microbubble shell, size range of microbubbles shifted to the right which means that larger microbubbles were produced.

4.6. Effect of Gas Type on Microbubble Stability

Since it is known that air filled microbubbles prepared with current formulation (DSPC:PEG40St, 9:1) shows low stability in circulation, currently different types of gas are used as osmotic stabilizers (Riess, Schutt et al. 2003). It has been reported that microbubble dissolution rate decreases with increasing the molecular weight of the gas. Therefore, due to higher molecular weight and low water solubility (Riess, Schutt et al. 2003), perfluorocarbon gas is currently used to produce more stable microbubbles. To evaluate the impact of different gasses on stability of our new microbubbles, microbubbles filled with perfluorocarbon (PFC) instead of air were prepared with different formulations. Microbubble formulations chosen for this investigation were DSPC:PEG40St 9:1, DSPC:PEG40St 5:5 and DSPC:PEG40St:DSPG 2:5:3. Change in number of these microbubbles filled with PFC is shown in Figure 4.60. As shown, trend of the microbubble stability did not change compared to air filled microbubbles having same formulations. Moreover, comparison of onset time of air and PFC filled microbubbles is given in Figure 4.61. As seen in the figure, for microbubble species

prepared with DSPC:PEG40St:DSPG at molar ratios of 5:5:0 and 2:5:3, PFC did not enhance the stability since the larger area per hydrophobic chain of PEG40S provides more free volume through which PFC molecules can penetrate. As reported by *Borden et al*. larger head-group of PEG40St, which allows baggier packing of the hydrophobic chains, leads to a much lower resistance in the fully condensed state (Borden and Longo 2004). On the other hand, PFC raised the stability of microbubbles prepared with DSPC and PEG40St at a molar ratio of 9:1 (current formulation of microbubbles) since fully formed monolayer shells for the long-chain lipids (DSPC) displayed a significant barrier to PFC transport. It is clearly seen from our results that enhancement of microbubble stability by using DSPC instead of air showed a difference according to the formulation of microbubbles. Our results indicated that microbubbles prepared with DSPC, PEG40St and DSPG at molar ratios of 5:5:0 and 2:5:3 reached to their maximum stability with the component that we used and could not be improved any further even if a gas with low water solubility is used with a different type of gas. This also provides us cost effective contrast agents for ultrasound imaging.
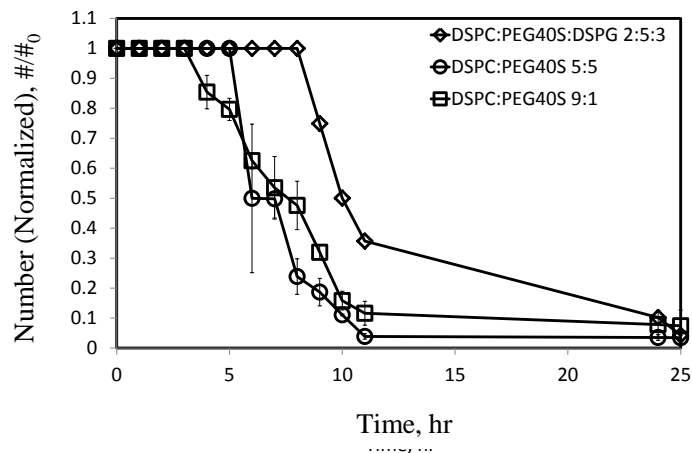
Figure 4.60. Change in number of microbubble species over time at 38°C
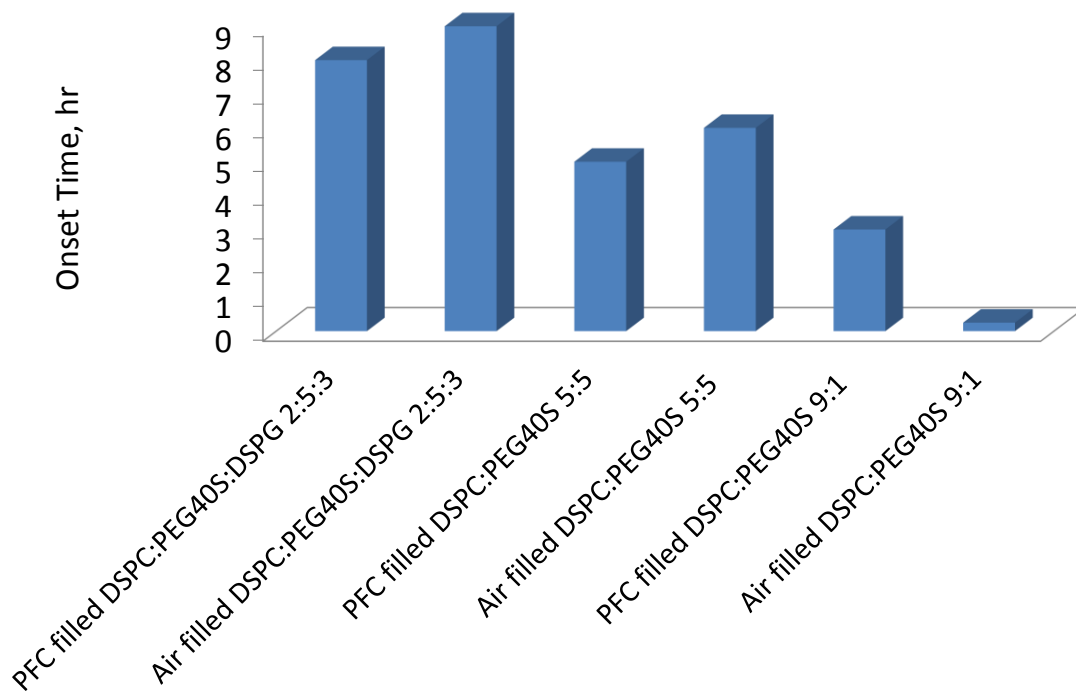
Figure 4.61. Onset time of air-filled and PFC-filled microbubbles.

The comparison of the size distributions of air-filled and PFC-filled is shown in Figure 4.62. It is obviously realized that by using PFC instead of air, smaller microbubbles can be produced probably due to strong synergistic effect between the perfluorocarbon gas and phospholipids. This synergy between microbubble shell and gas core causes more rigid microbubble shell structure resulting in smaller microbubbles. Another observation was that use of PFC gas increased the microbubble yield.
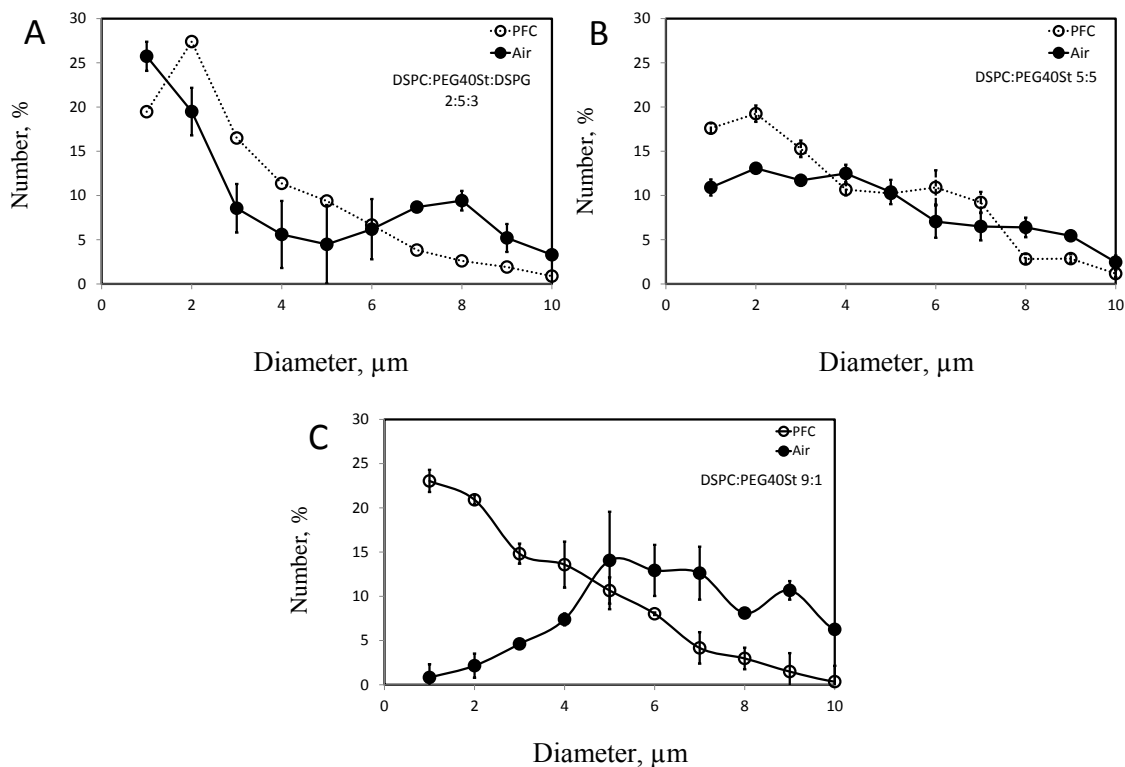
Figure 4.62. Comparison of size distributions of the air-filled and PFC filled microbubbles. (A) 2:5:3, (B) 5:5:0 and (C) 9:1

4.7. Characterization of Targeted Microbubbles

4.7.1. Streptavidin Quantification

Flow cytometry was used to measure the streptavidin densities on microbubble shell. In order to quantify streptavidin coverage, microbubbles including 10mol% of DSPE-PEG2000-biotin were labeled with phycoerythrin (PE) labeled streptavidin. Various percentages of streptavidin-PE were used between 0% and %200 (0.1μg/mL-20 μg/mL). Flow cytometric data from samples of microbubbles incubated with various percentage of streptavidin-PE (0%, 10%, 25%, 50%, 75% and 100%) are shown in Figure 4.64 and Figure 4.65. In Figure 4.65, measured streptavidin surface density on microbubbles is expressed as number of events. Flow cytometry results indicated that microbubbles incubated with 200% streptavidin-PE and resulted in approximately same number of events suggesting that streptavidin density is saturated at 100%.
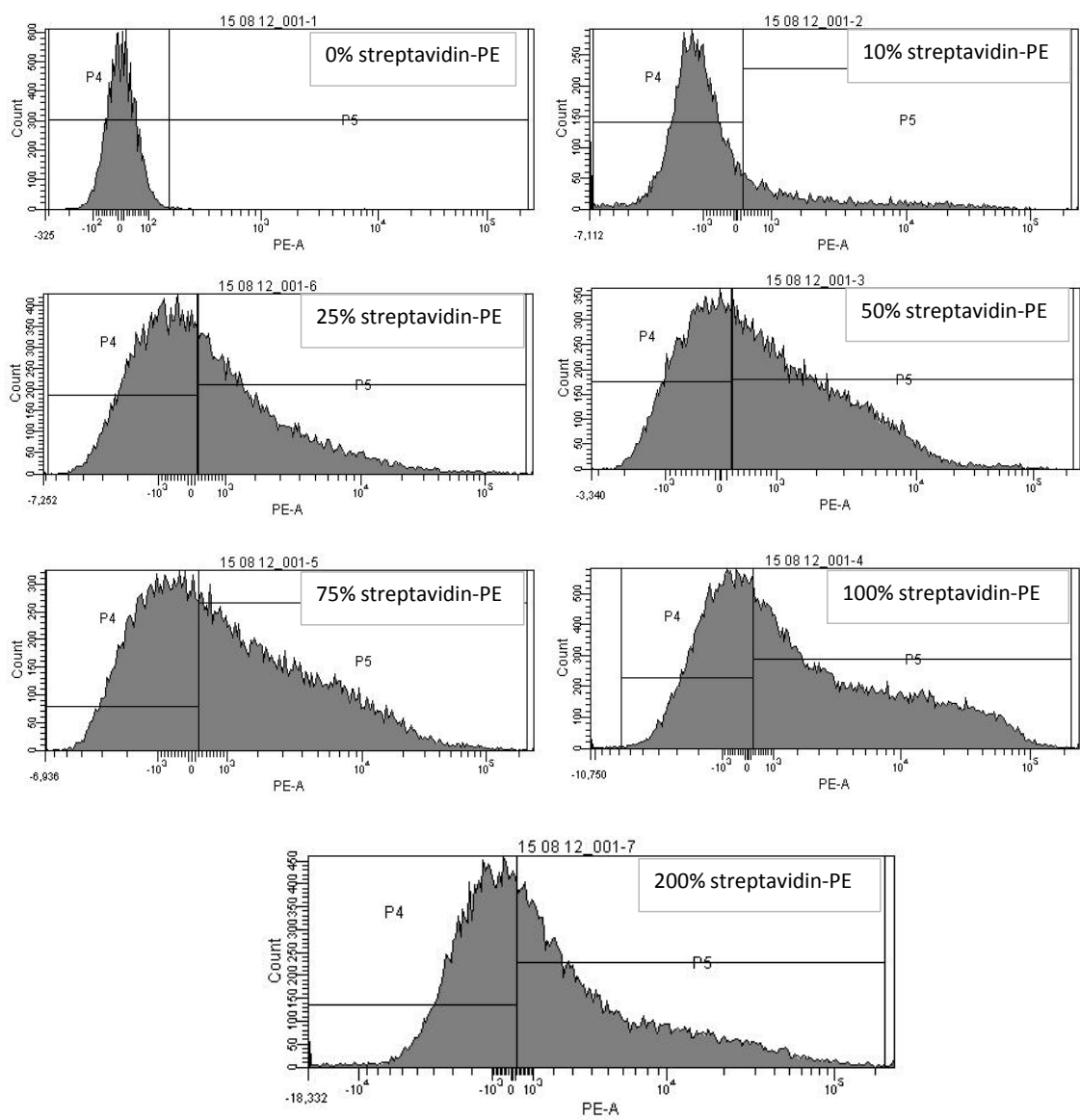
Figure 4.63. Histogram of the detection of Streptavidin-PE bound to microbubbles. The shift in fluorescence shows the labeled streptavidin binds to the microbubbles made with DSPE-PEG-biotin
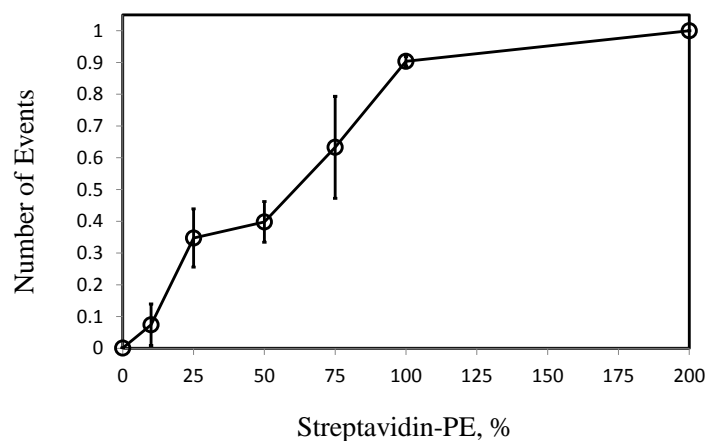
Figure 4.64. Change in fluorescence intensity corresponding to streptavidin-PE

The main finding of this investigation was that maximum streptavidin density was achieved at 100% (10μg/mL). Microbubbles with varied streptavidin densities might be maximally conjugated with a saturating solution of biotinylated antibody. This primarily study was performed since target studies may result in microbubble with unoccupied streptavidins and ligands.

4.7.2. Cellular Adhesion of Targeted Microbubbles

Microbubbles prepared with DSPC, PEG40St and DSPG at molar ratios of 9:1:0, 5:5:0 and 2:5:3 described above were chosen for ligand conjugation with Epidermal Growth Factor (EGF) using a streptavidin-biotin bridge. These EGF modified microbubbles should have an affinity to the $\alpha_v\beta_3$ receptors present on MDA-MB-231 human breast cancer cells. A rectangular parallel plate flow chamber was used to examine adhesion of microbubbles to cultured MDA-MB-231. Figure 4.65 shows a sketch of this flow chamber comprising a transparent polydimethylsiloxane (PDMS) block and a standard microscope slide. The distal ends of the outlet and inlet ports were connected to tubing. The microscope slide covered with MDA-MB-231 was mounted over the channel with the cells facing the inside. The inlet port was connected to a syringe pump. The syringe filled with imaging buffer (HEPES buffer) was hooked to the syringe pump. Tubing connected to the inlet port was adapted 3 way valve. For this study, adhesion of 3 different microbubble species (DSPC:PEG40St:DSPG 9:1:0, 5:5:0 and 2:5:3) was investigated. A solution of microbubbles was perfused under controllable shear conditions a monolayer of cultured MDA-MB-231 grown on the

microscope slide. Microbubbles 2×10^6 ml^{-1} were drawn through the flow chamber at various shear rates (76 s^{-1}, 152 s^{-1} and 229 s^{-1}) for additional 3 min. Adhered microbubbles to cells were then incubated for additional 3 min. After washing step (for 3 min.), their adhesion to the target surface was assessed. We hypothesized that EGF-labeled microbubble adhesion depends on the shear rate at cell surface. Data from flow chamber exposed with targeted and untargeted (control groups) microbubble species at various shear rates followed by a bubble-free wash at matching shear rates are shown in Figure 4.66. Microbubble adhesion is shown as the adhered microbubble number normalized to the cell number. For all three microbubble species, adhesion of microbubbles decreased with increasing the shear rate. Beside comparison of adhesion associated with shear rate, it was compared related to the microbubble type. It was observed that microbubbles prepared with DSPC and PEG40St at a molar ratio of 9:1 showed lower adhesion while microbubbles prepared with PEG40St at mol fraction of 0.5 illustrated higher adhesions to the cells. It may be possible that this difference in adhesion occurred due to the different stability of microbubbles.
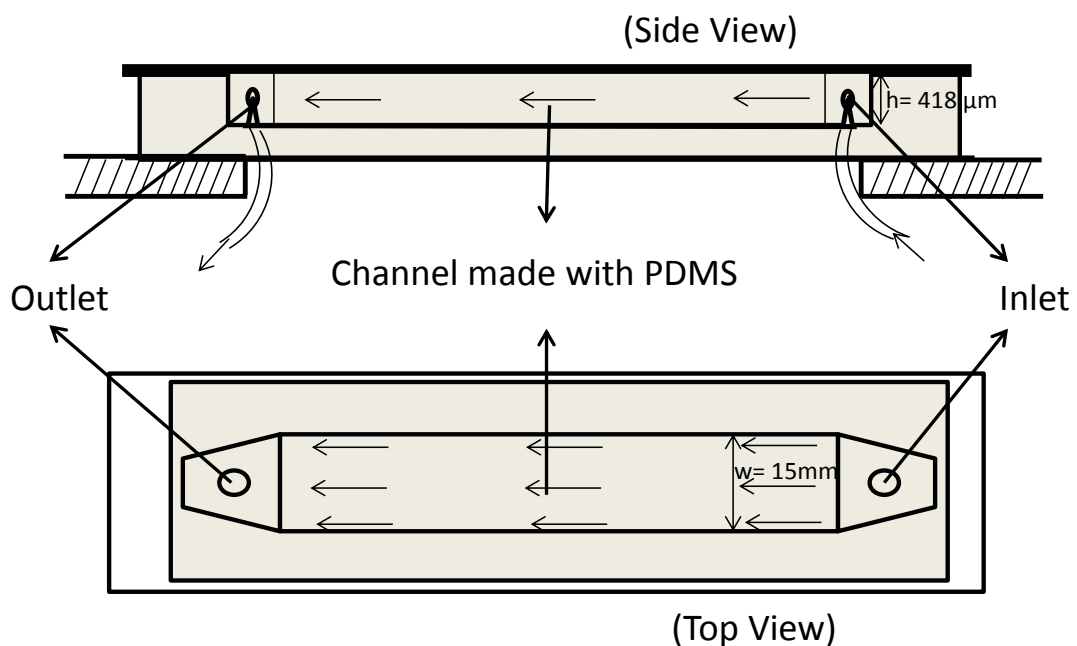
Figure 4.65. Schematic illustration of the flow chamber used in examination adhesion of microbubbles to cultured MDA-MB-231
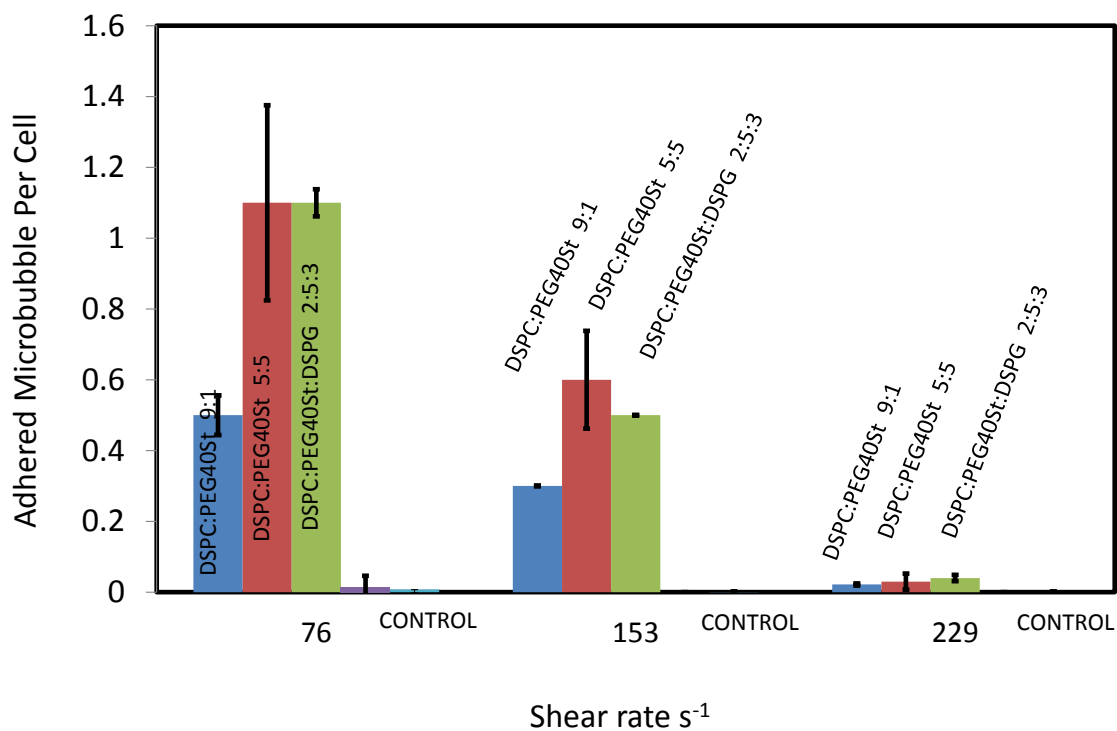
Figure 4.66. Comparison of adhered microbubble number associated with microbubble species and shear rate

Figure 4.67, Figure 4.68 and Figure 4.69 shows optical microscope images of adhered EGF labeled microbubbles prepared with DSPC:PEG40St:DSPG at molar ratios of 9:1:0, 5:5:0 and 2:5:3 at various shear rates. The MDA-MB-231 cell monolayer is seen in the background and as the shear rate decreased adhesion to MDA-MB-231 cell increased.
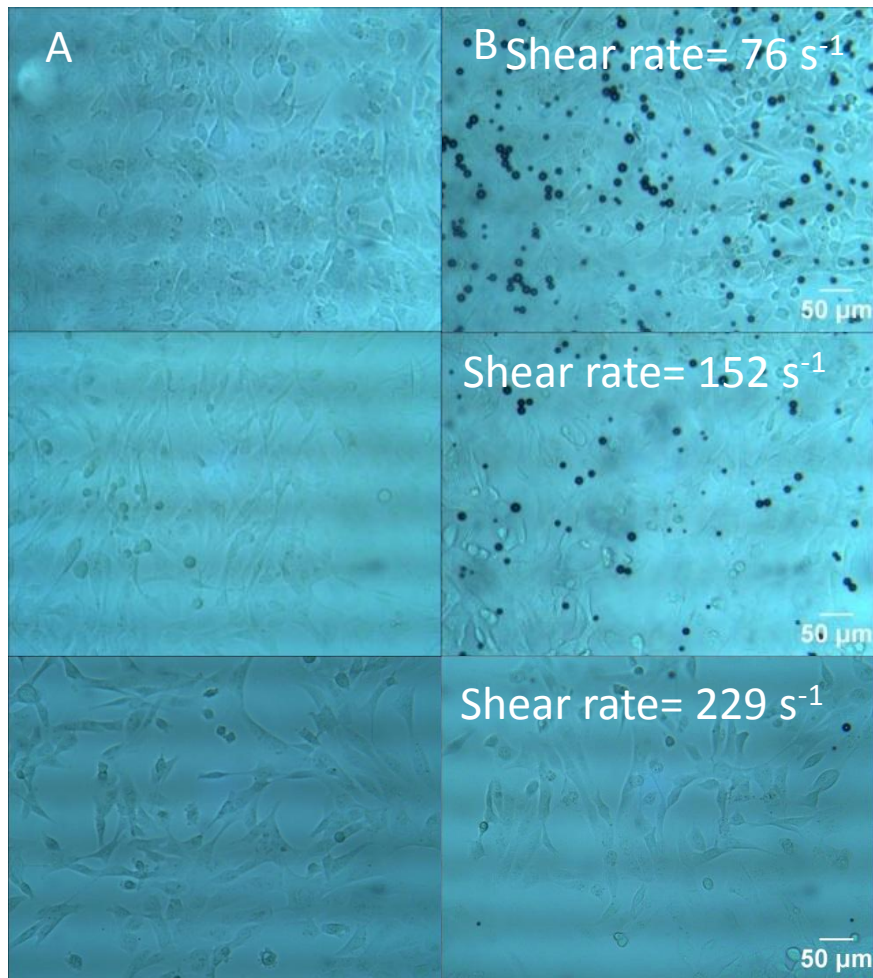
Figure 4.67. Light micrograph of cell lines (A) before perfusion of microbubbles and (B) adhered EGF labeled microbubbles prepared with DSPC:PEG40St at molar ratios of 9:1 to cells at various shear rates.
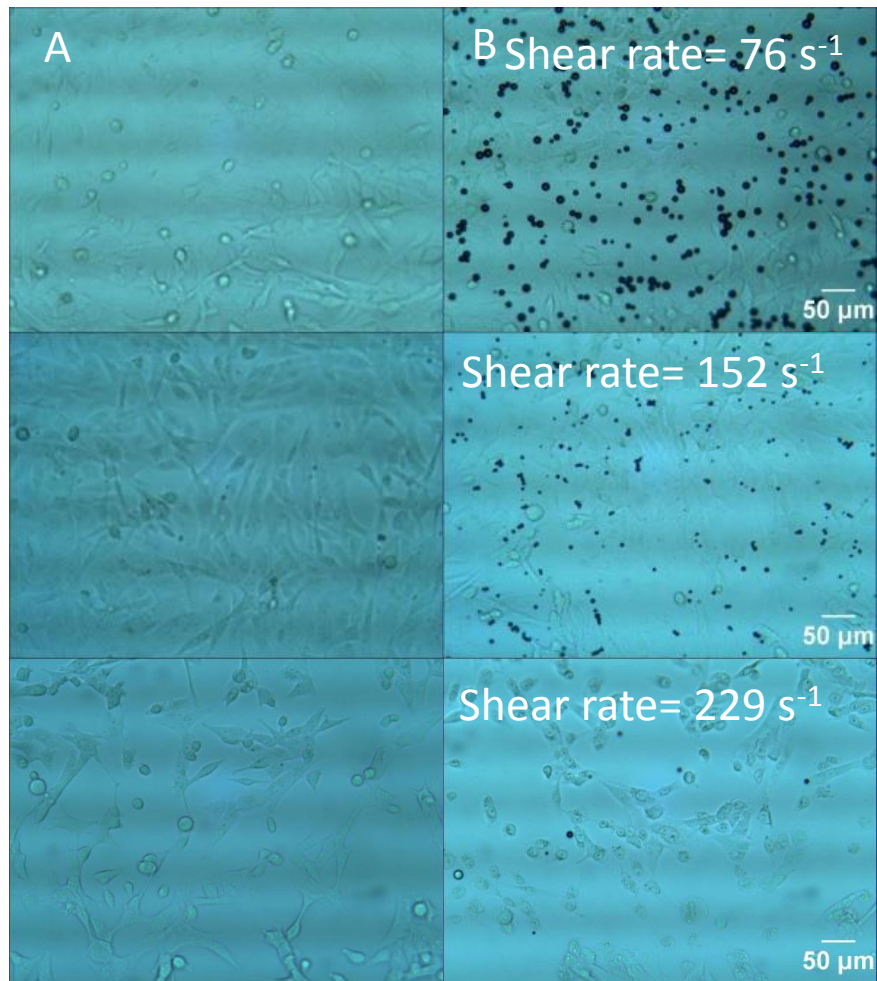
Figure 4.68. Light micrograph of cell lines (A) before perfusion of microbubbles and (B) adhered EGF labeled microbubbles prepared with DSPC:PEG40St at molar ratios of 5:5 to cells at various shear rates.
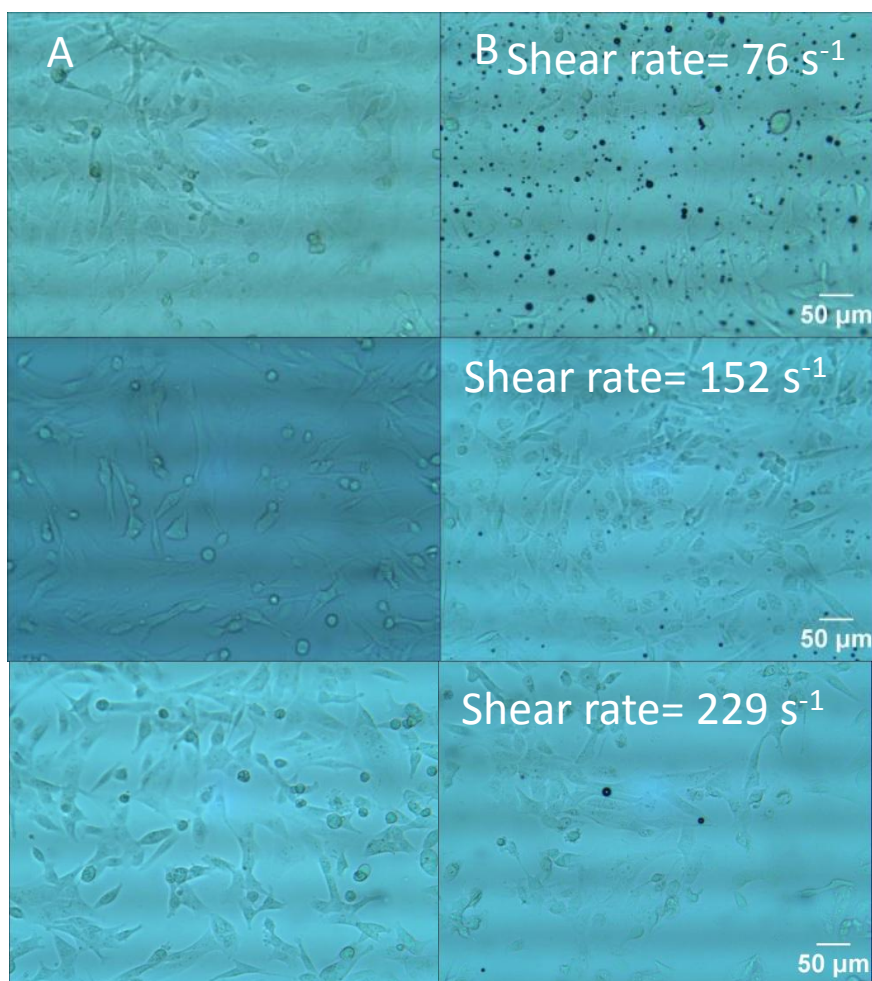
Figure 4.69. Light micrograph of cell lines (A) before perfusion of microbubbles and (B) adhered EGF labeled microbubbles prepared with DSPC:PEG40St:DSPG at molar ratios of 2:5:3 to cells at various shear rates.

Furthermore, control experiments were performed with microbubbles labeled with BSA instead of EGF. Control experiments demonstrated minimal accumulation of microbubbles compared to that when EGF was present on microbubble shell (Figure 4.66). BSA labeled microbubbles prepared with DSPC and PEG40St at a molar ratio of 9:1 adhered to the cells more than the other microbubble species produced with PEG40St at molar fraction of 0.5. As it is known that besides steric barrier function of PEG40St, it has ability of avoiding the unspecific binding to protein based materials such as endothelial cells and blood cells. Therefore, our result is not unexpected.

Moreover, dynamic stability of adhered microbubbles was examined at a shear rate of $153s^{-1}$. In this investigation, adhered EGF-labeled microbubbles prepared with the mixture of DSPC, PEG40St and DSPG at molar ratios 9:1:0, 5:5:0 and 2:5:3 to MDA-MB-231 were washed with imaging buffer under a shear rate of $153s^{-1}$ for 30

minutes and their stability on the cell line was examined. As seen from Figure 4.70, microbubbles prepared with current formulation started to burst with the effect of shear within few seconds. However, dissolution time of microbubbles increased when they were coated with DSPC:PEG40St at a molar ratio of 5:5. As we examined the dynamic stability of adhered microbubbles prepared with the mixture of DSPC, PEG40St and DSPG at molar ratios 2:5:3 to breast cancer cell line, it was observed that dynamic stability of microbubbles produced with this formulation was found to be the greatest at a shear rate of $153s^{-1}$ as compared to the other microbubble species.
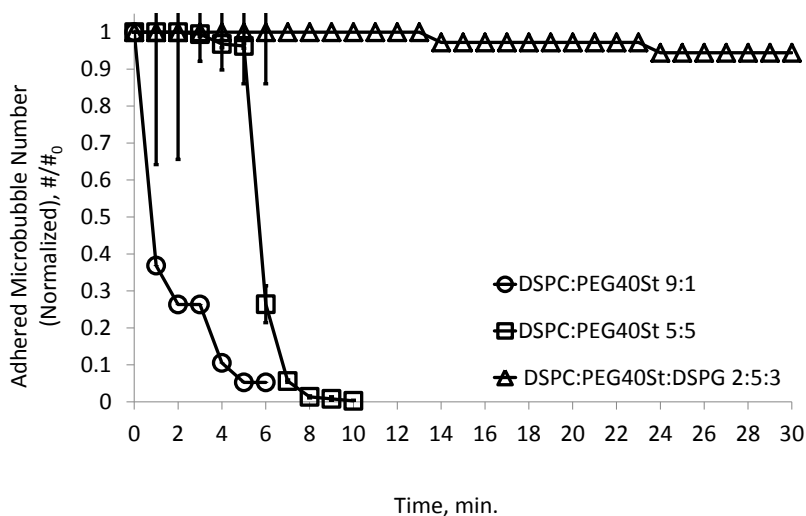
Figure 4.70. Change in number of microbubbles at a shear rate of $153s^{-1}$ over time.

It is known that avidin-biotin chemistry is the one of the most preferred way to bind the two biomolecules due to extremely high association equilibrium constant which is approximately 3×10^{15} M^{-1} (Rekharsky, Mori et al. 2007). In this study, streptavidin was chosen instead of avidin to bind the EGF to microbubbles since it generally has lower non-specific binding than avidin due to its non-glycosylated nature (Bayer, Ben-Hur et al. 1989). While developing a targeted microbubble species the absolute adhesion should be measured as bound microbubbles per cell. Adhesion of microbubbles is essential to obtain sufficient acoustic signal for ultrasound imaging. As reported in this study 100% (10μg/mL) streptavidin (corresponding to 100% ligand density) was chosen for production targeted microbubbles since microbubbles labeled with 100% streptavidin showed maximum saturation to streptavidin molecule indicating offered higher acoustic intensity. The main finding of this study was that adhesion of EGF-labeled microbubbles is dependent on local shear conditions and microbubble

stability. Since shear rates vary throughout the vascular system, ranging between 50 and 2000 s^{-1} (Weller, Villanueva et al. 2002), it is important to investigate the adherence of new targeted contrast agents under different shear conditions. Each microbubble species (formed with DSPC:PEG40St:DSPG 9:1:0, 5:5:0 and 2:5:3) showed this relationship between the adhesion and the shear rate. Another observation is that our new formulations provided much more adhesion to cell of interest compared to microbubble with current formulation (DSPC:PEG40St 9:1). These findings have indication that to detect the breast cancer, ultrasound might be a good alternative to mammography.

CHAPTER 5

CONCLUSIONS

In this study, stability and adhesion characteristics of microbubbles composed of different types of phospholipids, fatty acids and emulsifier were investigated. Phospholipids and fatty acids used in this study had the same hydrocarbon chain length but different head groups. In addition to phospholipids, the effect of cholesterol on microbubble stability was also examined. For current formulation of microbubbles prepared with DSPC and PEG40St at a molar ratio of 9:1, the change in size and concentration of microbubbles were investigated at temperature range from 4 oC to 48 oC in an effort to elucidate temperature response of microbubbles. Our results showed that stability of microbubbles decreased and size of the microbubbles increased with increasing temperature. Therefore, in the remaining part of the study microbubble stability was investigated at 38°C. Our results indicated that microbubbles prepared with current formulation (DSPC:PEG40St 9:1) disappeared in less than 30 min especially at 38°C, suggesting that these microbubbles are not very suitable for prolonged examination under ultrasound and for targeted delivery. Microbubble formulation was modified by increasing PEG40St amount. It was observed that increase in PEG40St up to 50mol% caused a significant improvement in bubble stability, resulting in prolonged (about 6 hours) onset time at 38 oC. Based on this observation, molar fraction of PEG40St was kept constant at 0.5 for examination of effect of the additional component on microbubble stability. Additional components were selected from the group of phospholipids and fatty acids which have a capability of secondary interactions such as hydrogen bonding, ionic interactions, van der Waals interactions etc. Selected components (DSPG, DSPA, DSPE, DSPS, DSTAP as lipids and Stearoyl-rac-glycerol, and Stearyl amine as fatty acids) were mixed at varying ratio with DSPC and PEG40 St and their effect on size and concentration of microbubbles were investigated. The results showed that the effect of additional component is highly dependent on the type of the head group of the additional component and its content in the formulation. Among the various components, the microbubble prepared with DSPC:PEG40St:DSPG at molar ratio of 2:5:3 resulted in the most stable microbubble

species. These microbubbles exhibited onset time of 9 hours at 38 oC. Besides the stability, microbubbles produced with this formulation had the narrowest size distribution and resulted in higher yield compared to the other microbubble species. In addition to effect of shell component, we also examined gas core type on microbubble stability. We observed that stability of the microbubbles prepared with current formulation can be enhanced further with the use of a gas less soluble in water, as observed by the other researchers in the literature. In contrast to expected, we found that the change of the gas core type did not have any effect on stability microbubbles prepared with DSPC, PEG40St and DSPG at molar ratios of 5:5:0 and 2:5:3. This result may suggest that the components forming the monolayer formed very dense shell around the gas core such that diffusion of gas through the shell is almost inhibited or at least enormously minimized. To figure out the effect of emulsifier type on microbubble stability, microbubbles were prepared with DSPC:PEG40St and DSPC:DSPE-PEGn (n=350, 1000, 2000), It was observed that using lipopolymers (DSPE-PEGn) as an emulsifier exhibited decrease in microbubble stability. Investigations for the adhesion of selected microbubbles to cultured human breast cancer cell line as a model system showed that adhesion ratio of the microbubbles depended on the formulation and shear rate, exhibiting lower adhesion with increasing shear rate. The results indicated that new microbubbles formulations prepared with DSPC:PEG40St at a molar ratio of 5:5 and DSPC:PEG40St:DSPG at a molar ratio of 2:5:3 provided much more adhesion to cell of interest and remained attached much longer to the cell line under the same shear rate applied compared to current formulation of microbubbles.

REFERENCES

Askvik, K. M., S. Are Gundersen, et al. (1999). "Complexation between lignosulfonates and cationic surfactants and its influence on emulsion and foam stability." Colloids and Surfaces A: Physicochemical and Engineering Aspects **159**(1): 89-101.

Bachmann, C., A. L. Klibanov, et al. (2006). "Targeting mucosal addressin cellular adhesion molecule (MAdCAM)-1 to noninvasively image experimental Crohn's disease." Gastroenterology **130**(1): 8-16.

Bagatolli, L. and E. Gratton (2000). "Two photon fluorescence microscopy of coexisting lipid domains in giant unilamellar vesicles of binary phospholipid mixtures." Biophysical journal **78**(1): 290-305.

Bayer, E. A., H. Ben-Hur, et al. (1989). "Postsecretory modifications of streptavidin." Biochemical Journal **259**(2): 369.

Bekeredjian, R., S. Chen, et al. (2003). "Ultrasound-targeted microbubble destruction can repeatedly direct highly specific plasmid expression to the heart." Circulation **108**(8): 1022-1026.

Bekeredjian, R., H. F. Kuecherer, et al. (2007). "Ultrasound-targeted microbubble destruction augments protein delivery into testes." Urology **69**(2): 386-389.

Borden, M. A., C. F. Caskey, et al. (2007). "DNA and polylysine adsorption and multilayer construction onto cationic lipid-coated microbubbles." Langmuir **23**(18): 9401-9408.

Borden, M. A., J. A. Feshitan, et al. (2009). "Microbubble size isolation by differential centrifugation." Journal of Colloid and Interface Science **329**(2): 316-324.

Borden, M. A., D. E. Kruse, et al. (2005). "Influence of lipid shell physicochemical properties on ultrasound-induced microbubble destruction." Ultrasonics, Ferroelectrics and Frequency Control, IEEE Transactions on **52**(11): 1992-2002.

Borden, M. A. and M. L. Longo (2002). "Dissolution behavior of lipid monolayer-coated, air-filled microbubbles: Effect of lipid hydrophobic chain length." Langmuir **18**(24): 9225-9233.

Borden, M. A. and M. L. Longo (2004). "Oxygen permeability of fully condensed lipid monolayers." The Journal of Physical Chemistry B **108**(19): 6009-6016.

Borden, M. A., G. Pu, et al. (2004). "Surface phase behavior and microstructure of lipid/PEG-emulsifier monolayer-coated microbubbles." Colloids and Surfaces B: Biointerfaces **35**(3-4): 209-223.

Chomas, J. E., P. Dayton, et al. (2001). "Mechanisms of contrast agent destruction." Ultrasonics, Ferroelectrics and Frequency Control, IEEE Transactions on **48**(1): 232-248.

Christiansen, C., H. Kryvi, et al. (1994). "Physical and biochemical characterization of Albunex, a new ultrasound contrast agent consisting of air-filled albumin microspheres suspended in a solution of human albumin." Biotechnology and applied biochemistry **19**(3): 307-320.

Christiansen, J. P., B. A. French, et al. (2003). "Targeted tissue transfection with ultrasound destruction of plasmid-bearing cationic microbubbles." Ultrasound in medicine & biology **29**(12): 1759-1767.

Coester, C., S. Tinkov, et al. (2009). "Microbubbles as Ultrasound Triggered Drug Carriers." Journal of Pharmaceutical Sciences **98**(6): 1935-1961.

Cox, D. J. and J. L. Thomas (2010). "Ultrasound-induced dissolution of lipid-coated and uncoated gas bubbles." Langmuir **26**(18): 14774-14781.

Deckers, R. and C. T. W. Moonen (2010). "Ultrasound triggered, image guided, local drug delivery." Journal of Controlled Release **148**(1): 25-33.

Dey, T., K. Anam, et al. (2000). "Antileishmanial activities of stearylamine-bearing liposomes." Antimicrobial Agents and Chemotherapy **44**(6): 1739-1742.

Dickey, A. and R. Faller (2008). "Examining the contributions of lipid shape and headgroup charge on bilayer behavior." Biophysical journal **95**(6): 2636-2646.

Dowhan, W. (1997). "Molecular basis for membrane phospholipid diversity: why are there so many lipids?" Annual review of biochemistry **66**(1): 199-232.

Dressaire, E., R. Bee, et al. (2008). "Interfacial polygonal nanopatterning of stable microbubbles." Science **320**(5880): 1198-1201.

Ellegala, D. B., H. Leong-Poi, et al. (2003). "Imaging tumor angiogenesis with contrast ultrasound and microbubbles targeted to $\alpha v \beta 3$." Circulation **108**(3): 336-341.

Fahy, E., S. Subramaniam, et al. (2009). "Update of the LIPID MAPS comprehensive classification system for lipids." Journal of lipid research **50**(Supplement): S9-S14.

Farook, U., E. Stride, et al. (2007). "Microbubbling by co-axial electrohydrodynamic atomization." Medical and Biological Engineering and Computing **45**(8): 781-789.

Farook, U., H. Zhang, et al. (2007). "Preparation of microbubble suspensions by co-axial electrohydrodynamic atomization." Medical engineering & physics **29**(7): 749-754.

Feinstein, S. B., J. Cheirif, et al. (1990). "Safety and efficacy of a new transpulmonary ultrasound contrast agent: initial multicenter clinical results." Journal of the American College of Cardiology **16**(2): 316-324.

Feinstein, S. B., F. J. Ten Cate, et al. (1984). "Two-dimensional contrast echocardiography. I. In vitro development and quantitative analysis of echo contrast agents." Journal of the American College of Cardiology **3**(1): 14-20.

Ferrara, K., R. Pollard, et al. (2007). "Ultrasound microbubble contrast agents: fundamentals and application to gene and drug delivery." Annu. Rev. Biomed. Eng. **9**: 415-447.

Forsberg, F., R. Roy, et al. (1998). "Conventional and hypobaric activation of an ultrasound contrast agent." Ultrasound in medicine & biology **24**(8): 1143-1150.

Gañán-Calvo, A. M. and J. M. Gordillo (2001). "Perfectly monodisperse microbubbling by capillary flow focusing." Physical review letters **87**(27): 274501.

Gerber, F., M. P. Krafft, et al. (2006). "Microbubbles with exceptionally long life—synergy between shell and internal phase components." New journal of chemistry **30**(4): 524-527.

Goldberg, B. B., D. A. Merton, et al. (2004). "Sentinel Lymph Nodes in a Swine Model with Melanoma: Contrast-enhanced Lymphatic US1." Radiology **230**(3): 727-734.

Gramiak, R. and P. M. Shah (1968). "Echocardiography of the aortic root." Investigative radiology **3**(5): 356-366.

Guiot, C., R. Cavalli, et al. (2004). "Temperature monitoring using ultrasound contrast agents: in vitro investigation on thermal stability." Ultrasonics **42**(1-9): 927-930.

Guiot, C., G. Pastore, et al. (2006). "Thermal response of contrast agent microbubbles: Preliminary results from physico-chemical and US-imaging characterization." Ultrasonics **44**: E127-E130.

Hédreul, C. and G. Frens (2001). "Foam stability." Colloids and Surfaces A: Physicochemical and Engineering Aspects **186**(1-2): 73-82.

Henry, C. L. and V. S. J. Craig (2009). "Inhibition of bubble coalescence by osmolytes: sucrose, other sugars, and urea." Langmuir **25**(19): 11406-11412.

Hernot, S. and A. L. Klibanov (2008). "Microbubbles in ultrasound-triggered drug and gene delivery." Advanced drug delivery reviews **60**(10): 1153-1166.

Hettiarachchi, K., E. Talu, et al. (2007). "On-chip generation of microbubbles as a practical technology for manufacturing contrast agents for ultrasonic imaging." Lab on a Chip **7**(4): 463-468.

Hohmann, J., T. Albrecht, et al. (2003). "Ultrasonographic detection of focal liver lesions: increased sensitivity and specificity with microbubble contrast agents." European journal of radiology **46**(2): 147-159.

Hristova, K. and D. Needham (1994). "The influence of polymer-grafted lipids on the physical properties of lipid bilayers: a theoretical study." Journal of colloid and interface science **168**(2): 302-314.

Huang, J. (2009). "Development of heat-sensitive microbubbles for cancer ablation margin assessment."

Isken, S. and J. A. M. de Bont (1998). "Bacteria tolerant to organic solvents." Extremophiles **2**(3): 229-238.

Jaworek, A. and A. Krupa (1999). "Classification of the modes of EHD spraying." Journal of Aerosol Science **30**(7): 975.

Jebrail, M., R. Schmidt, et al. (2008). "Effect of aliphatic chain length on stability of poly (ethylene glycol)-grafted phospholipid monolayers at the air/water interface." Colloids and Surfaces A: Physicochemical and Engineering Aspects **321**(1): 168-174.

Kaneko, O. F. and J. K. Willmann (2012). "Ultrasound for molecular imaging and therapy in cancer." Quantitative Imaging in Medicine and Surgery **2**(2): 87-97.

Kapp, D. S. and R. S. Cox (1995). "Thermal treatment parameters are most predictive of outcome in patients with single tumor nodules per treatment field in recurrent adenocarcinoma of the breast." International Journal of Radiation Oncology Biology Physics **33**: 887-900.

Karshafian, R., P. D. Bevan, et al. (2009). "Sonoporation by ultrasound-activated microbubble contrast agents: effect of acoustic exposure parameters on cell membrane permeability and cell viability." Ultrasound in medicine & biology **35**(5): 847-860.

Kaya, M., T. S. Gregory V, et al. (2009). "Changes in lipid-encapsulated microbubble population during continuous infusion and methods to maintain consistency." Ultrasound in medicine & biology **35**(10): 1748-1755.

Kenworthy, A. K., K. Hristova, et al. (1995). "Range and magnitude of the steric pressure between bilayers containing phospholipids with covalently attached poly (ethylene glycol)." Biophysical journal **68**(5): 1921-1936.

Kim, D. H., M. J. Costello, et al. (2003). "Mechanical properties and microstructure of polycrystalline phospholipid monolayer shells: Novel solid microparticles." Langmuir **19**(20): 8455-8466.

Kim, K., C. Kim, et al. (2000). "Preparation of a PEG-grafted phospholipid Langmuir-Blodgett monolayer for blood-compatible material." Journal of biomedical materials research **52**(4): 836-840.

Kim, K., C. Kim, et al. (2004). "Biostability and biocompatibility of a surface-grafted phospholipid monolayer on a solid substrate." Biomaterials **25**(1): 33-41.

Kirby, C., J. Clarke, et al. (1980). "Effect of the cholesterol content of small unilamellar liposomes on their stability in vivo and in vitro." Biochemical Journal **186**(2): 591.

Klibanov, A. L. (1999). "Targeted delivery of gas-filled microspheres, contrast agents for ultrasound imaging." Advanced drug delivery reviews **37**(1-3): 139-157.

Klibanov, A. L., P. T. Rasche, et al. (2002). "Detection of individual microbubbles of an ultrasound contrast agent: fundamental and pulse inversion imaging." Academic radiology **9**: S279.

Koczo, K., L. Lobo, et al. (1992). "Effect of oil on foam stability: aqueous foams stabilized by emulsions." Journal of colloid and interface science **150**(2): 492-506.

Kono, Y., G. C. Steinbach, et al. (2002). "Mechanism of Parenchymal Enhancement of the Liver with a Microbubble-based US Contrast Medium: An Intravital Microscopy Study in Rats1." Radiology **224**(1): 253-257.

Kooijman, E. E., V. Chupin, et al. (2005). "Spontaneous curvature of phosphatidic acid and lysophosphatidic acid." Biochemistry **44**(6): 2097-2102.

Korpanty, G., P. A. Grayburn, et al. (2005). "Targeting vascular endothelium with avidin microbubbles." Ultrasound in medicine & biology **31**(9): 1279-1283.

Kwan, J. J. and M. A. Borden (2010). "Microbubble Dissolution in a Multigas Environment." Langmuir **26**(9): 6542-6548.

Kwan, J. J. and M. A. Borden (2012). "Lipid monolayer collapse and microbubble stability." Advances in Colloid and Interface Science.

Langmuir, I. and D. B. Langmuir (1927). "The Effect of Monomolecular Films on the Evaporation of Ether Solutions." The Journal of Physical Chemistry **31**(11): 1719-1731.

Langner, M. and K. Kubica (1999). "The electrostatics of lipid surfaces." Chemistry and physics of lipids **101**(1): 3-35.

Lentacker, I., B. G. De Geest, et al. (2006). "Ultrasound-responsive polymer-coated microbubbles that bind and protect DNA." Langmuir **22**(17): 7273-7278.

Lentacker, I., S. De Smedt, et al. (2006). "Microbubbles which bind and protect DNA against nucleases."

Lentz, B. R., D. R. Alford, et al. (1982). "Phase behavior of mixed phosphatidylglycerol/phosphatidylcholine multilamellar and unilamellar vesicles." Biochemistry **21**(18): 4212-4219.

Leong-Poi, H., J. Christiansen, et al. (2003). "Noninvasive assessment of angiogenesis by ultrasound and microbubbles targeted to αv-integrins." Circulation **107**(3): 455-460.

Leong-Poi, H., M. A. Kuliszewski, et al. (2007). "Therapeutic arteriogenesis by ultrasound-mediated VEGF165 plasmid gene delivery to chronically ischemic skeletal muscle." Circulation research **101**(3): 295-303.

Li, M. and H. Fogler (1978). "Acoustic emulsification. Part 1. The instability of the oil-water interface to form the initial droplets." Journal of Fluid Mechanics **88**(03): 499-511.

Li, M. and H. Fogler (1978). "Acoustic emulsification. Part 2. Breakup of the large primary oil droplets in a water medium." Journal of Fluid Mechanics **88**(03): 513-528.

Lindner, J. R., J. Song, et al. (2001). "Ultrasound assessment of inflammation and renal tissue injury with microbubbles targeted to P-selectin." Circulation **104**(17): 2107-2112.

Livnah, O., E. A. Bayer, et al. (1993). "Three-dimensional structures of avidin and the avidin-biotin complex." Proceedings of the National Academy of Sciences **90**(11): 5076-5080.

Lozano, M. M. and M. L. Longo (2009). "Microbubbles coated with disaturated lipids and DSPE-PEG2000: phase behavior, collapse transitions, and permeability." Langmuir **25**(6): 3705-3712.

Lu, Q., H. D. Liang, et al. (2003). "Microbubble ultrasound improves the efficiency of gene transduction in skeletal muscle in vivo with reduced tissue damage." Gene therapy **10**(5): 396-405.

Lum, A. F. H., M. A. Borden, et al. (2006). "Ultrasound radiation force enables targeted deposition of model drug carriers loaded on microbubbles." Journal of Controlled Release **111**(1): 128-134.

Meijering, B. D. M., L. J. M. Juffermans, et al. (2009). "Ultrasound and microbubble-targeted delivery of macromolecules is regulated by induction of endocytosis and pore formation." Circulation research **104**(5): 679-687.

Mulvana, H., E. Stride, et al. (2010). "Temperature dependent behavior of ultrasound contrast agents." Ultrasound in medicine & biology **36**(6): 925-934.

Narayan, P. and M. A. Wheatley (1999). "Preparation and characterization of hollow microcapsules for use as ultrasound contrast agents." Polymer Engineering & Science **39**(11): 2242-2255.

Overgaard, J. (1989). "The current and potential role of hyperthermia in radiotherapy." International Journal of Radiation Oncology* Biology* Physics **16**(3): 535-549.

Pancholi, K., U. Farook, et al. (2008). "Novel methods for preparing phospholipid coated microbubbles." European Biophysics Journal **37**(4): 515-520.

Perutková, Š., M. Daniel, et al. (2009). "Stability of the inverted hexagonal phase." Advances in Planar Lipid Bilayers and Liposomes **9**: 237-278.

Petrache, H. I., S. W. Dodd, et al. (2000). "Area per lipid and acyl length distributions in fluid phosphatidylcholines determined by (2) H NMR spectroscopy." Biophysical journal **79**(6): 3172.

Podell, S., C. Burrascano, et al. (1999). "Physical and biochemical stability of Optison®, an injectable ultrasound contrast agent." Biotechnology and applied biochemistry **30**(3): 213-223.

Polozov, I. V. and K. Gawrisch (2004). "Domains in binary SOPC/POPE lipid mixtures studied by pulsed field gradient 1H MAS NMR." Biophysical journal **87**(3): 1741-1751.

Pu, G., M. L. Longo, et al. (2005). "Effect of microstructure on molecular oxygen permeation through condensed phospholipid monolayers." Journal of the American Chemical Society **127**(18): 6524-6525.

Raisinghani, A. and A. N. DeMaria (2002). "Physical principles of microbubble ultrasound contrast agents." The American journal of cardiology **90**(10): 3-7.

Rekharsky, M. V., T. Mori, et al. (2007). "A synthetic host-guest system achieves avidin-biotin affinity by overcoming enthalpy–entropy compensation." Proceedings of the National Academy of Sciences **104**(52): 20737-20742.

Riaz, M. (1995). "Stability and uses of liposomes." Pak Pharm Sci **8**(2): 69-79.

Riess, J. G., E. G. Schutt, et al. (2003). "Injectable microbubbles as contrast agents for diagnostic ultrasound imaging: The key role of perfluorochemicals." Angewandte Chemie-International Edition **42**(28): 3218-3235.

Ross, M., C. Steinem, et al. (2001). "Visualization of chemical and physical properties of calcium-induced domains in DPPC/DPPS Langmuir-Blodgett layers." Langmuir **17**(8): 2437-2445.

Schlicher, R. K., H. Radhakrishna, et al. (2006). "Mechanism of intracellular delivery by acoustic cavitation." Ultrasound in medicine & biology **32**(6): 915-924.

Schneider, M. (2008). "Molecular imaging and ultrasound-assisted drug delivery." Journal of Endourology **22**(4): 795-802.

Seip, R. and E. S. Ebbini (1995). "Noninvasive estimation of tissue temperature response to heating fields using diagnostic ultrasound." Biomedical Engineering, IEEE Transactions on **42**(8): 828-839.

Shah, D., N. Djabbarah, et al. (1978). "A correlation of foam stability with surface shear viscosity and area per molecule in mixed surfactant systems." Colloid & Polymer Science **256**(10): 1002-1008.

Sharon, N. and H. Lis (1982). "Glycoproteins: research booming on long-ignored ubiquitous compounds." Molecular and Cellular Biochemistry **42**(3): 167-187.

Shen, Y., R. L. Powell, et al. (2008). "Interfacial and stability study of microbubbles coated with a monostearin/monopalmitin-rich food emulsifier and PEG40 stearate." Journal of colloid and interface science **321**(1): 186-194.

Silvius, J. R., P. M. Brown, et al. (1986). "Role of head group structure in the phase behavior of amino phospholipids. 1. Hydrated and dehydrated lamellar phases of saturated phosphatidylethanolamine analogs." Biochemistry **25**(15): 4249-4258.

Silvius, J. R. and J. Gagne (1984). "Calcium-induced fusion and lateral phase separations in phosphatidylcholine-phosphatidylserine vesicles. Correlation by calorimetric and fusion measurements." Biochemistry **23**(14): 3241-3247.

Singhal, S., C. Moser, et al. (1993). "Surfactant-stabilized microbubbles as ultrasound contrast agents: stability study of Span 60 and Tween 80 mixtures using a Langmuir trough." Langmuir **9**(9): 2426-2429.

Sirsi, S. and M. Borden (2009). "Microbubble compositions, properties and biomedical applications." Bubble science engineering and technology **1**(1-2): 3.

Sirsi, S., J. Feshitan, et al. (2010). "Effect of microbubble size on fundamental mode high frequency ultrasound imaging in mice." Ultrasound in medicine & biology **36**(6): 935-948.

Straube, W. and R. M. Arthur (1994). "Theoretical estimation of the temperature dependence of backscattered ultrasonic power for noninvasive thermometry." Ultrasound in medicine & biology **20**(9): 915-922.

Swanson, E. J., V. Mohan, et al. (2010). "Phospholipid-stabilized microbubble foam for injectable oxygen delivery." Langmuir **26**(20): 15726-15729.

Swanson, E. J., V. Mohan, et al. (2010). "Phospholipid-Stabilized Microbubble Foam for Injectable Oxygen Delivery." Langmuir.

Takalkar, A. M., A. L. Klibanov, et al. (2004). "Binding and detachment dynamics of microbubbles targeted to P-selectin under controlled shear flow." Journal of Controlled Release **96**(3): 473-482.

Takeuchi, M., K. Ogunyankin, et al. (1999). "Enhanced visualization of intravascular and left atrial appendage thrombus with the use of a thrombus-targeting ultrasonographic contrast agent (MRX-408A1): in vivo experimental echocardiographic studies." Journal of the American Society of Echocardiography **12**(12): 1015-1021.

Talu, E., K. Hettiarachchi, et al. (2006). <u>P2A-8 Lipid-Stabilized Monodisperse Microbubbles Produced by Flow Focusing for Use as Ultrasound Contrast Agents</u>. Ultrasonics Symposium, 2006. IEEE, IEEE.

Talu, E., K. Hettiarachchi, et al. (2008). "Maintaining monodispersity in a microbubble population formed by flow-focusing." <u>Langmuir</u> **24**(5): 1745-1749.

Talu, E., M. M. Lozano, et al. (2006). "Long-term stability by lipid coating monodisperse microbubbles formed by a flow-focusing device." <u>Langmuir</u> **22**(23): 9487-9490.

Vaddi, H., P. Ho, et al. (2002). "Terpenes in propylene glycol as skin-penetration enhancers: Permeation and partition of haloperidol, fourier transform infrared spectroscopy, and differential scanning calorimetry." <u>Journal of pharmaceutical sciences</u> **91**(7): 1639-1651.

van Wamel, A., K. Kooiman, et al. (2006). "Vibrating microbubbles poking individual cells: drug transfer into cells via sonoporation." <u>Journal of Controlled Release</u> **112**(2): 149-155.

Varghese, T., J. Zagzebski, et al. (2002). "Ultrasound monitoring of temperature change during radiofrequency ablation: preliminary in-vivo results." <u>Ultrasound in medicine & biology</u> **28**(3): 321-329.

Villanueva, F. S., R. J. Jankowski, et al. (1998). "Microbubbles targeted to intercellular adhesion molecule-1 bind to activated coronary artery endothelial cells." <u>Circulation</u> **98**(1): 1-5.

von Bibra, H., F. Hartmann, et al. (1989). "Contrast-color Doppler echocardiography. Improved right heart diagnosis following intravenous injection of Echovist]." <u>Zeitschrift für Kardiologie</u> **78**(2): 101.

Weber, F. J. and J. De Bont (1996). "Adaptation mechanisms of microorganisms to the toxic effects of organic solvents on membranes." <u>Biochimica et biophysica acta</u> **1286**(3): 225.

Weller, G. E. R., F. S. Villanueva, et al. (2002). "Modulating targeted adhesion of an ultrasound contrast agent to dysfunctional endothelium." <u>Annals of biomedical engineering</u> **30**(8): 1012-1019.

Weller, G. E. R., F. S. Villanueva, et al. (2005). "Targeted ultrasound contrast agents: In vitro assessment of endothelial dysfunction and multi-targeting to ICAM-1 and sialyl Lewisx." <u>Biotechnology and bioengineering</u> **92**(6): 780-788.

Wheatley, M. and S. Singhal (1995). "Structural studies on stabilized microbubbles: development of a novel contrast agent for diagnostic ultrasound." <u>Reactive Polymers</u> **25**(2): 157-166.

Wheatley, M. A., B. Schrope, et al. (1990). "Contrast agents for diagnostic ultrasound: development and evaluation of polymer-coated microbubbles." Biomaterials **11**(9): 713-717.

Williams, R., J. M. Hudson, et al. (2011). "Dynamic microbubble contrast-enhanced US to measure tumor response to targeted therapy: a proposed clinical protocol with results from renal cell carcinoma patients receiving antiangiogenic therapy." Radiology **260**(2): 581-590.

Wisner, E. R., K. W. Ferrara, et al. (2003). "Sentinel node detection using contrast-enhanced power Doppler ultrasound lymphography." Investigative radiology **38**(6): 358-365.

Wrenn, S. P., M. Mleczko, et al. (2009). "Phospholipid-stabilized microbubbles: influence of shell chemistry on cavitation threshold and binding to giant uni-lamellar vesicles." Applied Acoustics **70**(10): 1313-1322.

Wydro, P. (2011). "The interactions between cholesterol and phospholipids located in the inner leaflet of humane erythrocytes membrane (DPPE and DPPS) in binary and ternary films—The effect of sodium and calcium ions." Colloids and Surfaces B: Biointerfaces **82**(1): 209-216.

Xing, Z. W., H. T. Ke, et al. (2010). "Novel ultrasound contrast agent based on microbubbles generated from surfactant mixtures of Span 60 and polyoxyethylene 40 stearate." Acta Biomaterialia **6**(9): 3542-3549.

Zderic, V., S. Vaezy, et al. (2002). "Ocular drug delivery using 20-kHz ultrasound." Ultrasound in medicine & biology **28**(6): 823-829.

Zhao, W., T. Róg, et al. (2008). "Role of phosphatidylglycerols in the stability of bacterial membranes." Biochimie **90**(6): 930-938.

Zhou, Y., J. Cui, et al. (2008). "Dynamics of sonoporation correlated with acoustic cavitation activities." Biophysical journal **94**(7): L51-L53.

Zuna, I., P. Novak, et al. (2000). "Noninvasive monitoring of temperature distribution in the target field of hyperthermia by ultrasonic tissue characterization." Ultrasound in Medicine and Biology, Suppl **2**(26): A54.